

University of Louisville

## ThinkIR: The University of Louisville's Institutional Repository

---

Electronic Theses and Dissertations

---

8-2010

# Substance P and the tectothalamic pathway.

Sean Phillip Masterson 1974-  
*University of Louisville*

Follow this and additional works at: <https://ir.library.louisville.edu/etd>

---

### Recommended Citation

Masterson, Sean Phillip 1974-, "Substance P and the tectothalamic pathway." (2010). *Electronic Theses and Dissertations*. Paper 915.  
<https://doi.org/10.18297/etd/915>

This Doctoral Dissertation is brought to you for free and open access by ThinkIR: The University of Louisville's Institutional Repository. It has been accepted for inclusion in Electronic Theses and Dissertations by an authorized administrator of ThinkIR: The University of Louisville's Institutional Repository. This title appears here courtesy of the author, who has retained all other copyrights. For more information, please contact [thinkir@louisville.edu](mailto:thinkir@louisville.edu).

**SUBSTANCE P AND THE TECTOTHALAMIC PATHWAY**

By

Sean Phillip Masterson

B.A., Indiana University, 2001

M.A., University of Louisville, 2005

A Dissertation

Submitted to the faculty of the

Graduate School of the University of Louisville

in Partial Fulfillment of the Requirements

for the Degree of

Doctor of Philosophy

Department of Anatomical Sciences and Neurobiology

University of Louisville

Louisville, Kentucky

August 2010



**SUBSTANCE P AND THE TECTOTHALAMIC PATHWAY**

By

Sean Phillip Masterson

B.A., Indiana University, 2001

M.A., University of Louisville, 2005

A Dissertation Approved on

July 28, 2010

By the Following Dissertation Committee:

---

Martha Bickford, Ph.D., Dissertation Director

---

Paul DeMarco, Ph.D.

---

Charles Hubscher, Ph.D.

---

Robin Krimm, Ph.D.

---

David S.K. Magnuson, Ph.D.

## ACKNOWLEDGEMENTS

This dissertation is as much a testament to the patience and dedication of my advisor and mentor, Dr. Martha Bickford, as it is to my own. For her perseverance, I owe a debt of gratitude that can never be fully repaid. The members of my dissertation committee, Dr. Paul DeMarco, Dr. Charles Hubscher, Dr. Robin Krimm, and Dr. David S.K. Magnuson have generously given their time and have never threatened the autonomy which is peculiar to my personality. I only regret that the stratification of our research community created an irresistible illusion of separateness that prevented me from knowing some of the committee as well as I would have liked. I am grateful to Dr. Jianli Li for his assistance throughout my research and from whom I adopted a most dependable electrophysiology rig. I must acknowledge the many friends, Dr. Ranida Chomsung, Haiyang Wei, Johnathan Day-Brown II, and Dmitry Familstev who assisted, advised and guided my research in addition to making life more interesting. Arkadiusz Slusarczyk, Cathie Capel, and Michael Eisenback were instrumental in much of my research and I thank them for their technical assistance. I am grateful too for the support of the department staff. I must express my gratitude to Mindy, my wife, for her continued support and encouragement. This work was supported by NINDS grants R01NS35377 and F31NS052012.

## **ABSTRACT**

### **SUBSTANCE P AND THE TECTOTHALAMIC PATHWAY**

Sean Masterson

July 28, 2010

Cortical and tectal inputs to the caudal LPN in the rat were examined using anatomical and physiological techniques. Pyramidal cells in layer 6 of the visual cortex and wide-field vertical cells in the stratum opticum of the superior colliculus (SC) project to the caudal LPN. Ultrastructural examination revealed that cortical terminals within the caudal LPN were small, contacted small dendrites, and could be identified through vGLUT1 immunohistochemistry. In contrast, tectal terminals were much larger, contacted large dendrites, and could be identified through vGLUT2 immunohistochemistry. In whole cell current clamp recording, stimulation of corticothalamic fibers elicited EPSPs that showed a frequency dependent facilitation and stimulation of the tectothalamic fibers elicited stable EPSPs.

The neuropeptide Substance P (SP) and the receptor to which it binds, neurokinin-1 (NK-1), can both be found within the LPN of the rat. We examined the origin of the SP-positive terminals, their anatomical relationship to the NK-1 receptor, and the physiological effects of SP within the LPN. Light and confocal microscopy revealed that NK-1 positive cells were localized in the caudal LPN and were embedded within a SP positive terminal field. At the ultrastructural level, SP terminals were the same size as tecto-LPN terminals and terminals that contain vGLUT2 and they synapsed with large

NK-1 positive dendrites. Lesions of the superior colliculus (SC) with ibotenic acid reduced the level of SP and vGLUT2 immunoreactivity in the caudal LPN. Bath application of SP depolarized the neurons, increased their membrane resistance, and produced long-term potentiation (LTP) of the EPSPs. These effects were blocked by simultaneous application of the NK-1 antagonist L-703,606. Considering that high-frequency firing is often necessary for the release of neuropeptides, both the corticothalamic and tectothalamic fibers were stimulated at 100Hz. Stimulation of the corticothalamic fibers had no effect on the membrane resistance or on EPSP amplitudes. In contrast, stimulation of the tectothalamic fibers depolarized the neurons, increased their membrane resistance, and produced LTP. These results suggest that wide-field vertical cells in the stratum opticum of the SC project to the caudal LPN and when activated at high frequency produce LTP through the activation of NK-1 receptors.

## TABLE OF CONTENTS

	PAGE
ACKNOWLEDGEMENTS.....	iii
ABSTRACT .....	iv
LIST OF FIGURES .....	ix
CHAPTERS	
I. INTRODUCTION.....	1
SYNAPTIC ORGANIZATION OF THE TECTORECIPIENT ZONE OF THE RAT LATERAL POSTERIOR NUCLEUS .....	6
Abstract.....	6
Introduction.....	7
Methods and materials .....	9
Animals .....	9
Tract tracing .....	10
Antibody characterization.....	11
Vesicular glutamate transporter immunohistochemistry .....	12
Electron Microscopy .....	12
Computer generated figures .....	13
Results.....	14
Distribution and morphology of inputs to the LPN .....	14
Synaptic organization of the tecto-LPN terminals.....	15



Synaptic organization of the corticothalamic terminals in the	
tecto-recipient LPN .....	16
Distribution of vGLUT1 and vGLUT2 in the LPN .....	17
Synaptic organization of vGLUT1- and vGLUT2-stained terminals ..	18
Discussion .....	19
The tectorecipient LPN: “second order” nucleus.....	19
vGLUT1 and vGLUT2: markers for corticothalamic and	
tectothalamic terminals .....	21
Functional considerations .....	22
III. FREQUENCY-DEPENDENT RELEASE OF SUBSTANCE P MEDIATES	
HETEROSYNAPTIC POTENTIATION OF GLUTAMATERGIC RESPONSES IN	
THE RAT VISUAL THALAMUS.....	54
Abstract .....	54
Introduction.....	55
Methods and materials .....	57
Tract tracing and lesions .....	57
Histochemistry .....	58
Preparation of LPN slices .....	59
Recording procedures .....	60
Results.....	62
SP is presynaptic, and NK1 is postsynaptic in the LPN .....	62
Tecto-LPN terminals contain SP .....	63
Stimulation of cortico-LPN and tecto-LPN inputs in slices .....	64

Cortico and tecto inputs are glutamatergic and convergent.....	65
Tecto-LPN and cortico-LPN EPSPs display distinct short term synaptic plasticity.....	65
SP increases the amplitude of cortico-LPN and tecto-LPN EPSPs .....	66
SP effects are mediated by postsynaptic NK1 receptors .....	67
SP is released from tecto-LPN terminals by high frequency Stimulation.....	67
Discussion.....	69
Tectothalamic synapses: a third type of glutamatergic response.....	69
Substance P in the LPN.....	71
Functional implications.....	72
IV. SUMMARY AND FUTURE DIRECTIONS.....	94
Summary.....	94
Future directions .....	96
Resolution of the anatomy within the tectothalamic circuit .....	96
Receptors and mechanisms of SP potentiation.....	97
REFERENCES .....	99
LIST OF ABBREVIATIONS.....	110
CURRICULUM VITAE.....	113

## LIST OF FIGURES

FIGURE	PAGE
Chapter II	
1. Retrogradely labeled cortico-LPN cells.....	25
2. Retrogradely labeled tecto-LPN cells.....	27
3. Anterogradely labeled tecto-LPN terminals.....	29
4. Anterogradely labeled type I cortico-LPN terminals from visual cortex....	31
5. Anterogradely labeled type II cortico-LPN terminals from visual cortex...	33
6. Anterogradely labeled cortico-LPN terminals from visual cortex.....	35
7. Three terminal types were identified in the LPN.....	37
8. Tecto-LPN terminals are nonGABAergic and contact large nonGABAergic dendrites.....	39
9. Cortico-LPN terminals are small and nonGABAergic and contact small nonGABAergic dendrites.....	41
10. The caudal LPN stains for both vGLUT1 and vGLUT2.....	43
11. SC lesions decrease vGLUT2 staining in the caudal LPN.....	45
12. vGLUT1 terminals are small and nonGABAergic and contact small nonGABAergic dendrites.....	47

13. vGLUT2 terminals are nonGABAergic and contact large nonGABAergic dendrites.....	49
14. Histograms of terminal and dendritic sizes.....	51
15. Summary of synaptic terminal morphology in the rat visual thalamus .....	53

### Chapter III

1. SP is presynaptic and NK1 is postsynaptic in the LPN .....	76
2. Tecto-LPN terminals contain SP .....	78
3. Cortico-LPN and tecto-LPN inputs are glutamatergic and convergent .....	80
4. Tecto-LPN and cortico-LPN EPSPs display distinct short term synaptic plasticity.....	82
5. Substance P increases the amplitude of cortico and tecto EPSPs.....	84
6. SP effects are mediated by postsynaptic NK1 receptors .....	86
7. High frequency stimulation of tecto-LPN axons increases the amplitude of subsequent tecto- and cortico-LPN EPSPs .....	88
8. High frequency stimulation of cortico-LPN input does not change the amplitude of subsequent tecto- or cortico-LPN EPSPs .....	90
9. Schematic summary of rat LPN glutamatergic synapses.....	93

## CHAPTER I

### INTRODUCTION

The visual world presents a multitude of foci that range in complexity and relevance. The central nervous system is limited in its capacity to process sensory information and is incapable of attending to all possible stimuli. Therefore, neural mechanisms must exist that are capable of weighting visual stimuli and determining their salience. There are two established routes by which visual information reaches the cortex. In the primary visual pathway, information from the retina is conveyed to the cortex by the lateral geniculate nucleus (LGN) of the thalamus. Retinogeniculate terminals are large, contact proximal dendrites, and terminate in potent synaptic arrangements known as glomeruli (Li et al., 2003a). In vivo physiology studies indicate that the response properties of LGN neurons are defined, or “driven”, primarily by their retinal inputs (Cleland et al., 1971). In contrast, input from the visual cortex to the LGN, in the form of small terminals that innervate distal dendrites, has relatively minor, “modulatory” effects on the visual responses of geniculate neurons.

In the secondary visual pathway, information from the retina reaches the cortex by way of the superior colliculus (SC) and the pulvinar nucleus (primates) or the LPN (rodents). The secondary visual system has been implicated in visual orientation and spatial attention (Bender and Butter 1987, Fabre-Thorpe et al. 1986, Laberge and Buchsbaum 1990). The activity of the LPN is especially intriguing because it has diverse

visual input and has reciprocal connections with the cortex. The LPN receives sparse projections from retinal ganglion cells and extensive projections from both the cortex and the SC. The projection cells (also referred to as relay cells) in the LPN are glutamatergic cells that project to visual cortical areas, striatum and amygdala. The LPN has been termed a "higher order" nucleus (Guillery, 1995, Sherman and Guillery, 2002) because its anatomical organization suggests that its activity might be defined not by the retina but by the cortex. Pyramidal cells from layers 5 and 6 of the visual cortex project to the LPN. The layer 5 axons are large, contact proximal dendrites, and terminate glomeruli, similar to the synaptic arrangements of retinogeniculate terminals (Bourassa and Deschênes, 1995; Li et al., 2003a). Stimulation of layer 5 axons elicits a frequency dependent depression in LPN neurons (Li et al., 2003b). This response is similar to the response of LGN neurons to stimulation of retinogeniculate axons (Turner and Salt, 1998; Chen et al., 2002). In contrast, layer 6 axons that innervate the LPN are small and contact distal dendrites, similar to the terminations of corticogeniculate terminals (Bourassa and Deschênes, 1995; Li et al., 2003a). Cells in the LPN respond to stimulation of the layer 6 axons with a frequency dependent facilitation, a response that is similar to the cortical input to the LGN (Li et al., 2003b; Lindstöm and Wróbel 1990; Turner and Salt, 1998; von Krosigk et al., 1999). These anatomical and physiological findings support the idea that layer 5 afferents may be "drivers" of LPN activity while layer 6 afferents may be "modulators" of LPN activity (Sherman and Guillery, 1998). In this scenario, visual information from the cortex both drives and modulates the activity of the LPN which then projects back to the cortex. This thalamo-cortico-thalamo loop might coordinate cortical regions and contribute to the generation of attention.

Within the concept of drivers and modulators, classification of the tectal input to the LPN remains unclear. The SC is divided into superficial and deep layers. The superficial layer is subdivided into the stratum zonale (SZ), stratum griseum superficiale (SGS), and the stratum opticum (SO). The superficial layers of the SC receive topographically organized inputs from retinal ganglion cells (Wassle and Illing, 1980) and layer 5 pyramidal cells of the visual cortex (Hubener and Bolz, 1988). Neurons in the SGS and SO possess large visual receptive fields (Chalupa et al., 1983, Major et al. 2000), are multisensory (Burnett et al., 2004) and innervate the LPN (Ling et al., 1997, Hilbig et al., 2000). Neurons in the tectorecipient region of the LPN display different response properties to visual stimuli and possess larger visual receptive fields than the cells in the superficial layers of the SC (Chalupa et al., 1983). The larger receptive fields of the tectorecipient neurons connote a possible convergence of tectal afferents onto relay cells in the LPN.

Although a large variation has been found in the morphology of tecto-LPN synapses in the hamster (Ling et al., 1997), these synapses could still be grouped into two categories: individual terminals and tubular clusters. The individual terminals were smooth with a sparse distribution of swellings. The tubular clusters consisted of 20-40 tightly packed boutons around the shaft of a large, proximal dendrite. The synaptic morphology of the tubular clusters suggests that the SC might profoundly influence the behavior of the LPN. Unfortunately, experiments that removed the tectal input to the LPN produced contrasting results. Lesion of the SC was found to have negligible effects on the visual responsiveness of cells within the monkey pulvinar, a structure comparable to the LPN (Bender, 1983). Conversely, inhibition of the rabbit SC was found to

significantly decrease the visual responsiveness of cells within the LPN (Casanova and Molotchnikoff, 1990). Functional MRI (Buchel and Josephs, 1998) and PET scans (Bundesen et al., 2002) of humans have shown that the SC and pulvinar are active during periods of visual attention. The functional and anatomical relationship between the SC and the LPN relative to visual attention is undetermined.

Immunocytochemical studies have found that cells within the SGS and SO stain for SP. It has been demonstrated in the cat that a large number of these SP-immunoreactive cells project to the LPN (Hutsler and Chalupa, 1991). The ultrastructure of substance P stained terminals is similar to that of tectal terminals labeled by anterograde transport (Kelly et al., 2003). In the rat, there is a dense network of fibers that stain for SP in the caudal regions of the LPN (Battaglia et al., 1992). This is the region of the LPN that receives the densest input from the SC. Lesioning of the SC in the cat (Hutsler and Chalupa, 1991) and in the rat (Miguel-Hidalgo et al., 1991) caused a reduction in the SP-immunoreactivity within the tectorecipient region the LPN.

The SP receptor, neurokinin-1 (NK1) has also been localized to the LPN (Ogawa-Meduro et al., 1994, Saffroy et al., 2003) and is most densely distributed in the caudal tectorecipient zones. Substance P has diverse effects throughout the central nervous system many of which are facilitating. Substance P was found to increase the susceptibility of neurons to long term potentiation in the cortex (Kato and Yoshimura 1993) and spinal cord (Afrah et al. 2002). Substance P has also been found to inhibit pyramidal neurons in the hippocampus by exciting interneurons through a decrease in  $K^+$  conductance and an increase in  $Na^+$  conductance (Ogier and Raggenbass 2003). Application of SP onto dissociated dorsal root ganglion cells potentiated an NMDA



activated current (Wu et al., 2004). This effect was blocked by NK1 antagonists. This potentiation was slow-acting and long-lasting; peaking after 5-10 minutes and lasting up to 3 hours.

The visual system has been studied extensively. Yet, the mechanism by which the simplest visual image is selected, deconstructed, processed, and then reconstructed into a percept remains largely a mystery. In the following chapters, I will describe anatomical and physiological experiments that characterize tecto-LPN circuit and its modulation by SP. The results contribute to our understanding of mammalian visual pathways and mechanisms to manipulate thalamic synaptic efficacy which could be used to modify abnormal thalamic activity patterns. In addition, the data collected could have a broader impact because the design of the tecto-LPN circuit and the function of its components are likely common to other areas of the central nervous system.

**CHAPTER II**  
**SYNAPTIC ORGANIZATION OF THE TECTORECIPIENT ZONE OF**  
**THE RAT LATERAL POSTERIOR NUCLEUS**

Published: Masterson SP, Li J, Bickford ME. J Comp Neurol 515:647-663.2009

**Abstract**

Dorsal thalamic nuclei have been categorized as either “first order” nuclei that gate the transfer of relatively unaltered signals from the periphery to the cortex, or “higher order” nuclei that transfer signals from one cortical area to another. To classify the tectorecipient lateral posterior (LPN), we examined the synaptic organization of tracer-labeled cortical and tectal terminals, and terminals labeled with antibodies against the type 1 and type 2 vesicular glutamate transporters (vGLUT1 and vGLUT2) within the caudal/lateral LPN of the rat. Within this zone, we found that all tracer-labeled cortical terminals, as well as vGLUT1 antibody-labeled terminals, are small profiles with round vesicles (RS profiles) that innervate small caliber dendrites. Tracer-labeled tecto-LPN terminals, as well as vGLUT2 antibody-labeled terminals, were medium-sized profiles with round vesicles (RM profiles). Tecto-LPN terminals were significantly larger than cortico-LPN terminals, and contacted significantly larger dendrites. These results indicate that within the tectorecipient zone of the rat LPN, cortical terminals are located distal to tectal terminals, and that vGLUT1 and vGLUT2 antibodies may be used as markers for cortical and tectal terminals respectively. Finally, comparisons of the synaptic patterns formed by tracer-

labeled terminals with those of vGLUT antibody-labeled terminals suggest that individual LPN neurons receive input from multiple cortical and tectal axons. We suggest that the tectorecipient LPN constitutes a third category of thalamic nucleus (“second order”) that integrates convergent tectal and cortical inputs. This organization may function to signal the movement of novel or threatening objects moving across the visual field.

## **Introduction**

Recent studies suggest that nuclei of the dorsal thalamus fall into two general categories. First order nuclei, such as the dorsal lateral geniculate nucleus (dLGN), receive ascending sensory input (e.g. from the retina) that drives neuronal response properties, and feedback input from cortical layer VI that modulates these responses (Guillery, 1995; Sherman and Guillery, 1998). In contrast, higher order nuclei receive little ascending sensory input, and are innervated by cortical cells located in both layers V and VI. Anatomical and physiological studies suggest that within higher order nuclei, the function of the ascending sensory input is supplanted by inputs from cortical layer V (Ogren and Hendrickson, 1979; Vidnyanszky et al., 1996; Feig and Harting, 1998; Bartlett et al., 2000; Li et al., 2003a; Li et al., 2003c; Reichova and Sherman, 2004; Baldauf et al., 2005), and that this cortically driven circuitry may be involved in corticocortical communication rather than the relay of ascending sensory signals (Guillery, 1995; Sherman and Guillery, 2002).

Previous studies indicate that the rostral regions of the rat lateral posterior nucleus (LPN) can be considered higher order. This region receives few ascending inputs and is innervated by two types of cortical terminals that resemble either corticogeniculate terminals (type I), or retinogeniculate terminals (type II) (Bourassa and Deschenes, 1995;

Li et al., 2003a). In addition, stimulation of cortical inputs to the rostral LPN elicits two types of excitatory postsynaptic responses (EPSPs). Type I responses facilitate with increasing stimulation frequency (Li et al., 2003b), similar to corticogeniculate EPSPs (Lindstrom and Wrobel, 1990; Turner and Salt, 1998; von Krosigk et al., 1999; Granseth et al., 2002), while type II responses depress with increasing stimulation frequency (Li et al., 2003a), similar to retinogeniculate responses (Turner and Salt, 1998; Chen et al., 2002; Chen and Regehr, 2003). Thus, it appears that the rostral LPN should be considered higher order in that the morphology and physiology of synaptic terminals that originate from cortical layer 5 are quite similar to the ascending sensory inputs of first order nuclei.

However, a third category may be necessary to describe the organization of thalamic regions that receive input from the superior colliculus (SC). Recent studies of the primate mediodorsal nucleus indicate that inputs from the SC can significantly impact thalamic and cortical activity patterns (Wurtz and Sommer, 2004) yet, when examined, tectothalamic terminals form unique synaptic arrangements that do not fall into driver or modulator categories (Mathers, 1971; Partlow et al., 1977; Crain and Hall, 1980; Ling et al., 1997; Kelly et al., 2003; Chomsung et al., 2008). Furthermore, we previously found that the membrane properties and responses to stimulation of cortical fibers recorded within the caudal LPN of the rat are distinct from those recorded in the rostral LPN (Li et al., 2003b; Li et al., 2003c).

The unique response properties we recorded in the caudal LPN were likely located in the tectorecipient zone of the LPN (Mason and Groos, 1981; Mooney et al., 1984; Takahashi, 1985; Hilbig et al., 2000). However, it is difficult to accurately relate

our physiological findings to LPN input zones because precise histological markers for LPN subdivisions are lacking. In addition, the synaptic organization of tecto-LP terminals and their relation to cortico-LP terminals has not previously been examined. Therefore, in preparation for further *in vitro* studies of the rat LPN, we have characterized the tectorecipient zone of the rat LPN using histochemical markers, tract tracing and electron microscopy.

## **Methods**

A total of 19 hooded rats were used for these experiments. Five rats received injections of Fluorogold (FG, Fluorochrome LLC, Denver, CO) in the LPN to label corticothalamic and tectothalamic cells by retrograde transport. Four rats received injections of biotinylated dextran amine (BDA, 3,000 MW; Molecular Probes, Eugene, OR) in the visual cortex to label corticothalamic terminals by anterograde transport. Three rats received injections of phaseolus vulgaris leucoagglutinin (PHAL, Vector Laboratories, Burlingame, CA) in the SC to label tectothalamic terminals by anterograde transport. Brains from an additional 4 rats were used for the immunocytochemical localization of the type 1 and type 2 vesicular glutamate transporters (vGLUT1 and vGLUT2). Finally, 3 rats received injections of ibotenic acid (MP Biomedicals, Aurora, OH) in the SC to determine whether vGLUT1 or vGLUT2 staining of the LPN was diminished after the destruction of tectothalamic cells. All procedures conformed to the National Institutes of Health guidelines for the care and use of laboratory animals and were approved by the University of Louisville Animal Care and Use Committee.

### ***Tract tracing***

The rats were anesthetized with intraperitoneal injections of sodium pentobarbital (initially 50mg/kg, with supplements injected as needed to maintain anesthesia) or intramuscular injections of ketamine and xylazine (initially 100 mg/kg and 6.7 mg/kg respectively, with supplements to maintain anesthesia). They were placed in a stereotaxic apparatus and prepared for aseptic surgery. BDA (5% in saline) PHAL (2.5% in water), or FG (10% in saline) were injected through a glass micropipette (20-30  $\mu\text{m}$  tip diameter) using 5  $\mu\text{A}$  of continuous positive current for 10-20 minutes. 2  $\mu\text{L}$  of ibotenic acid (2% in saline) was ejected from a glass micropipette (10-20  $\mu\text{m}$  tip diameter) using a PV830 pneumatic PicoPump (WPI, Sarasota, FL). After a survival time of one week, the rats were perfused transcardially with artificial cerebrospinal fluid (ACSF) or Tyrode solution followed by a fixative solution of 4 % paraformaldehyde, or 2.5-3% paraformaldehyde and 1-1.5% glutaraldehyde in 0.1 M phosphate buffer pH 7.4 (PB).

The brain was removed from the skull, and the thalamus was sectioned to a thickness of 50  $\mu\text{m}$  using a vibratome and placed in PB. The transported FG was revealed by incubating sections overnight at 4°C in the goat anti-FG antibody diluted 1:10,000. The next day the sections were incubated one hour in a biotinylated rabbit anti-goat antibody (Vector) diluted 1:100, followed by 2 hours in a solution containing a complex of avidin and biotinylated horseradish peroxidase (ABC). The transported PHAL was revealed by incubating sections overnight at 4°C in the biotinylated goat anti-PHAL antibody diluted 1:200, followed by 2 hours in ABC. The transported BDA was revealed by incubating sections overnight at 4°C in ABC solution. Sections containing FG, PHAL or BDA were subsequently reacted with nickel intensified diaminobenzidine (DAB) for five to 10 minutes, and washed in PB. Sections were then mounted on slides

for light microscopic examination, or prepared for electron microscopy. Light level photographs were taken using a digitizing camera (Spot RT, Diagnostic Instruments Incorporated, Sterling Heights, MI), and terminal distributions were plotted using a Neurolucida system.

### ***Antibody characterization***

The antibodies used in this study are listed in Table 1. Preabsorption of the type 1 and type 2 vesicular glutamate transporter (vGLUT1 and vGLUT2) antiserums with their corresponding immunogen peptides (Chemicon catalogue #AG208 and AG209; 1  $\mu$ g/ml immunogen peptide added to the diluted antibody) eliminated all terminal staining in tissue sections containing the thalamus and cortex (mouse, rat, tree shrew and cat tissue perfusion fixed with 4 % paraformaldehyde, or 2% paraformaldehyde and 2% glutaraldehyde for previous studies). Western blot of rat cerebral cortex tissue with the vGLUT1 antibody reveals a single band at approximately 60kDa (Melone et al., 2005). Using the vGLUT1 antibody, the thalamic staining pattern we obtained was similar to that obtained in rat by Kaneko and Fujiyama (2002). Western blot of cultured astrocytes from rat visual cortex with the vGLTU2 antibody reveals a single band at approximately 62kDa (Montana et al., 2004). The vGLUT2 antibody stains terminals in the tectorecipient zones of the tree shrew pulvinar nucleus (Chomsung et al., 2008). As described in the results section, the vGLUT2 antibody revealed a similar pattern in rat tissue.

The gamma amino butyric acid (GABA) antibody shows positive binding with GABA and GABA-keyhole limpet hemocyanin, but not BSA, in dot blot assays (manufacturer's product information). In rat tissue, the GABA antibody stains most

neurons in the thalamic reticular nucleus and a subset of neurons in the dorsal thalamus. This labeling pattern is consistent with other GABAergic markers used in a variety of species (Houser et al., 1980; Oertel et al., 1983; Fitzpatrick et al., 1984; Montero and Singer, 1984, 1985; de Biasi et al., 1986; Rinvik et al., 1987).

All Fluoro-Gold antibody binding was confined to cells that contained Fluoro-Gold (as determined by their fluorescence under ultraviolet illumination). Staining with the PHAL antibody was restricted to injection sites in the SC, and axons and terminals in the pretectum and LPN.

#### ***Vesicular glutamate transporter immunohistochemistry***

Sections through the caudal LPN were stained with antibodies vGLUT1 or vGLUT2. 4 rats were perfused transcardially with ACSF followed by a fixative solution of 4% paraformaldehyde, or 2% paraformaldehyde and 2% glutaraldehyde in PB. The brains were removed and 50 $\mu$ m thick parasagittal sections were cut on a vibratome and collected in PB. The sections were incubated overnight in a 1:10,000 dilution of either the guinea pig anti-vGLUT1 or guinea pig anti-vGLUT2 antibodies. The following day the sections were incubated in a 1:100 dilution of a biotinylated goat-anti guinea pig antibody (Vector) for 1 hour, followed by incubation in ABC (Vector) for 1 hour, and a reaction with nickel enhanced DAB.

#### ***Electron microscopy***

Sections were postfixed in 2% osmium tetroxide in PB for 1 hour and then dehydrated through a graded series of ethyl alcohol (70%-100%) and embedded in Durcupan resin (Ted Pella, Redding, CA) between sheets of Aclar plastic (Ladd Industries Inc., Burlington, VT). A light microscope was used to identify areas of interest



which were excised and mounted on resin blocks. A diamond knife was used to cut ultrathin sections which were placed on Formvar-coated nickel slot grids. Selected sections that contained tracer labeled terminals were additionally stained for GABA using previously described postembedding immunocytochemical techniques (Li et al., 2003c). Briefly, we used a rabbit polyclonal antibody against GABA at a dilution of 1:500-1:2000, and a goat-anti-rabbit IgG conjugated to 15 nm gold particles at a dilution of 1:25 (Amersham, Arlington Heights, IL) to reveal the distribution of GABA. All sections were air dried and stained with a 10% solution of uranyl acetate in methanol for 30 minutes before examination with an electron microscope. Labeled terminals involved in synaptic contacts were photographed, or digitally captured, and the size of the pre- and postsynaptic profiles were measured (SigmaScan software; SPSS Inc., Chicago, IL). Profiles were considered GABA-positive if the density of gold particles overlying them exceeded that found in 95% of small profiles with round vesicles. Profile measurements are expressed as means  $\pm$  SD. Statistical significance was tested using an unpaired T-test.

### ***Computer Generated Figures***

Light level photographs were taken using a digitizing camera (Spot RT; Diagnostic Instruments Inc., Sterling Heights, MI). Electron microscopic images were taken using a digitizing camera (SIA-7C; SIA, Duluth, GA) or negatives, which were subsequently scanned and digitized (SprintScan 45i; Polaroid, Waltham, MA). A Neurolucida system (MicroBrightField, Inc., Williston, VT) was used to plot the distribution of labeled cells and terminals, and the figures were composed using Photoshop software (Adobe Systems Inc, San Jose, CA). Photoshop software was also

used to adjust the brightness and contrast to optimize the images, and in some cases the images were inverted (Figure 2) or sharpened (Figure 13).

## **Results**

### ***Distribution and morphology of tectal and cortical inputs to the LPN***

As illustrated in Figures 1 and 2, FG injections in the caudal LPN labeled a dense band of cells in the lower stratum griseum superficiale (SGS) and stratum opticum (SO) of the SC, and a dense cluster of cells in the caudal, lateral cortex, a region corresponding to V2 (Paxinos and Watson, 2007). The majority of cortical cells were distributed in layer VI, but a sparser band of labeled cells was also present in layer V. The labeled cortico-LPN cells, and the vast majority of labeled tecto-LPN cells, were distributed ipsilateral to the injections. As illustrated in Figure 3, PHAL injections into the SGS and SO of the superior colliculus labeled terminals in the caudal/lateral regions of the LPN, as well as the pretectum (PT).

As illustrated in Figures 4 and 5, injections of BDA into the lateral cortex (which contained the densest distribution of labeled cells following caudal LPN FG injections) labeled terminals in the LPN, laterodorsal nucleus (LDN), pretectum (PT) and SC. BDA injections into the lateral cortex also labeled cells in the LPN and LDN (by retrograde transport), but for clarity, they are not illustrated. Figure 6 illustrates that injections of BDA in more medial regions of the cortex labeled many terminals in the LDN, LPN, PT, SC, dLGN and vLGN, but very few terminals in the caudal tectorecipient zone of the LPN. This suggests that the caudal LPN FG injections labeled cells in the more medial regions of the cortex via uptake by fibers of passage.

Figure 7 illustrates the morphology of tecto-LPN and cortico-LPN terminals. Terminals labeled by the anterograde transport of BDA injected into the cortex exhibited two morphologies. The most common type of corticothalamic axon (type I, illustrated in Figure 7A) was thin and gave rise to sparsely distributed small boutons. Occasional en passant boutons were observed, but the most common arrangement was a single bouton at the end of a short axon side branch (“drumstick” ending). More rarely, type II axons (illustrated in Figure 7B) were observed. These were thicker axons that gave rise to large boutons in discrete clusters. As illustrated in Figure 4, type I corticothalamic terminals were distributed throughout the LPN, but type II terminals (Figure 5) were primarily confined to the rostral LPN.

The morphology of terminals labeled by the anterograde transport of PHAL injected into the SC was different than that of either type I or type II cortical terminals. Tecto-LPN boutons were of medium size and often form distinct tubular clusters (illustrated in Figure 7C). Comparison of the distribution of tecto-LPN terminals (Figure 3) to that of cortico-LPN terminals, reveals that the tectal terminal field partially overlaps the distribution of type I terminals (Figure 4), but has virtually no overlap with type II cortical terminals (Figure 5).

#### ***Synaptic organization of tecto-LPN terminals***

To characterize the synaptic organization of tracer-labeled tecto-LPN terminals, we analyzed electron micrographs of 100 PHAL-labeled terminals involved in synapses by measuring the size of the stained terminals and their postsynaptic partners. The PHAL-labeled terminals were of medium size ( $0.71 \pm 0.32 \mu\text{m}^2$ ), in other words larger than our previous measurements of type I cortical terminals in the LPN ( $0.34 \pm 0.11 \mu\text{m}^2$ ;

Li et al., 2003b), but smaller than our previous measurements of type II cortical terminals in the LPN ( $2.72 \pm 1.27 \mu\text{m}^2$ ; Li et al., 2003b). Thus the previous nomenclature of RM (for medium sized terminals that contain round vesicles; Robson and Hall, 1977) is an appropriate classification of rat tecto-LPN terminals.

As illustrated in Figure 8, PHAL-labeled tecto-LPN terminals contacted relatively large caliber dendrites (minimum diameter  $0.98 \mu\text{m} \pm 0.30 \mu\text{m}$ ;  $n=100$ ). Frequently, several labeled terminals were observed surrounding one dendrite. Using GABA postembedding immunocytochemical techniques, we additionally analyzed the gold particle density overlying 98 tracer labeled terminals and their postsynaptic targets. We found 91% (89/98) of the terminals contacted GABA-negative dendritic shafts (Figure 8 A-E), and 9% (9/98) of the terminals contacted GABA-positive dendrites that contained vesicles (F2 profiles; Figure 8A). In addition, all 98 PHAL-labeled terminals were found to be GABA-negative.

#### ***Synaptic organization of corticothalamic terminals in the tecto-recipient LPN***

To characterize the synaptic organization of tracer-labeled cortico-LPN terminals, we analyzed electron micrographs of BDA-labeled terminals in the tectorecipient zone of the LPN. We photographed 100 labeled terminals involved in synapses by measuring the size of the stained terminals and their postsynaptic partners. The BDA-labeled terminals were of small size ( $0.27 \pm 0.12 \mu\text{m}^2$ ), similar to our previous measurements of type I cortical terminals throughout the LPN ( $0.34 \pm 0.11 \mu\text{m}^2$ ; Li et al., 2003b). Thus, all cortical terminals in the tectorecipient LPN can be classified as RS profiles (small terminals that contain round vesicles).

As illustrated in Figure 9, BDA-labeled cortico-LPN terminals contacted relatively small caliber dendrites (minimum diameter  $0.65 \mu\text{m} \pm 0.18 \mu\text{m}$ ;  $n=100$ ). Multiple labeled terminals were not observed to contact single dendrites. However, multiple unlabeled RS profiles frequently contacted dendrites that were postsynaptic to labeled cortico-LPN terminals (Figure 9 A-C). Using GABA postembedding immunocytochemical techniques, we additionally analyzed the gold particle density overlying 100 tracer labeled terminals and their postsynaptic targets. We found 98% (98/100) of the terminals contacted GABA-negative dendritic shafts (Figure 9 A-E), and 2% (2/100) contacted GABA-positive dendrites. In addition, all 100 BDA-labeled terminals were found to be GABA-negative.

#### ***Distribution of vGLUT1 and vGLUT2 in the LPN***

Figure 10 illustrates the thalamic staining patterns obtained with antibodies against vGLUT1 or vGLUT2. Terminals stained with the vGLUT1 antibody were densely distributed throughout the entire thalamus, but terminals stained with the vGLUT2 antibody were most densely distributed in the caudal and lateral LPN, overlapping the distribution of tecto-LPN terminals (Figure 3). To determine whether vGLUT2 can be considered a marker for tectal terminals, we injected ibotenic acid into the SC to destroy tecto-LPN cells and then stained the LPN for vGLUT2. As illustrated in Figure 11, vGLUT2 staining was still present in the tectorecipient zone of the contralateral LPN, but was greatly diminished in the ipsilateral LPN. In contrast, vGLUT1 staining was unchanged. This suggests that tecto-LPN terminals contain vGLUT2, but not vGLUT1.

### ***Synaptic organization of vGLUT1- and vGLUT2-stained terminals***

To compare the synaptic contacts made by tectal and cortical terminals in the caudal/lateral LPN to those made by vGLUT1 and vGLUT2 stained terminals, we examined tissue stained for vGLUT1 or vGLUT2 using an electron microscope. Examples are illustrated in Figures 12 and 13. We photographed 200 stained terminals involved in synapses (100 stained for vGLUT1 and 100 stained for vGLUT2) and measured the size of the stained terminals and their postsynaptic partners. As illustrated in Figure 14, vGLUT1-stained terminals were smaller ( $0.33 \pm 0.17\mu\text{m}^2$ ) than vGLUT2-stained terminals ( $0.63 \pm 0.29\mu\text{m}^2$ ), and this difference was significant ( $P < 0.001$ ). In addition, the average minimum diameter of dendrites postsynaptic to vGLUT1 terminals ( $0.62 \mu\text{m} \pm 0.14 \mu\text{m}$ ) was smaller than the average minimum diameter of dendrites postsynaptic to vGLUT2 terminals ( $0.89 \mu\text{m} \pm 0.25 \mu\text{m}$ ), and this difference was significant ( $P < 0.001$ ).

There was no significant difference between the size of the tecto-LPN terminals labeled by anterograde transport and the size of the vGLUT2-stained terminals ( $P > 0.05$ ), nor was there a significant difference between the sizes of the dendrites they contacted ( $P > 0.05$ ). However, there was a slight difference between the size of cortico-LPN terminals labeled by anterograde transport and the size of vGLUT1-stained terminals ( $P = 0.04$ ), although there was no significant difference between the size of the dendrites they contacted ( $P > 0.05$ ).

## **Discussion**

### ***The tectorecipient LPN: “second order” nucleus***

Our results indicate that tectal terminals innervate the caudal and lateral LPN, as previously described (Mason and Groos, 1981; Takahashi, 1985), where they form clusters that surround and contact relatively large caliber, nonGABAergic, projection cell dendrites. These observations correlate well with previous anatomical studies of tectothalamic terminals in a variety of other species. Robson and Hall (1977) first described tectothalamic terminals in the grey squirrel pulvinar nucleus as RM profiles, and illustrated the manner in which they encircle relatively large caliber dendrites. Similar patterns have also been observed in the squirrel monkey (Mathers, 1971), Rhesus monkey (Partlow et al., 1977), hamster (Crain and Hall, 1980; Ling et al., 1997), cat (Kelly et al., 2003), and tree shrew (Chomsung et al., 2008).

Our results also indicate that in the caudal/lateral LPN, cortical terminals are small profiles that contact relatively small caliber projection cell dendrites. The size and synaptic location of these terminals suggests that the majority of cortical input to the tectorecipient zones of the LPN arises from layer VI (Bourassa and Deschenes, 1995). In fact, most cells labeled by the retrograde transport of FG injected into the caudal LPN were located in layer VI. However, caudal LPN injections additionally labeled cells in layer V. It seems most likely that, in addition to cortico-LPN cells, our injections labeled corticotectal cells; the axons of corticotectal cells pass through the brachium of the superior colliculus, which was included in most of our injection sites (Figure 2A). The fact that our caudal LPN FG injections labeled cells in both layers V and VI of medial cortical regions that do not project to the tectorecipient LPN (Figure 6) also indicates that

FG was taken up by fibers of passage. Alternatively, layer V cells do innervate the caudal LPN, but their axons do not display the type II morphology typically associated with layer V corticothalamic cells (Bourassa and Deschenes, 1995). In either case, we can conclude that cortical terminals are located distal to tectal terminals in the caudal LPN. Similar results have been described in the tectorecipient thalamus of the squirrel monkey (Mathers, 1972), grey squirrel (Robson and Hall, 1977), cat (Li et al., 2000) and tree shrew (Chomsung et al., 2007). Together, these results indicate that the organization of thalamic nuclei innervated by the retinorecipient layers of the SC is different from that observed in either first order or higher order nuclei (summarized in Figure 13).

The organization of the tectorecipient LPN, which we will refer to as a “second order” nucleus, is unique not only because tectal terminals form distinctive tubular clusters, but also because the SC is innervated by the same cortical areas that are targeted by the LPN. Although the precise nature of the signals transmitted by tectothalamic cells is still unclear, their location within the SC suggests that their response properties are created by converging retinal and visual cortical inputs. Thus, caudal LPN activity is influenced directly by layer VI corticothalamic projections, and may be indirectly influenced by layer V corticotectal projections as well. This organization is clearly different from the dLGN, which is innervated directly by retinal ganglion cells, or the rostral LPN which receives little ascending input and is innervated directly by cortical layer V (Bourassa and Deschenes, 1995). It is also clear that tectal inputs do not drive the response properties of LPN cells in a manner similar to retinal inputs to the dLGN. While the response properties of geniculocortical cells are almost identical to the retinal cells that innervate them (Cleland et al., 1971), the receptive fields of tectorecipient LPN cells



are much larger than those recorded in the superficial layers of the SC (Chalupa et al., 1983).

***vGLUT1 and vGLUT2: markers for corticothalamic and tectothalamic terminals***

We found that terminals stained with a vGLUT2 antibody are concentrated in the caudal/lateral LPN, where we found tectothalamic terminals labeled by anterograde transport. Furthermore, lesions of the SC diminished vGLUT2 staining (but not vGLUT1 staining), in the caudal/lateral LPN. Finally, we found no significant difference between the sizes of vGLUT2 stained terminals and tecto-LPN terminals labeled with PHAL, or between the sizes of their postsynaptic dendrites. Together, these results strongly suggest that vGLUT2 is contained within tectothalamic terminals. Tectothalamic terminals in the tree shrew also appear to contain vGLUT2 (Chomsung et al., 2008).

Previous studies have suggested that vGLUT1 can be used as a marker for corticothalamic terminals because vGLUT1 mRNA is found only in the cortex, while vGLUT2 mRNA is found only in subcortical cells (Fremeau et al., 2001; Herzog et al., 2001; Kaneko and Fujiyama, 2002). In addition, vGLUT1 stained terminals are very densely distributed throughout the thalamus, which correlates well with the fact that the majority of terminals in the thalamus are of cortical origin (Erisir et al., 1997). Finally, although we found a slight difference between the sizes of vGLUT1 stained terminals and cortico-LPN terminals labeled with BDA, the majority of the vGLUT1 stained terminals and BDA stained terminals were similar in size. Together, these results suggest that vGLUT1 is contained within corticothalamic terminals, but might also be expressed in a small population of terminals of subcortical origin.

### ***Functional considerations***

Robson and Hall (1977) suggested that the clustered arrangements of synaptic terminals in the tectorecipient zone of the grey squirrel pulvinar nucleus allow axons from different areas to converge on single dendrites. This was based on the fact that few terminals in any one cluster degenerated following large lesions of the SC. Similarly, we found that only one or two terminals contacting any one dendrite were labeled by anterograde transport following relatively large injections of PHAL in the SC. In contrast, in material labeled with the vGLUT2 antibody, dendrites were often surrounded by multiple labeled terminals. This suggests that terminals from many tectal axons converge on single dendrites.

This organization is similar to that observed in the pulvinar nucleus of the tree shrew, where we also observed that multiple tectal terminals converge on single dendrites (Chomsung et al., 2008). In the tree shrew, two tectorecipient zones have been identified in the dorsal (Pd) and central (Pc) subdivisions of the pulvinar nucleus (Luppino et al., 1988; Lyon et al., 2003). We concluded that both the Pd and Pc receive topographic (specific) projections from the SC, and the Pd receives additional nontopographic (diffuse) projections, possibly arising from convergent axon collaterals (Chomsung et al., 2008).

For this study, the goal of our FG injections was to label all of the inputs to the tectorecipient zone of the LPN. Therefore, we are unable to address the topography of rat tecto-LPN projections. However, a previous study in the hamster concluded that there is a large degree of convergence in the rodent tecto-LPN pathway (Mooney et al., 1984). Thus the available results suggests that individual LPN neurons can be innervated by

multiple tectal axons, and each tectal axon can make multiple synaptic connections with LPN cells via dense terminal clusters (Ling et al., 1997; current study Figure 7C).

Our comparison of BDA-labeled cortico-LPN terminals to vGLUT1-labeled terminals also indicates that multiple cortical axons converge to innervate single cells. This is further supported by our *in vitro* physiological studies. In the caudal LPN, the amplitude of corticothalamic EPSPs gradually increased with increased stimulation currents, suggesting the recruitment of multiple convergent axons (Li et al., 2003a). Together, our results indicate that cells in the tectorecipient LPN receive input from multiple tectal axons on their proximal dendrites, and input from multiple cortical axons on their distal dendrites. Thus, as opposed to the dLGN, where small receptive fields are preserved by restricted retinogeniculate innervation (Cleland et al., 1971), and enhanced by inhibitory circuitry (Hirsch, 2003), the tectorecipient LPN appears to be organized to expand receptive fields (although tectal contacts on interneurons may provide filtering). In the deep layers of the cat SC, the responses of output cells have been shown to be enhanced by converging visual, auditory and somatosensory signals (Rowland et al., 2007). However, this integration is blocked by cooling of the anterior ectosylvian sulcus (Alvarado et al., 2007), which forms a loop with the SC via connections in the suprageniculate nucleus (Norita and Katoh, 1986; McHaffie et al., 1988; Harting et al., 1992; Benedek et al., 1996). The connections of the tectorecipient LPN may perform a similar function. The relatively large receptive fields of the SC and tectorecipient zones of the thalamus may function to enhance activity related to novel or threatening objects moving across the visual field (Krout et al., 2001).

**Figure 1.**

Following an iontophoretic injection of fluorogold (indicated in black) in the lateral posterior nucleus (LPN), cells labeled by retrograde transport are primarily distributed in the visual cortex (layers V and VI) and the superior colliculus (SC). Each labeled cell is indicated by a black dot in the series of parasagittal sections arranged from lateral (A) to medial (F). Scale bar = 1 mm and applies to all sections. IC, inferior colliculus.

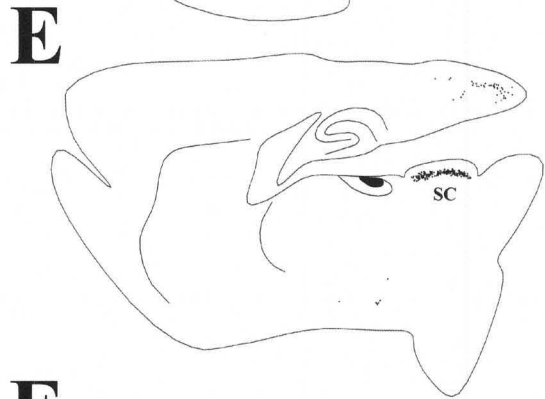
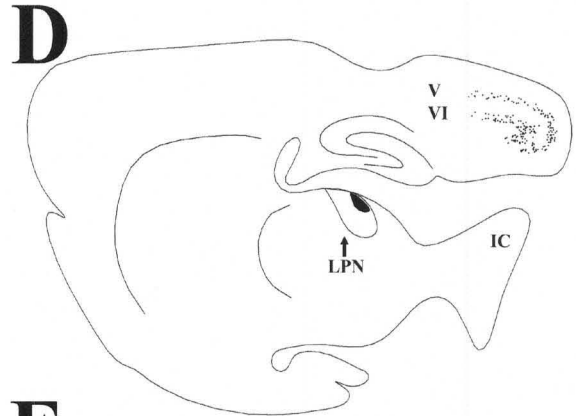
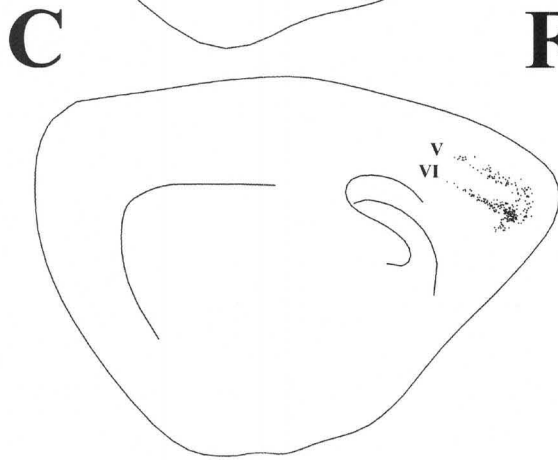
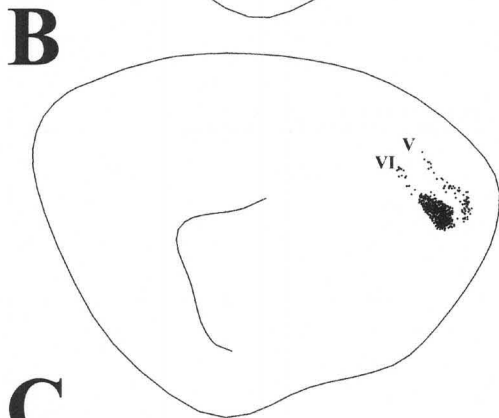
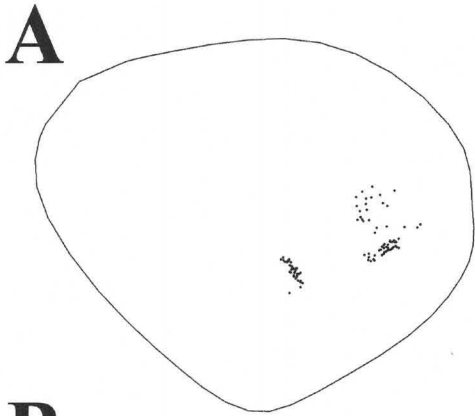


**Figure 2.**

Following an iontophoretic injection of fluorogold in the lateral posterior nucleus (LPN, panel A), cells labeled by retrograde transport in the superior colliculus (B, shown at higher magnification in panel D) are primarily distributed in the stratum opticum (SO) and lower stratum griseum superfiale (SGS). Cells labeled by retrograde transport in the visual cortex (C) are primarily distributed in layer VI (shown at higher magnification in panel E), but a smaller band of labeled cells is present in layer V. BSC, brachium of the superior colliculus, PT, pretectum, SGI, stratum griseum intermediale, STR, superior thalamic radiation. Scale bar in C = 300  $\mu\text{m}$  and applies to A and B. Scale bars in D and E = 50  $\mu\text{m}$ .

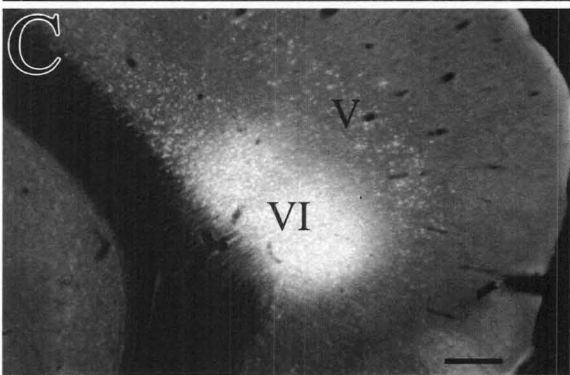
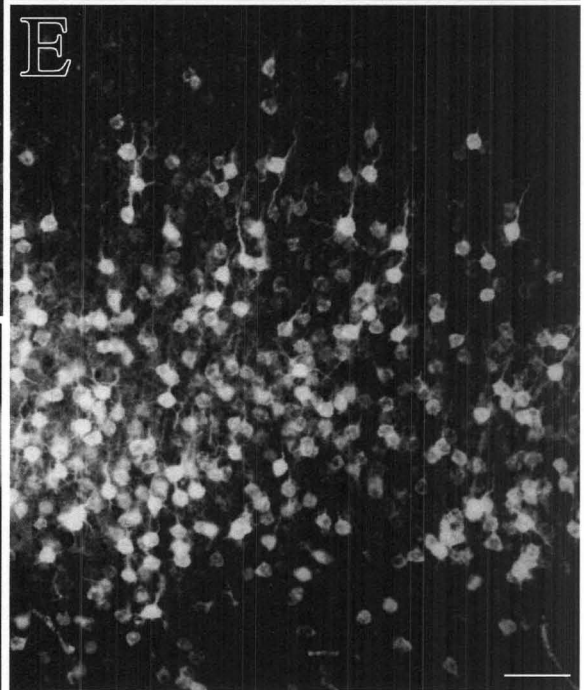
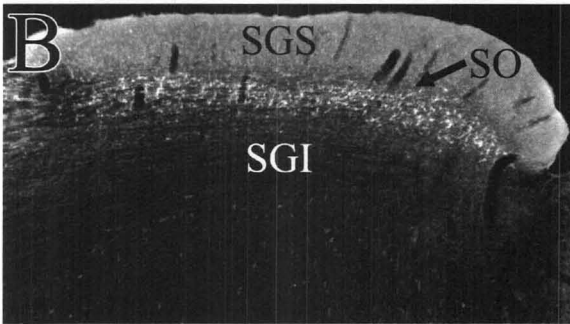
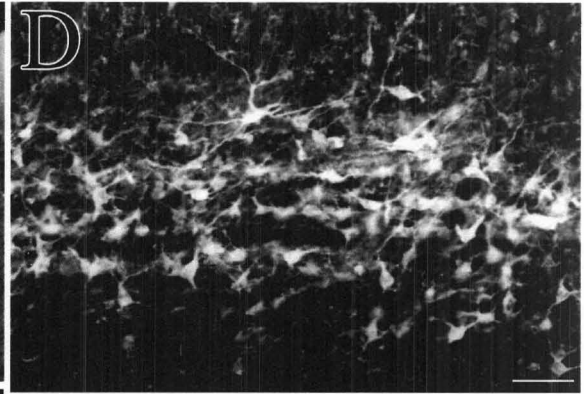
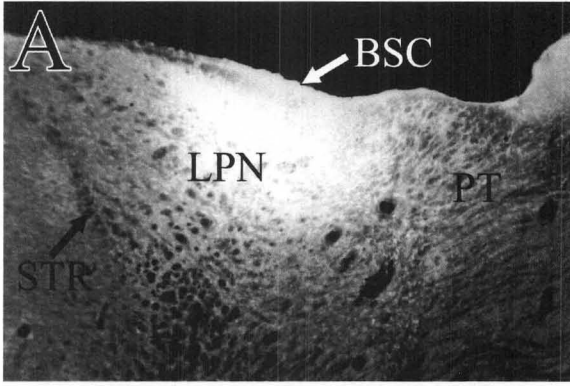


**Figure 3.**

Following an iontophoretic injection of phaseolus leucoagglutinin in the superior colliculus (SC, indicated in black), terminals labeled by anterograde transport are primarily distributed in pretectum (PT) and the caudal/lateral regions of the lateral posterior nucleus (LPN). The black dots indicate the relative distribution of labeled terminals in the series of parasagittal sections arranged from lateral (A) to medial (F). Scale bar = 1 mm and applies to all sections. IC, inferior colliculus.



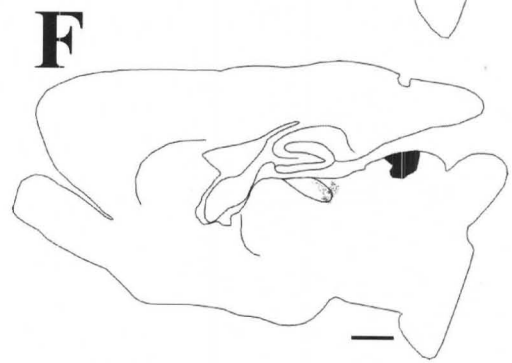
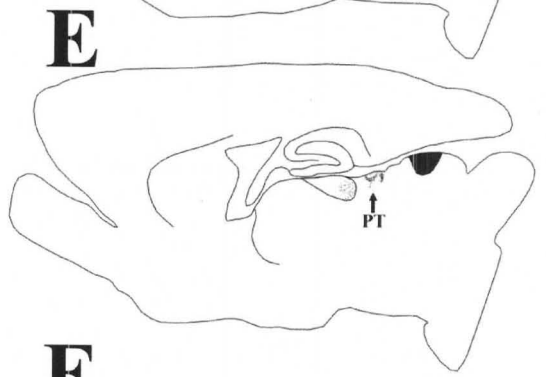
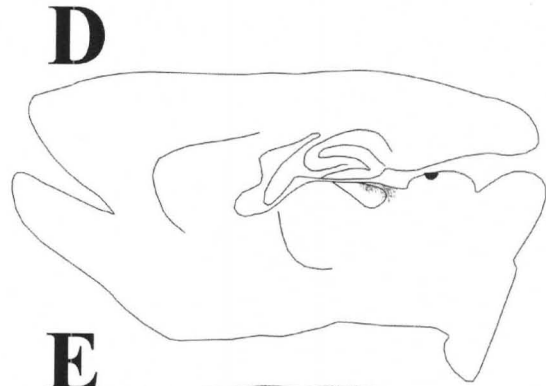
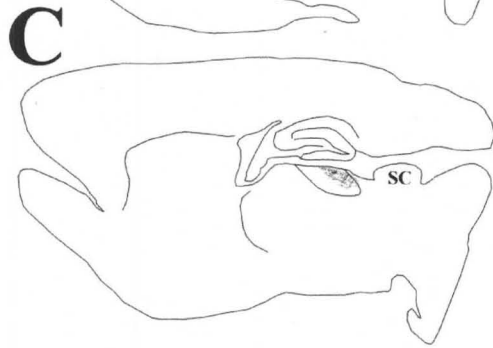
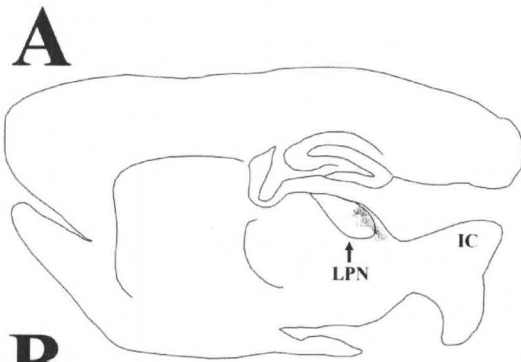


**Figure 4.**

Following an iontophoretic injection of biotinylated dextran amine in the lateral visual cortex, type I terminals labeled by anterograde transport are distributed throughout the lateral posterior nucleus (LPN), including the caudal tectorecipient zone. The black dots indicate the relative distribution of labeled type I terminals in the series of parasagittal sections arranged from lateral (A) to medial (F). Terminals are also labeled in the laterodorsal nucleus (LDN), pretectum (PT) and superior colliculus (SC). Scale bar = 1 mm and applies to all sections. IC, inferior colliculus.

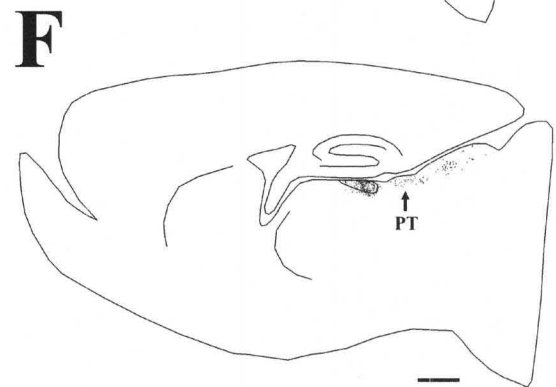
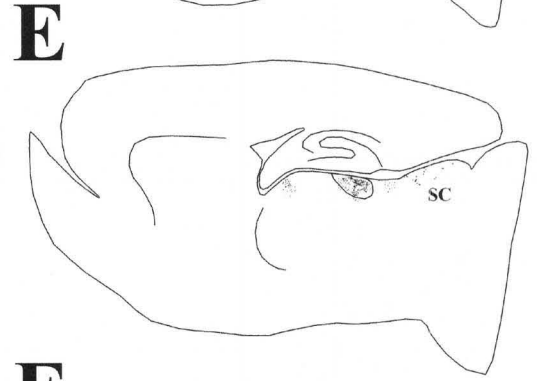
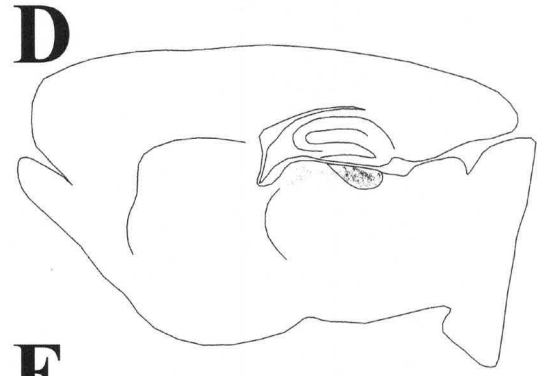
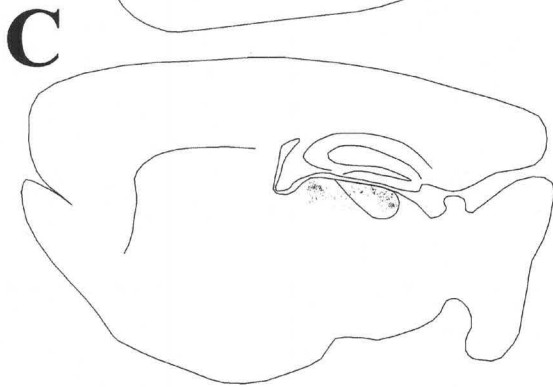
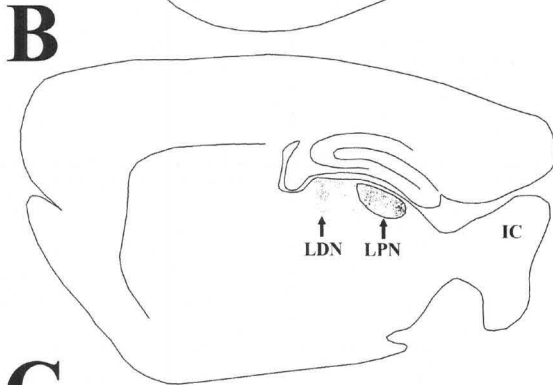
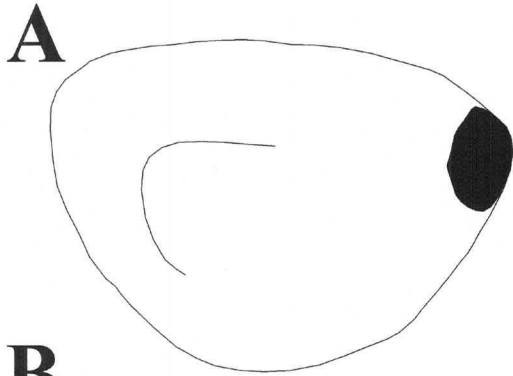


**Figure 5.**

Following an iontophoretic injection of biotinylated dextran amine in the lateral visual cortex (same injection as that illustrated in Figure 4), type II terminals labeled by anterograde transport are distributed primarily in the rostral lateral posterior nucleus (LPN) and laterodorsal nucleus (LDN). The black dots indicate the relative distribution of labeled type II terminals in the series of parasagittal sections arranged from lateral (A) to medial (F). Scale bar = 1 mm and applies to all sections. IC, inferior colliculus, PT, pretectum, SC, superior colliculus.

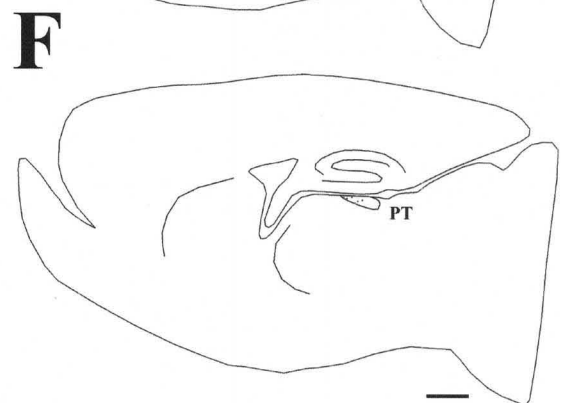
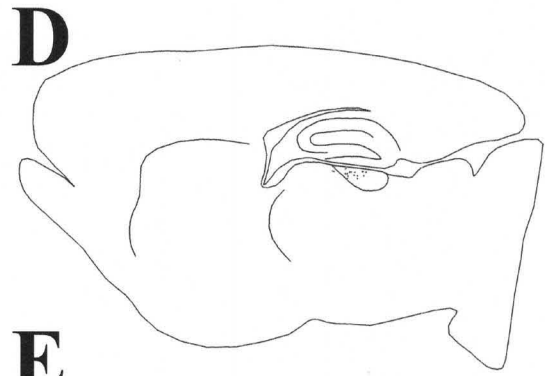
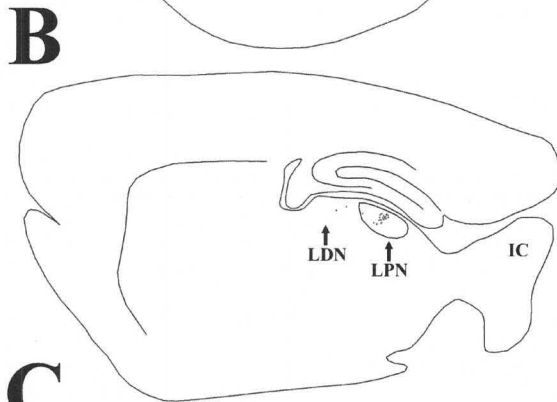
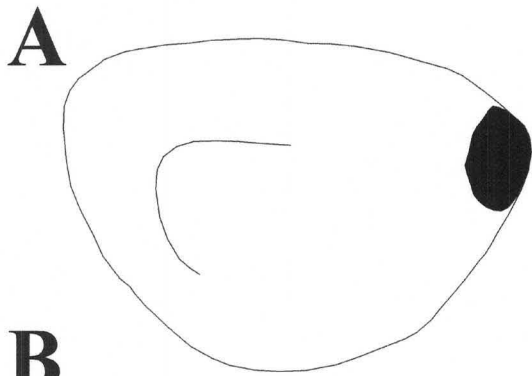


**Figure 6.**

Following a syringe injection of biotinylated dextran amine in the medial visual cortex, terminals labeled by anterograde transport are distributed in the rostral lateral posterior nucleus (LPN) and laterodorsal nucleus (LDN), but do not extend into the caudal, tectorecipient LPN. The black dots indicate the relative distribution of labeled terminals in the series of parasagittal sections arranged from lateral (A) to medial (D). Labeled terminals are also distributed in the dorsal and ventral lateral geniculate nucleus (dLGN, vLGN), as well as pretectum (PT), and superior colliculus (SC). Scale bar = 1 mm and applies to all sections. IC, inferior colliculus.

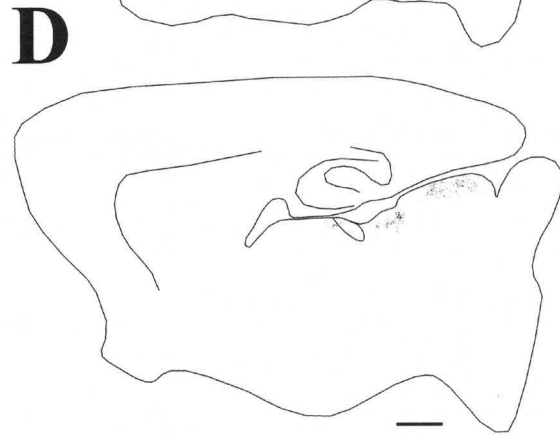
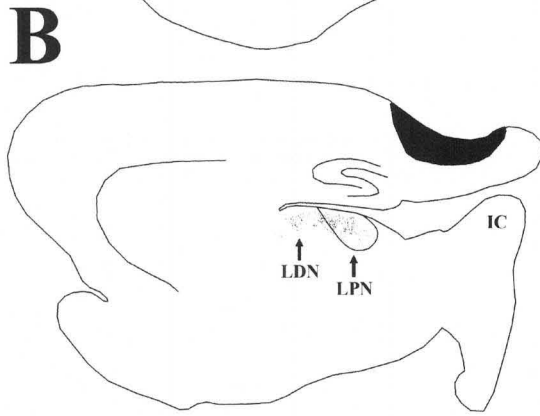
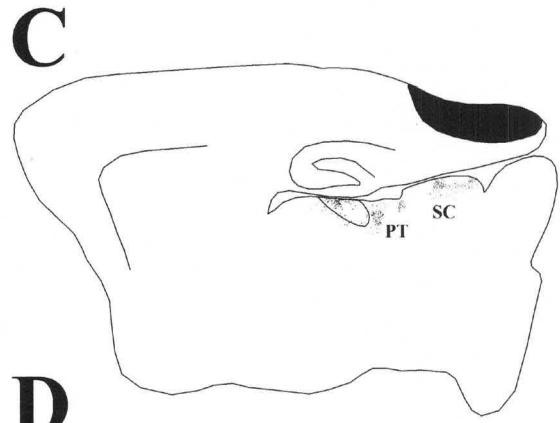
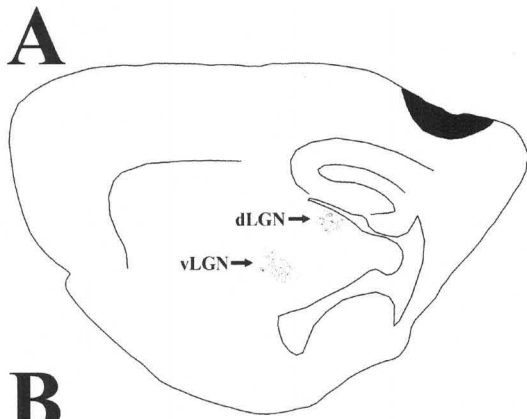


**Figure 7.**

Three terminal types were identified in the lateral posterior nucleus. Terminals labeled by the anterograde transport of biotinylated dextran amine injected into the cortex exhibited two morphologies. Type I terminals (A) are small boutons that are sparsely distributed along relatively thin axons. Type II terminals (B) are large boutons that emanate from thick axons and form discrete clusters. Terminals labeled by the anterograde transport of phaseolus leucoagglutinin injected into the superior colliculus (C) form tubular clusters of medium sized boutons. Scale bar = 20  $\mu\text{m}$  and applies to all panels.



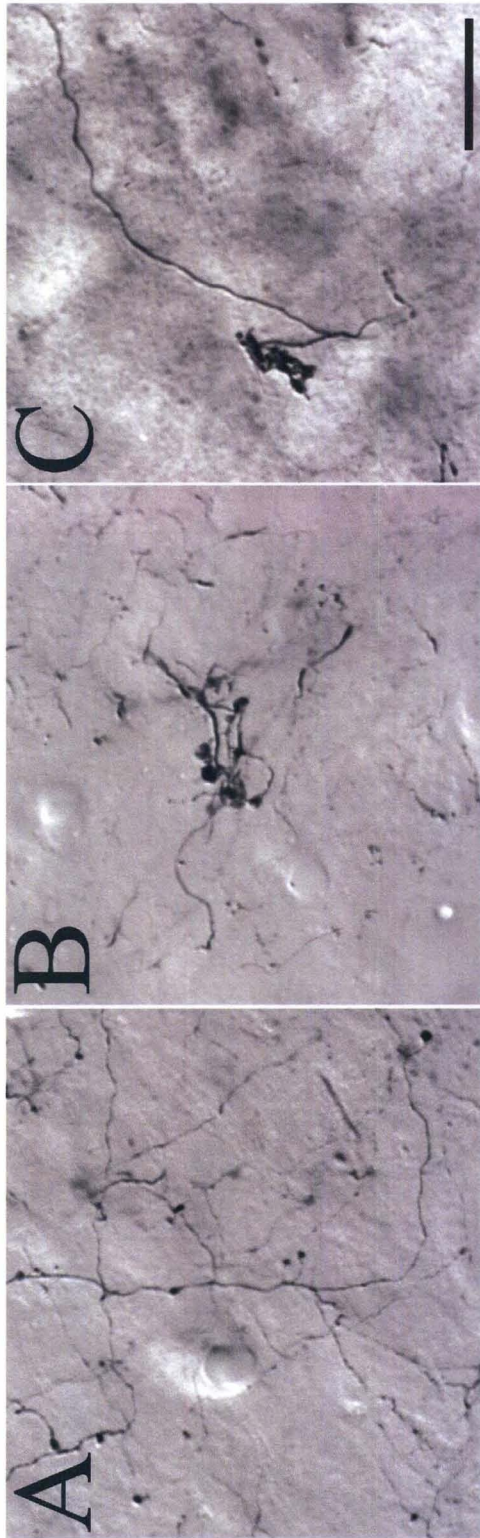


**Figure 8.**

Terminals in the caudal lateral posterior nucleus labeled by the anterograde transport of phaseolus leucoagglutinin injected into the superior colliculus are nonGABAergic (low density of gold particles) and primarily contact (white arrows) nonGABAergic dendrites of relatively large caliber (A-E). Occasional contacts on GABAergic profiles (+) were observed (panel A). Many dendrites received input from multiple labeled terminals (A, C-E). Scale bar = 1  $\mu\text{m}$  and applies to all panels.

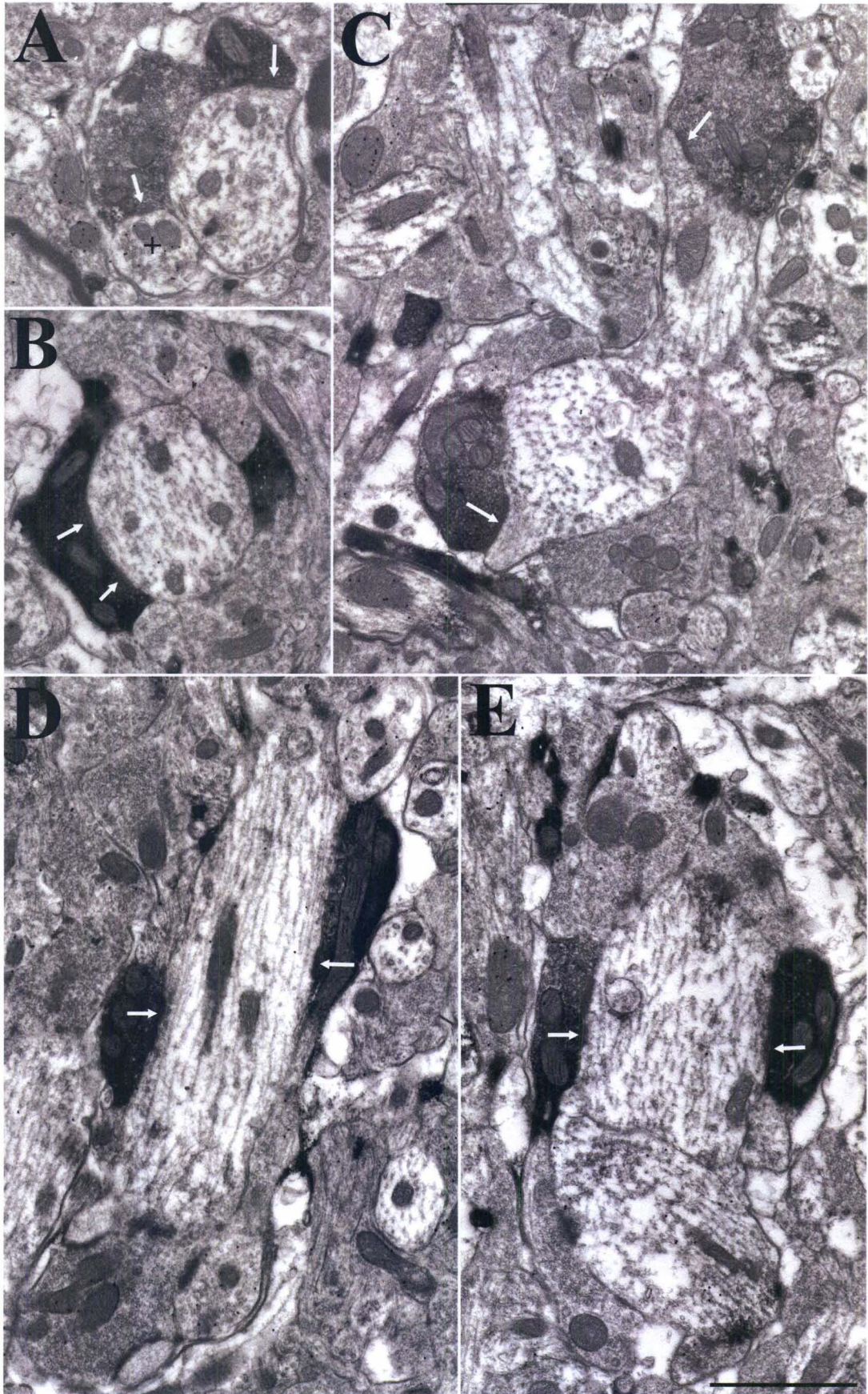


**Figure 9.**

Terminals in the caudal lateral posterior nucleus labeled by the anterograde transport of biotinylated dextran amine injected into the cortex are small and primarily contact (white arrows) nonGABAergic (low density of gold particles) dendrites of relatively small caliber (A-C). Scale bar = 0.5  $\mu\text{m}$  and applies to all panels.

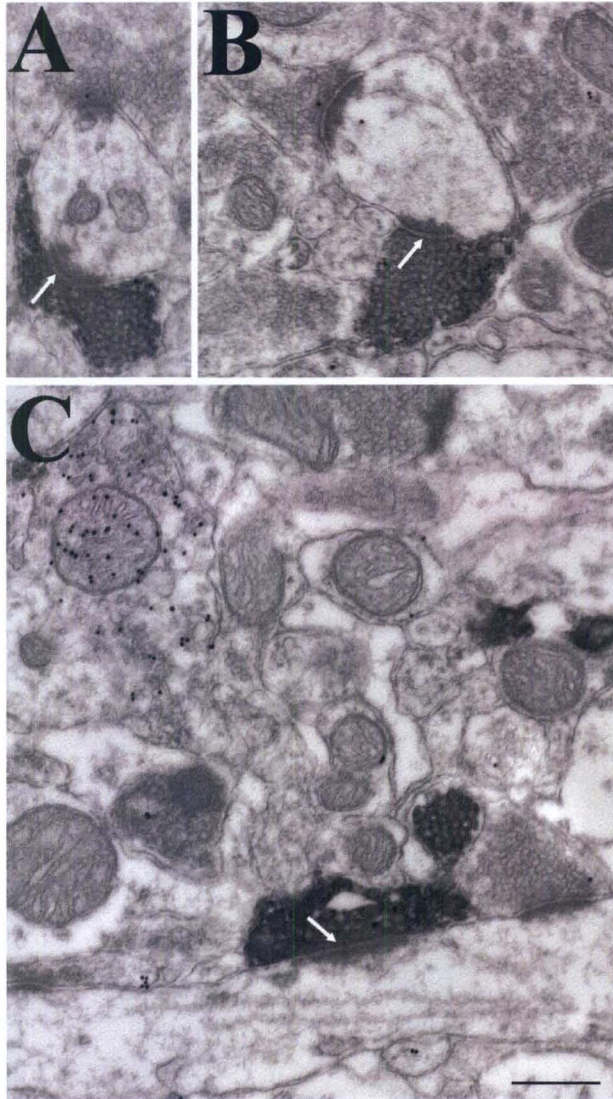


**Figure 10.**

The caudal part of the lateral posterior nucleus (LPN) stains densely for both the type 1 and type 2 vesicular glutamate transporters (vGLUT1 and vGLUT2). A) The boundaries of the LPN are illustrated in adjacent sections stained for vGLUT1 (white dots) and vGLUT2 (black dots). Scale bar = 1 mm. IC, inferior colliculus, SC superior colliculus. B) Within the LPN, vGLUT2-stained terminals are confined to the caudal LPN, defining the tectorecipient zone (small black dots). vGLUT2-stained terminals are also distributed in the nucleus of the optic tract (NOT). Scale bar = 500  $\mu\text{m}$  and also applies to C. C) Terminals stained for vGLUT1 are densely distributed throughout the LPN (large white dots), but are relatively sparsely distributed in the NOT and anterior pretectal nucleus (APN). Therefore vGLUT1 staining delineates the caudal border of the LPN. The location of the tectorecipient zone of the LPN is indicated with small white dots.

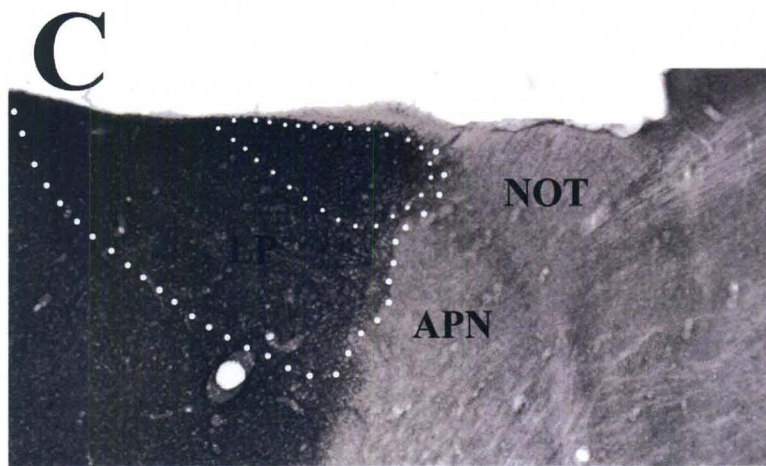
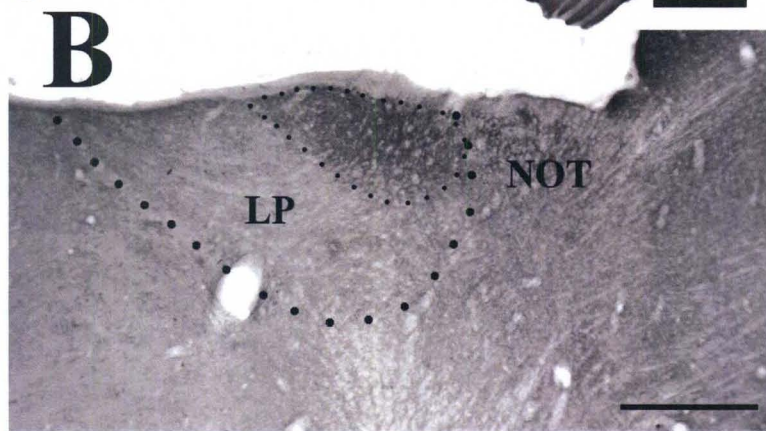


**Figure 11.**

Immunocytochemical staining for the type 2 vesicular glutamate transporter (vGLUT2) is decreased in the lateral posterior nucleus (LPN) following superior colliculus (SC) lesions. A) An ibotenic acid lesion of the SC is illustrated in a section stained with an antibody against NeuN. B) Contralateral to the SC lesion illustrated in A, vGLUT2 staining is present in the caudal LPN. C) Ipsilateral to the SC lesion illustrated in A, vGLUT2 staining is diminished. Scale bar = 500  $\mu$ m and applies to all panels.



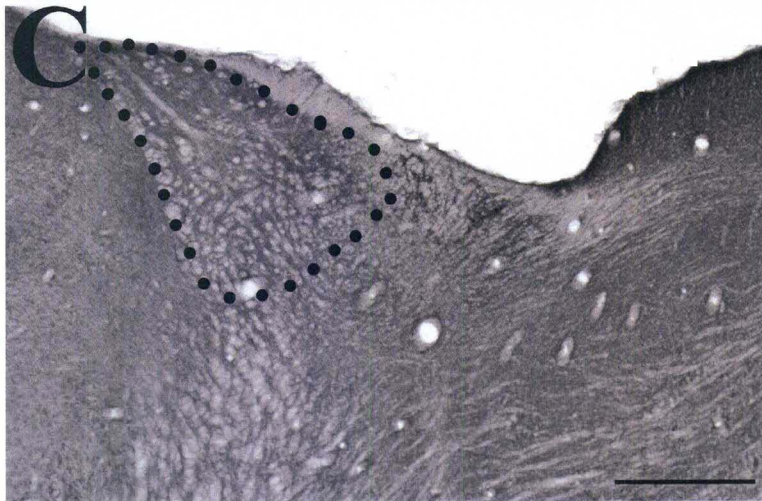
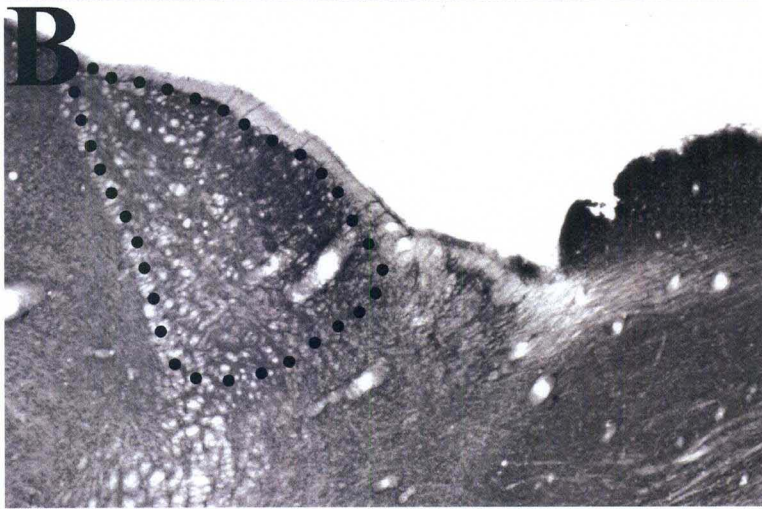
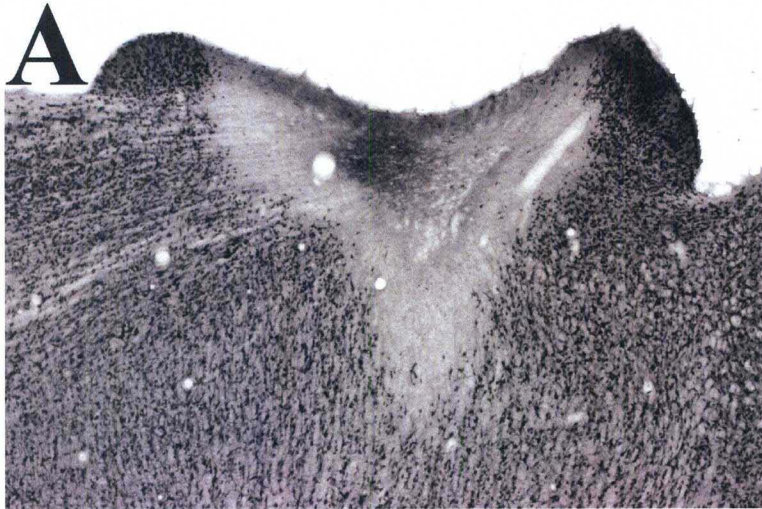


**Figure 12.**

Terminals in the caudal lateral posterior nucleus labeled with an antibody against the type 1 vesicular glutamate transporter are small and primarily contact (white arrows) nonGABAergic (low density of gold particles) dendrites of relatively small caliber (A-F). Many dendrites are surrounded by multiple labeled terminals (D-F), and labeled terminals form multiple contacts on single dendrites (E). Scale bar = 0.5  $\mu\text{m}$  and applies to all panels.

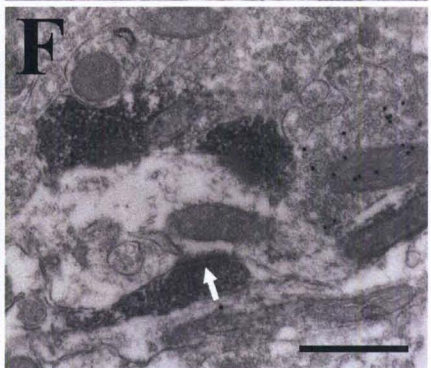
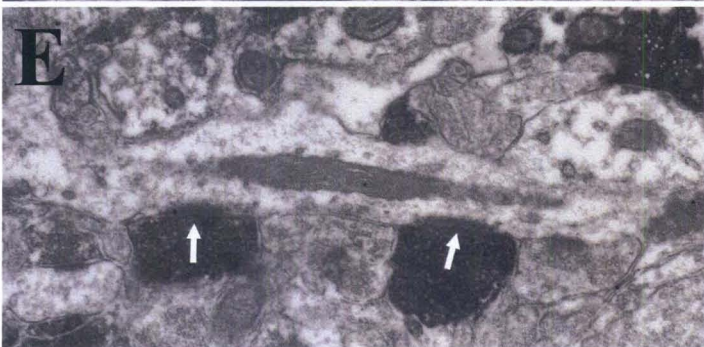
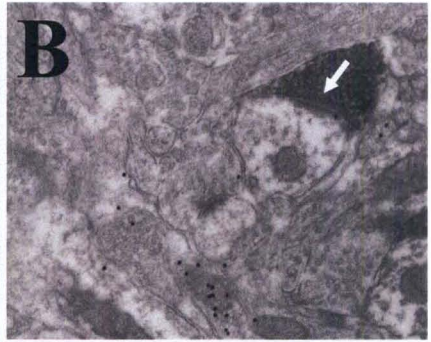
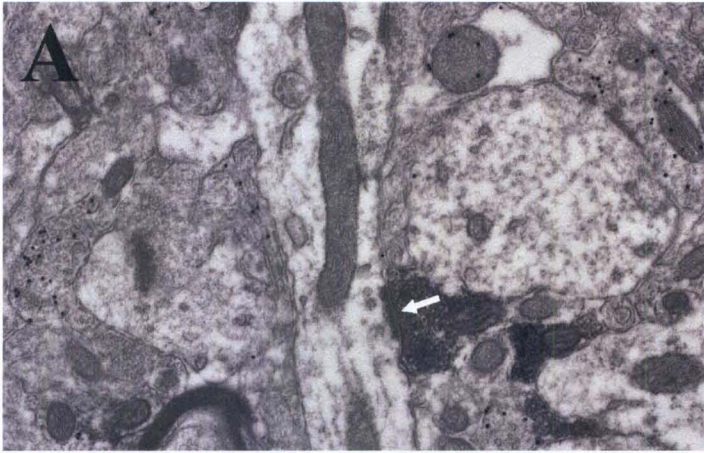


**Figure 13.**

Terminals in the caudal lateral posterior nucleus against the type 2 vesicular glutamate transporter surround and make multiple contacts (white arrows) with nonGABAergic dendrites (low density of gold particles) of relatively large caliber (A-C). Occasional contacts with GABAergic profiles (+) are observed (panel C). Scale = 1  $\mu$ m and applies to all panels.

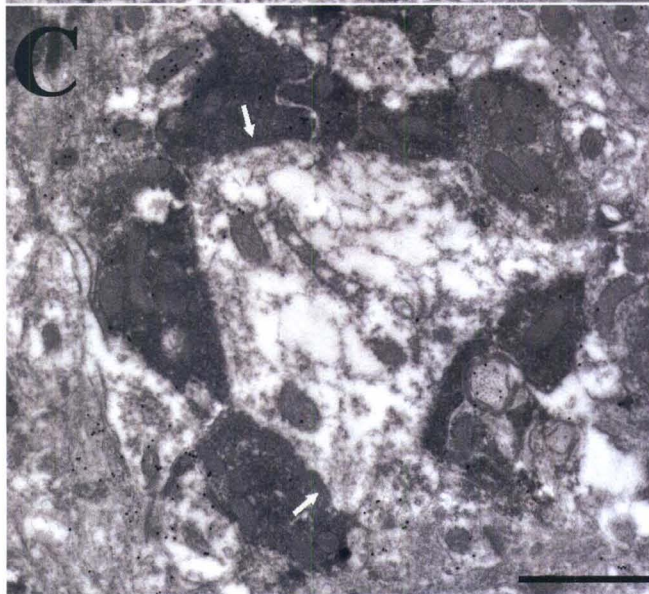
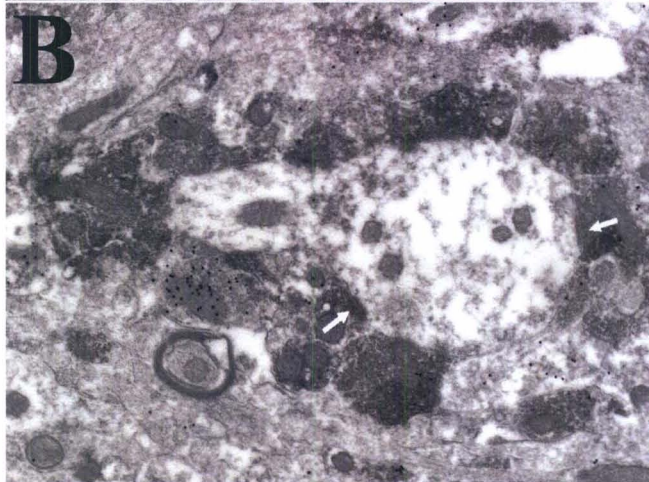
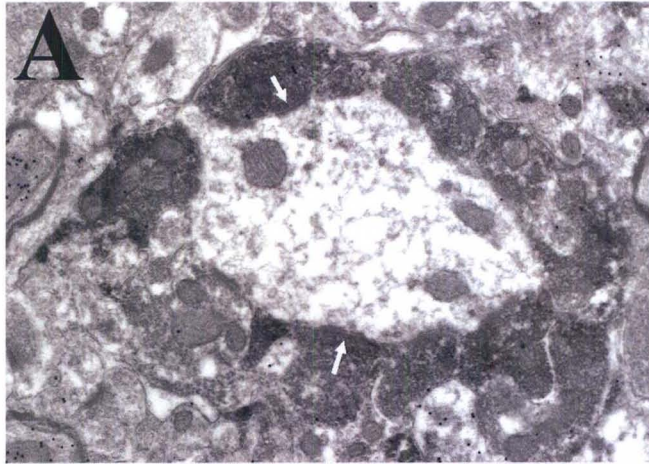


**Figure 14.**

In the tectorecipient regions of the lateral posterior nucleus, terminals labeled via tracer injections in the superior colliculus (tectal) are larger than terminals labeled via tracer injections in the cortex (cortical), and they contact larger dendrites. Similarly, terminals labeled with an antibody against the type 2 vesicular glutamate transporter (vGLUT2) are larger than terminals labeled with an antibody against the type 1 vesicular glutamate transporter (vGLUT1), and vGLUT2-labeled terminals contact larger dendrites than vGLUT1-labeled terminals. The histogram in A compares the areas of the 4 types of labeled terminals, and the histogram in B compares the minimum diameters of their postsynaptic dendrites.

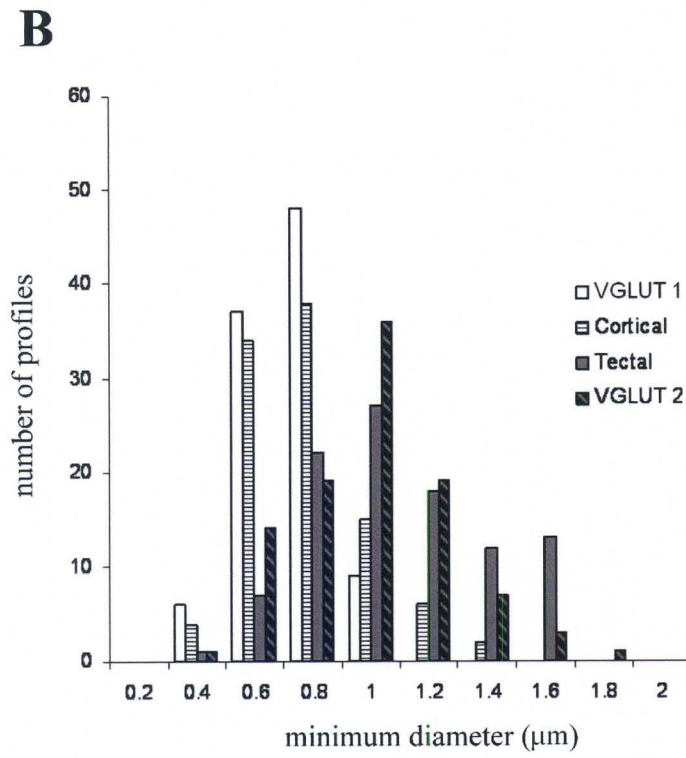
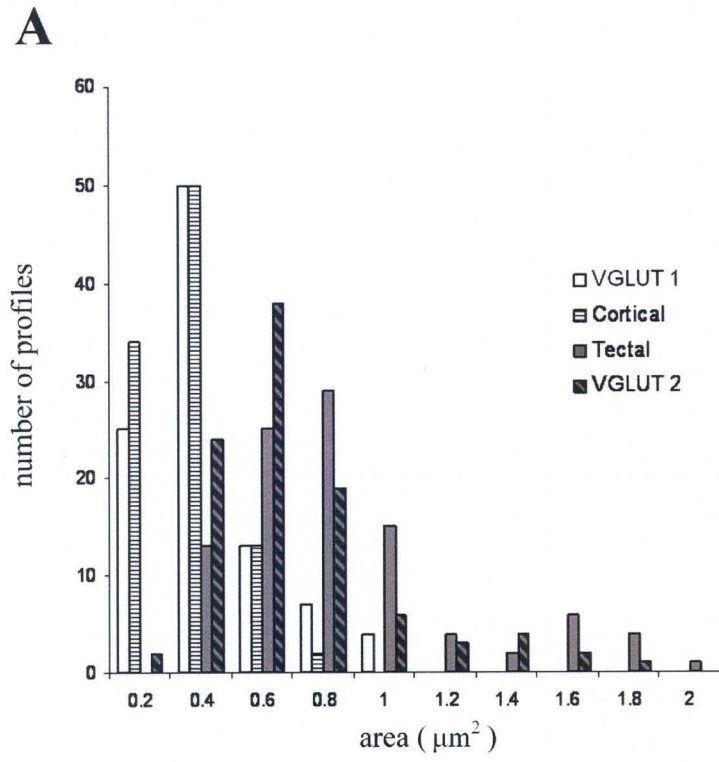
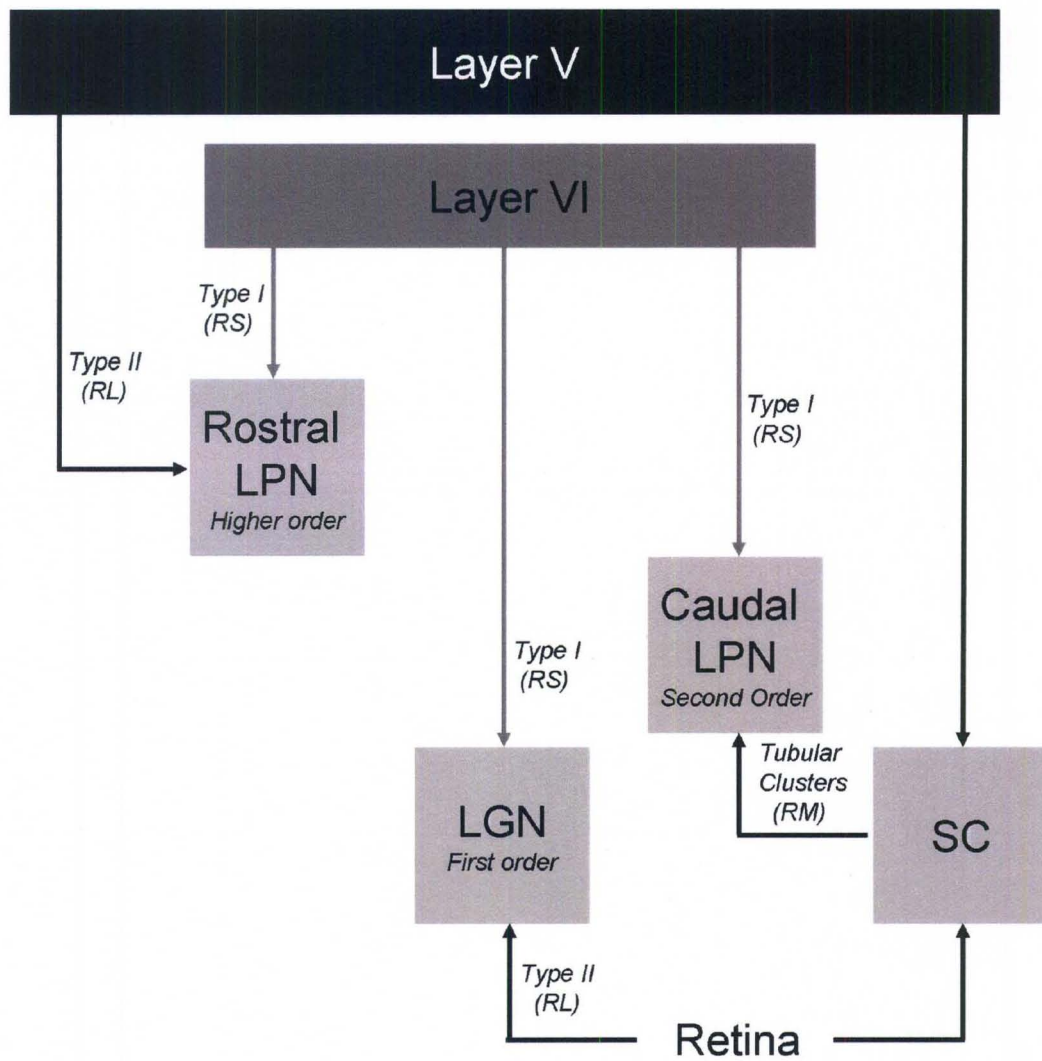


**Figure 15.**

Summary of synaptic terminal morphology in the rat visual thalamus. Type I terminals are small terminals that emanate from the relatively thin axons of layer VI corticothalamic cells. At the ultrastructural level they are small terminals with round vesicles that innervate distal dendrites (RS profiles). Type II terminals are large terminals that emanate from the relatively thick axons of layer V corticothalamic cells, or from the retina. At the ultrastructural level they are large terminals with round vesicles that innervate more proximal dendrites (RL profiles). Tectothalamic terminals form tubular clusters that surround proximal dendrites. At the ultrastructural level they are medium sized terminals with round vesicles (RM profiles). See text for details.





**CHAPTER III**

**FREQUENCY-DEPENDENT RELEASE OF SUBSTANCE P MEDIATES  
HETEROSYNAPTIC POTENTIATION OF GLUTAMATERGIC RESPONSES IN  
THE RAT VISUAL THALAMUS**

Published: Masterson SP, Li J, Bickford ME. J. Neurophysiology (in press)

**Abstract**

To investigate the interaction between peptides and glutamatergic synapses in the dorsal thalamus, we compared the frequency-dependent plasticity of excitatory postsynaptic potentials (EPSPs) in the tectorecipient zone of rodent lateral posterior nucleus (LPN), which is densely innervated by axons that contain the neuromodulator substance P (SP). Immunocytochemistry and confocal and electron microscopy revealed that neurokinin 1 (NK1) receptors are distributed on the dendrites of LPN cells, while SP is contained in axons originating from the superior colliculus (SC) and is reduced following SC lesions. *In vitro* whole cell recordings in parasagittal slices revealed that stimulation of the SC or optic radiations (CTX) evoked LPN EPSPs that increased in amplitude with increasing stimulation intensity, suggesting convergence. With 0.5-10Hz stimulus trains, CTX EPSP amplitudes displayed frequency-dependent facilitation, while SC EPSP amplitudes were unchanged. High frequency SC stimulation (100Hz for 0.5 seconds), or bath application of SP, resulted in gradual increases in both SC and CTX

EPSP amplitudes, which peaked 20 minutes post stimulation/application an average of 2.5 (SC) and 2.0 (CTX) fold above baseline. This enhancement correlated with increases in input resistance, and both the potentiation and resistance change were abolished in the presence of the NK1 antagonist L-703,606. These results indicate that SP is released when SC-LPN neurons fire at high frequency, and SP acts postsynaptically via NK1 receptors to potentiate subsequent LPN responses to both cortical and tectal inputs. We suggest that the SP-mediated potentiation of synaptic responses may serve to amplify responses to threatening objects that move across large regions of the visual field.

### **Introduction**

The efficacy of sensory information transfer through the dorsal thalamus is subject to state-dependent fluctuations in the membrane properties of thalamic neurons and their synaptic inputs (Sherman, 2001). A particularly robust transformation of sensory signals is mediated by the frequency-dependent plasticity of glutamatergic synapses. For example, the amplitudes of retinogeniculate excitatory postsynaptic potentials (EPSPs) remain stable at low stimulation frequencies (< 1 Hz), but decrease in amplitude as the stimulation frequency is increased (2-20Hz; Turner and Salt, 1998, Chen et al., 2002, Chen and Regehr, 2003). In contrast, the amplitudes of corticogeniculate EPSPs remain stable at low stimulation frequencies, but facilitate with increasing stimulation frequency (Lindstrom and Wrobel, 1990, Turner and Salt, 1998, von Krosigk et al., 1999, Granseth et al., 2002). Higher frequency stimulation (50-500Hz) of corticogeniculate fibers activates metabotropic glutamate receptors, resulting in slow EPSPs that can increase the membrane potential of geniculate neurons for 20 seconds or more (McCormick and von Krosigk, 1992). Moreover, tetanic stimulation of

corticothalamic fibers in the ventrobasal nucleus results in a long-term (1 hour or more) potentiation of these synapses (Castro-Alamancos and Calcagnotto, 1999).

Further modulation of thalamic transmission is made possible by a rich network of fibers that contain a wide variety of neuropeptides. However, while a number of studies have demonstrated that the membrane properties of thalamic neurons can be significantly altered by the exogenous application of neuropeptides (Cox et al., 1997, Sun et al., 2002, Govindaiah and Cox, 2006, Lee and Cox, 2006, Brill et al., 2007, Lee and Cox, 2008; Paul and Cox, 2010), or by their release from intrinsic interneurons (Sun et al., 2003), little is known regarding the conditions under which neuropeptides are released by extrinsic inputs to the thalamus, or their effects on neuronal responses to conventional neurotransmitters. This is an important avenue of investigation because the ability to manipulate thalamic synaptic efficacy could be used to modify abnormal thalamic activity patterns that occur in conditions such as epilepsy or neuropathic pain.

In other areas of the brain, neuropeptides have been shown to amplify glutamatergic postsynaptic responses. For example, in the spinal cord SP release from C fibers is dependent on the frequency of their stimulation, and the binding of SP to neurokinin 1 (NK1) receptors results in the amplification of glutamatergic EPSPs (Adelson et al., 2009). To examine conditions that induce thalamic neuropeptide release and subsequent effects on glutamatergic transmission, we examined the frequency-dependency of corticothalamic and tectothalamic responses in the rat lateral posterior nucleus (LPN). We previously demonstrated that within the tectorecipient zone of the LPN cortical terminals (which contain the type 1 vesicular glutamate transporter, vGLUT1) are located distal to tectal terminals (which contain the type 2 vesicular

glutamate transporter, vGLUT2) on the dendrites of projection neurons (Masterson et al., 2009). The LPN is also densely innervated by fibers that contain SP, which likely arise from the superior colliculus (SC; Hutsler and Chalupa, 1991). Thus the LPN provides a model system to examine the interactions of peptides and glutamatergic synapses in the thalamus. Our results demonstrate that substance P release from tecto-LPN axons is frequency-dependent and, via binding to NK1 receptors, can provide a sustained potentiation of both tectal and cortical glutamatergic synaptic responses.

## **Methods**

All procedures conformed to the National Institutes of Health guidelines for the care and use of laboratory animals and were approved by the University of Louisville Animal Care and Use Committee.

### ***Tract tracing and lesions***

Two adult Long Evans (hooded) rats received bilateral injections of biotinylated dextran amine (BDA; Molecular Probes, Carlsbad, CA) in the SC, and 2 rats received unilateral injections of ibotenic acid (Sigma Chemical Company, St Louis, MO) in the SC. The rats were anesthetized with intraperitoneal injections of ketamine (initially 75mg/kg) and xylazine (initially 8mg/kg), with supplements injected as needed to maintain anesthesia. They were placed in a stereotaxic apparatus and prepared for aseptic surgery. A small craniotomy was made above the SC and BDA (5% in saline, 5  $\mu$ l) or ibotenic acid (Sigma Chemical Company, St Louis, MO, 10  $\mu$ l) was injected through a glass micropipette (10  $\mu$ m tip diameter) using a PV83 pneumatic picopump (WPI, Sarasota, FL). After a survival time of one week, the rats were transcardially perfused with ACSF followed by a fixative solution of 4% paraformaldehyde in 0.1 M phosphate

buffer pH 7.4 (PB). The brain was removed from the skull, and a vibratome was used to cut sections in the parasagittal plane to a thickness of 50  $\mu\text{m}$ .

### ***Histochemistry***

To examine the distribution of SP and NK1 in the LPN, 8 rats were deeply anesthetized and transcardially perfused with ACSF followed by a fixative solution of 4% paraformaldehyde or 4% paraformaldehyde and 0.5% glutaraldehyde in 0.1 M phosphate buffer pH 7.4 (PB). The brain was removed from the skull, and a vibratome was used to cut sections in the parasagittal plane to a thickness of 50  $\mu\text{m}$ . Sections from these rats, as well as sections from rats that received ibotenic acid injections in the SC, were incubated in either a rat-anti-SP antibody (Accurate Chemical Company, Westbury, NY) diluted 1:500 or a rabbit-anti-NK1 antibody (Chemicon, Billerica, MA) diluted 1:4000 in 0.01M phosphate buffer, 0.9% NaCl (PBS) and 1% normal goat serum. The following day the sections were rinsed in PB and incubated for 1 hour in biotinylated goat-anti-rat or biotinylated-goat-anti-rabbit antibodies (Vector Laboratories, Burlingame, CA) diluted 1:100. They were then incubated for an hour in a solution of 1:100 dilution of avidin and biotinylated-horseradish peroxidase (ABC solution), reacted with nickel-enhanced diaminobenzidine, and mounted on slides or prepared for electron microscopy.

For electron microscopy, sections were postfixated in 2% osmium tetroxide in PB for 1 hour and then dehydrated through a graded series of ethyl alcohol (70-100%) and embedded in Durcupan resin (Ted Pella, Redding, CA) between sheets of Aclar plastic (Ladd Industries Inc., Burlington, VT). A light microscope was used to identify areas of interest, which were excised and mounted on resin blocks. A diamond knife was used to cut ultrathin sections, which were placed on Formvar-coated nickel slot grids, air dried,

and stained with a 10% solution of uranyl acetate in methanol for 30 minutes before examination with an electron microscope. SP or NK1-labeled profiles were digitally captured and categorized based on ultrastructural features. The size of SP-stained profiles was measured using SigmaScan software (SPSS Inc., Chicago, IL). Profile measurements are expressed as mean  $\pm$  SD. Statistical comparison to previous data (Masterson et al., 2009) was tested with an unpaired *t*-test.

To determine whether tectothalamic terminals contain SP, sections from rats that received SC BDA injections were incubated overnight at 4°C in a solution of streptavidin conjugated to Alexa 546 (Molecular Probes, Carlsbad, CA) diluted 1:100 and rat-anti-SP antibody (Accurate Chemical Company) diluted 1:250 in PBS and 1% normal goat serum. The following day the sections were rinsed in PB and incubated for 1 hour in a goat-anti-rat antibody conjugated to Alexa 488 diluted 1:100. After rinsing in PB, the sections were mounted on slides and viewed with a laser scanning confocal microscope (Olympus, Center Valley, PA).

### ***Preparation of LPN slices***

Long Evans (hooded) rats of both sexes (16-45 days old) were anesthetized with carbon dioxide and decapitated. The brains were hemisected and quickly transferred to a cold (4°C) oxygenated cutting solution containing (in mM): sucrose 206; KCl 2.5; CaCl<sub>2</sub> 1; MgSO<sub>4</sub> 1; MgCl<sub>2</sub> 1; NaH<sub>2</sub>PO<sub>4</sub> 1.25; NaHCO<sub>3</sub> 26; and *d*-glucose 10 at a pH of 7.4. After the tissue was chilled for 3 minutes, parasagittal slices (400µm thick) were cut on a vibratome (Leica VT 100E, Deerfield, IL) and placed back into cutting solution for 20 minutes. The slices were further trimmed into blocks with a razor blade to include the SC, thalamus, and striatum. The slices were then transferred into oxygenated artificial

cerebrospinal fluid (ACSF) containing (in mM): NaCl 124; KCl 2.5; CaCl<sub>2</sub> 2; MgSO<sub>4</sub> 1; NaH<sub>2</sub>PO<sub>4</sub> 26; and *d*-glucose 10, at a pH of 7.4.

### ***Recording procedures***

After 2 hours of incubation in oxygenated ACSF at 35°C, the slice was placed in a temperature controlled recording chamber and maintained in an interface of warmed (35°C) humidified air (95% O<sub>2</sub>-5% CO<sub>2</sub>) and ACSF. Bicuculline (10μM, Tocris, Ellisville, MO) and CGP55845 (5μM, Tocris) were routinely included in the ACSF to block GABA<sub>A</sub> and GABA<sub>B</sub> receptors. In certain experiments, CNQX (20μM, Sigma Chemical Company, St Louis, MO) and/or APV (25μM, Sigma) were added to the ACSF and bath applied to block AMPA/kainate and NMDA receptors respectively. In other experiments substance P (2 μM, Sigma) and/or the NK1 antagonist L703,606 (5 μM, Sigma) were added to the ACSF.

Borosilicate glass microelectrodes (tip resistance, 3.5-7.0 MΩ) were pulled horizontally (P97, Sutter Instruments) and filled with a solution containing (in mM): K-gluconate 115, MgCl<sub>2</sub> 2, ATP 3, GTP 0.3, HEPES 10, KCl 120 and phosphocreatine 10 at a pH of 7.3. Blind whole cell patch-clamp recordings were made in current-clamp mode with an Axoclamp 2B amplifier (MDS Analytical Technologies, Sunnyvale, CA, USA). Positive pressure was maintained while penetrating the tissue, and when a neuron was encountered (as indicated by an increase in electrode resistance), a small negative pressure was applied to the pipette to rupture a patch of cellular membrane. Recordings were obtained from cells considered to be relay cells. These cells exhibited a low-threshold calcium conductance and a hyperpolarization-activated mixed cation conductance (Li et al., 2003a). Records were digitized at 10 kHz and stored directly on



computer. All membrane potential measurements were junction potential (9 mV) corrected.

As schematically illustrated in Figure 3A, to stimulate tectothalamic fibers, a multipolar stimulation electrode (matrix microelectrode; FHC, Bowdoin, ME) was placed in the superficial layers of the SC. Corticothalamic axons (CTX) were stimulated with a second multipolar electrode placed in the optic radiations. Stimulating electrodes were always at least 1 mm from the recording electrode. The electrode array contained 8 tungsten electrodes with a spacing of 115  $\mu\text{m}$  between each electrode. Once a whole cell recording was obtained, SC or CTX stimulation was produced by using any two adjacent electrodes in the arrays. The anode and cathode positions were varied until the best response was achieved.

Current pulses of 50 $\mu\text{s}$  were generated with a stimulator (Grass S88, Grass Instrument, Warwick, RI) that was connected to a stimulus isolation unit (World Precision Instruments A365, Sarasota, FL) which controlled current intensity (100 $\mu\text{A}$ -3000 $\mu\text{A}$ ). Stimulus frequency was controlled by computer using pClamp 8.2 software (MDS Analytical Technologies). To measure short term plasticity, repetitive stimuli were delivered in trains of 20 pulses of variable frequency (0.5-10Hz). The responses to 5 trains delivered in 10s intervals were averaged. To examine long term plasticity, 100 Hz current pulses were delivered for a period of 0.5 sec, and then current pulses were delivered after 5, 10, 15 and 20 minutes (the average of 5 current pulses in 5s intervals was recorded for each time point). EPSP amplitudes were measured using pClamp 8.2 software. EPSP amplitudes were calculated as the difference between the membrane voltage 2ms before the stimulus and the peak of the synaptic response. For the stimulus

trains, the amplitudes of each EPSP of the 20 pulse train were quantified relative to the amplitude of the first EPSP of the train. For long term plasticity experiments, the amplitudes of EPSPs generated after high frequency stimulation were quantified relative to the amplitudes of EPSPs generated just prior to high frequency stimulation.

Depolarization of the membrane potential caused by application of SP or 100Hz SC stimulation was compensated for by current injection to maintain pre-application/stimulation potential levels. Input resistance changes were evaluated by comparing the voltage response to square wave current pulses prior to and 10 minutes following SP application of 100 Hz SC stimulation. Voltage responses were also recorded in response to brief (20ms) application of glutamate (100  $\mu$ M) from a pipette (8-12  $\mu$ m tip diameter) placed close to the recording electrode. The glutamate was ejected from the pipette using a PV83 pneumatic picopump (WPI) with the pressure adjusted to elicit a stable pre-SP response of greater than 1 mV. Student t-tests or ANOVA single factor analysis were used to test for statistical significance. Quantitative data are expressed as means  $\pm$  SD.

## **Results**

### ***SP is presynaptic, and NK1 is postsynaptic in the LPN***

Immunohistochemical staining for both SP and NK1 was densely distributed in the caudal and lateral regions of the LPN, which we previously identified as the tectorecipient zone of the LPN (Masterson et al., 2009). The SP antibody stained boutons (Figure 1A), while the NK1 antibody stained dendrites and occasional somata (Figure 1B). Double staining with both antibodies revealed that SP-positive boutons were closely

associated with NK1 stained cells, and SP-positive boutons did not stain for NK1 (Figure 1C).

To confirm that SP is confined to axon terminals and NK1 receptors are located postsynaptically, we prepared SP and NK1 stained tissue for electron microscopy. An ultrastructural analysis of a sample of 100 profiles stained with the SP antibody revealed that all SP staining was confined to synaptic boutons (identified by the presence of synaptic vesicles, Figure 1D, E). In contrast, a sample of 100 profiles stained with the NK1 antibody revealed that the NK1 receptor was expressed by dendrites postsynaptic to unstained terminals (Figure 1F) and occasional somata. Importantly, no NK1-stained profiles in the LPN contained synaptic vesicles, suggesting that SP activates postsynaptic NK1 receptors in the LPN.

#### ***Tecto-LPN terminals contain SP***

We measured SP-stained terminals in electron micrographs to compare their sizes to that of cortico-LPN and tecto-LPN terminals labeled by anterograde transport, as well as profiles stained for the type 1 and type 2 vesicular glutamate transporters (vGLUT1 and vGLUT2) analyzed in our previous study (Masterson et al., 2009). The minimum diameter of 100 SP-stained profiles involved in synapses ( $0.71 \pm 0.24 \mu\text{m}$ ) was not significantly different than the minimum diameters of tecto-LPN terminals involved in synapses ( $0.76 \pm 0.22 \mu\text{m}$ ) or vGLUT2-stained terminals involved in synapses ( $0.72 \pm 0.24 \mu\text{m}$ ). In contrast, synaptic SP-stained profiles were significantly larger than synaptic cortico-LPN terminals ( $0.43 \pm 0.13 \mu\text{m}$ ;  $p = 5.5 \times 10^{-11}$ ) and synaptic vGLUT1-stained terminals ( $0.43 \pm 0.09 \mu\text{m}$ ;  $p = 1 \times 10^{-12}$ ). This suggests that tecto-LPN terminals contain SP and cortico-LPN terminals do not contain SP.

To determine whether tectothalamic axons contain substance P, we stained tissue that contained BDA-labeled tecto-LPN axons for substance P and examined the LPN using a confocal microscope. Individual boutons double-labeled for BDA and SP were identified (Figure 2A), which indicates that at least a subset of tecto-LPN boutons contain substance P. Finally, ibotenic acid lesions of the SC diminished substance P staining in the ipsilateral, but not the contralateral LPN (Figure 2B-E).

### ***Stimulation of cortico-LPN and tecto-LPN inputs in slices***

As schematically illustrated in Figure 3A, to compare the synaptic responses of LPN neurons to stimulation of their cortical or tectal inputs, whole cell recordings were obtained from neurons in the caudal/lateral LPN (tectorecipient zone, Masterson et al., 2009) in 400  $\mu\text{m}$  thick parasagittal sections maintained *in vitro*, and EPSPs were recorded following stimulation of the optic radiations (CTX) or SC. All recorded neurons were identified as regular spiking (RS) projection neurons based on their pattern of firing in response to current pulses (Li et al., 2003a). Although our previous anatomical results suggest that projection neurons within the tectorecipient zone receive both tectal input on their proximal dendrites and cortical input on their distal dendrites, not all inputs can be preserved and/or activated within the reduced slice preparation. Nevertheless, tectal or cortical EPSPs could be evoked in over half of the recorded cells (47 of 78, or 60.3%, of cells tested for cortical input, and 53 of 96, or 55.2%, of cells tested for tectal input). We attribute this relatively high success rate to the use of the 8 electrode arrays that spanned a distance of 1 mm. While we were not able to move the arrays once a whole cell recording was obtained, stimulation could be produced between any two electrodes in the array and the anode and cathode positions were varied to obtain the best response.

### ***Cortico-LPN and tecto-LPN inputs are glutamatergic and convergent***

We previously determined that stimulation of the optic radiations activates both NMDA and AMPA/kainate receptors in the LPN (Li et al., 2003b). To test whether these receptors are also activated by the stimulation of tectothalamic fibers, we stimulated the SC in the presence of the NMDA receptor antagonist APV or the AMPA/kainate receptor antagonist CNQX (Figure 3B). APV caused a significant decrease in EPSP peak amplitude ( $39 \pm 12\%$ ;  $p = 0.040$ ,  $n = 4$ ) and shift in the latency of the peak amplitude from  $11.3 \pm 2.1$  to  $8.5 \pm 1.6$ ms ( $n = 4$ ,  $p = 8.1 \times 10^{-4}$ ). The AMPA/kainate receptor antagonist CNQX also caused a decrease in EPSP amplitude ( $60 \pm 19\%$ ;  $p = 0.016$ ,  $n = 6$ ) and a shift in the latency of peak amplitude ( $10.4 \pm 2.3$  to  $17.8 \pm 2.8$  ms,  $n = 6$ ,  $p = 3.4 \times 10^{-5}$ ).

As previously reported, all CTX EPSP amplitudes in the tectorecipient zone of the LPN increased in a graded manner as the stimulation intensity was increased (Li et al., 2003b). Similarly, SC EPSP amplitudes increased with increasing stimulation current (Figure 3 C-D,  $n = 7$ ). In addition, SC EPSP latencies decreased as the stimulation intensity was increased (Figure 3D), a feature we previously reported for corticothalamic EPSPs in the tectorecipient LPN (Li et al., 2003b). These results suggest that LPN neurons receive multiple convergent cortical and tectal inputs.

### ***Tecto-LPN and cortico-LPN EPSPs display distinct short term synaptic plasticity***

The short-term frequency dependency of tecto-LPN and cortico-LPN EPSPs was tested using stimulation intensities that evoked stable EPSPs with initial amplitudes of at least 1mV. Tecto-LPN fibers were stimulated with 20-pulse trains at frequencies of 0.5, 1, 2, 5, and 10 Hz. For each frequency, an analysis of variance was performed comparing

the amplitudes of EPSPs within the pulse-train. Repetitive stimulation of tecto-LPN fibers produced no significant differences between EPSP amplitudes at any frequency (Fig. 4: A and C, n = 40; 10Hz P=0.85; 5Hz P=0.90; 2Hz P=0.90; 1Hz P=0.99; 0.5Hz P=0.51; ANOVA single factor). A similar analysis of cortico-LPN EPSPs revealed no significant differences between EPSP amplitudes at frequencies of 0.5 and 1 Hz. However, stimulation frequencies of 2, 5, and 10 Hz showed significant facilitation within the 20-pulse trains (Fig. 4: B and D, n=39; 2-10Hz, P<0.001; 1Hz P=0.80; 0.5Hz P=1.0; ANOVA single factor).

### ***SP increases the amplitude of cortico-LPN and tecto-LPN EPSPs***

We next tested whether the exogenous application of SP affected CTX or SC responses. Control EPSPs were recorded, and then the slice was bathed for 20 minutes with ACSF that contained 2  $\mu$ M SP. EPSP amplitudes were recorded at 5, 10, 15, and 20 minutes after the initial addition of SP to the ACSF. Application of SP increased the SC EPSP amplitudes in 21/34 cells tested, and CTX EPSP amplitudes in 9/17 cells tested. The average increase in EPSP amplitude of the responding cells, and the time course of these increases, are illustrated in Figure 5.

After 5 minutes exposure to SP, SC responses (white bars in Figure 5, n = 21) increased by an average of 2.1 fold after 5 minutes, 2.4 fold after 10 minutes, 2.7 fold after 15 minutes and 2.4 fold after 20 minutes. All of these post-SP responses were significantly different from responses recorded before SP application ( $p < 0.05$ ). In the presence of SP, CTX responses (light gray bars in Figure 5, n = 9) increased by an average of 1.4 fold after 5 minutes, 1.7 fold after 10 minutes, 1.6 fold after 15 minutes

and 2.2 fold after 20 minutes. All of these post-SP responses were significantly different from responses recorded before SP application ( $p < 0.05$ ).

### ***SP effects are mediated by postsynaptic NK1 receptors***

When the NK1 antagonist L703,606 (5  $\mu$ M) was added simultaneously with the SP, CTX ( $n = 5$ , dark gray bars in Figure 5) and SC ( $n = 9$ , black bars in Figure 5) EPSP amplitudes were not significantly different from control responses (0 minutes;  $p > 0.3$  for amplitudes 5, 10, 15 and 20 minutes post-SP+L703,606), indicating that the SP effect is mediated through the NK1 receptors that are distributed on LPN cells (Figure 1). A postsynaptic effect is also supported by the fact that 10 minutes after SP application the average input resistance of the recorded neurons ( $122 \pm 77 \text{M}\Omega$ ) increased significantly ( $235 \pm 87 \text{M}\Omega$ ;  $p < 0.05$ ,  $n=21$ ). This is illustrated in Figure 6 (A,B) as an increase in the voltage responses to 10 ms 50pA hyperpolarizing current pulses after 10 minutes of bath application of SP. In addition, the amplitude of voltage responses to the brief (20 ms) application of glutamate from the tip of an adjacent pipette increased significantly after 10 minutes of SP bath application (Figure 6C). This increase in the peak amplitude of glutamate responses was correlated with the increase in input resistance (Figure 6D,  $r = 0.68$ ;  $n = 16$ ).

### ***SP is released from tecto-LPN terminals by high frequency stimulation***

We next tested whether high frequency stimulation (100Hz for 0.5 s) of the SC or CTX resulted in EPSP amplitude changes. In 28/40 cells tested, high frequency stimulation of the SC resulted in a gradual increase in tectal EPSP amplitudes, which peaked 20 minutes post stimulation an average of 2.4 fold above baseline (white bars in Figure 7 histogram). Analysis of all responding cells ( $n=28$ ) revealed that post-

stimulation amplitudes were significantly larger than pre-stimulation amplitudes ( $p = 0.5 \times 10^{-4}$  at 5 minutes,  $p = 3 \times 10^{-5}$  at 10 minutes,  $p = 1 \times 10^{-5}$  at 15 minutes and  $p = 0.015$  at 20 minutes post-stimulation when compared to control). These increases were completely blocked when the NK1 antagonist L703,606 was applied to the bath during the high frequency stimulation, and for the 20 minutes following stimulation during which the EPSP amplitude measurements were obtained ( $n = 10$ ; black bars in Figure 7 histogram;  $p = 0.26$  at 5 minutes,  $p = 0.16$  at 10 minutes,  $p = 0.16$  at 15 minutes and  $p = 0.31$  at 20 minutes post-stimulation +L703,606 when compared to control).

In our slice preparation, in approximately 20% of the recorded neurons both CTX and SC stimulation electrodes evoked stable EPSPs in the same cell. In these cells we tested whether high frequency SC stimulation affected CTX EPSP amplitudes. In 10/18 cells tested, we found that high frequency SC stimulation resulted in the subsequent facilitation of CTX responses in the same cell (up to 1.9 fold after 20 minutes, light gray bars in Figure 7 histogram). Analysis of all responding cells ( $n=10$ ) revealed that at 10, 15 and 20 minutes post-stimulation, amplitudes were significantly larger than pre-stimulation amplitudes ( $p = 0.079$  at 5 minutes,  $p = 0.04$  at 10 minutes,  $p = 0.042$  at 15 minutes,  $p = 0.031$  at 20 minutes post-stimulation when compared to control), and this effect was blocked by the simultaneous application of L703,606 to the bath ( $n = 6$ ; dark gray bars in Figure 7;  $p = 0.38$  at 5 minutes,  $p = 0.48$  at 10 minutes,  $p = 0.25$  at 15 minutes and  $p = 0.052$  at 20 minutes post-stim+L703,606 when compared to control). The effect of high frequency SC stimulation on neuron input resistance was similar to that seen following SP application (from  $193 \pm 86 \text{M}\Omega$  to  $251 \pm 98 \text{M}\Omega$ ;  $p < 0.05$ ,  $n=28$ ).



We also tested the effects of high frequency CTX stimulation on cells that responded to both SC and CTX stimulation (n= 9). As illustrated in Figure 8, high frequency CTX stimulation did not increase cortical or tectal EPSP amplitudes of LPN neurons >5 minutes post stimulation. In fact, CTX and SC EPSP amplitudes were slightly smaller than control (0 minute) amplitudes and this was found to be significant ( $p < 0.05$ ) at all post-stimulation time points.

### **Discussion**

As schematically illustrated in Figure 9, our results indicate that SC-LPN terminals contain both glutamate and SP. At stimulation frequencies up to 10Hz, glutamate is released, which activates both NMDA and AMPA receptors on postsynaptic neurons. The resulting glutamatergic SC-LPN EPSPs show little frequency-dependent plasticity. In contrast to CTX-LPN EPSPs, which show frequency-dependent facilitation, there was no significant difference between SC-LPN EPSP amplitudes generated by 1, 2, 5 or 10 Hz stimulus trains. However, after high frequency (100Hz) stimulation, SP is released from SC-LPN terminals, which activates NK1 receptors on postsynaptic neurons. The activation of NK1 receptors leads to a subsequent potentiation of both SC- and CTX-evoked responses in the postsynaptic neuron. As discussed below, the unique properties of SC-LPN synaptic terminals may produce amplified responses to threatening visual images.

### ***Tectothalamic synapses: a third type of glutamatergic response***

Previous studies of the dorsal thalamus have identified two main types of glutamatergic synaptic responses. The majority of inputs to the dorsal thalamus originate from cortical layer VI (type I inputs), (Guillery, 1969). *In vitro* studies of a variety of

thalamic nuclei have consistently shown that the EPSPs elicited by stimulation of layer VI corticothalamic inputs increase in a graded manner with increasing stimulation intensity, and facilitate at frequencies of 2 Hz or higher (Turner and Salt, 1998, Granseth et al., 2002). In contrast, EPSPs generated by stimulation of ascending sensory inputs, or inputs that originate from cortical layer V (type II inputs), show an all-or-none increase in amplitude with increasing stimulation levels, and are depressed at stimulation frequencies of 2 Hz or higher (Turner and Salt, 1998, Chen and Regehr, 2000, Chen et al., 2002, Granseth et al. 2002; Li et al., 2003c; Reichova and Sherman, 2004; Arsenault and Zhang, 2006).

In the current study, all CTX EPSPs increased in amplitude with increasing stimulation current, and showed a robust frequency-dependent facilitation, consistent with all previous studies of layer VI corticothalamic responses. In contrast, the SC EPSPs in the LPN were unlike either type I or type II synaptic responses in that their amplitudes remained relatively constant at stimulation frequencies up to 10 Hz. Very similar responses have been recorded in the paralamina thalamic nuclei (adjacent to the medial geniculate nucleus) following stimulation of the SC (Smith et al., 2007).

Like type I corticothalamic inputs, SC EPSPs show a graded increase in amplitude with increasing levels of stimulation current. This likely reflects the convergence of multiple tectal axons onto single LPN neurons. Previous studies indicate that the tecto-LPN projection in the rodent is nontopographic (Mooney et al., 1984), and our previous electron microscopic observations indicate that multiple tectal terminals innervate individual dendrites (Masterson et al., 2009). This supports the idea that LPN cells may integrate converging inputs from multiple tecto-LPN cells.

Smith et al (2007) recently proposed that inputs from the SC and inferior colliculus to the paralamina neurons be called “integrators” to distinguish them from the type I and type II glutamatergic synaptic responses which Sherman and Guillery (1998) have defined as “modulating” and “driving” inputs respectively. Smith et al further proposed that it may be the collective activities of multiple convergent integrator inputs that are critical for the formation of the postsynaptic neuron’s receptive field. This concept fits well with the known properties of the LPN; receptive fields within the tectorecipient LPN are much larger than those recorded in the superficial layers of the SC where tecto-LPN cells are located (Chalupa et al., 1983, Abramson and Chalupa, 1988, Casanova and Molotchnikoff, 1990, Hutsler and Chalupa, 1991, Ling et al., 1997, Hilbig et al., 2000, Major et al., 2000). In the hamster, Mooney et al (1984) demonstrated that receptive fields of LPN cells are on average 10 times larger than those of tecto-LPN cells.

#### ***Substance P release in the LPN***

We also found that tectothalamic synapses are distinguished from type I and type II glutamatergic synapses in that they release SP when stimulated at high frequencies. This is similar to the frequency-dependent release of SP in the spinal cord (Go and Yaksh, 1987, Adelson et al., 2009) substantia nigra (Diez-Guerra et al., 1988) and intestinal tract (Baron et al., 1983). In the LPN, a recent study demonstrated that SP reduces a  $K^+$  conductance, likely  $K_{leak}$ , via NK1 receptors (Paul and Cox, 2010). The increases in input resistance that we identified following bath application of SP or high frequency stimulation of the SC are consistent with this action. The net result of SP release from tectothalamic terminals is an increase in the response of postsynaptic neurons to all glutamatergic synaptic inputs.

Our studies suggest that when tectothalamic neurons fire at frequencies up to 10 Hz, glutamate is released and LPN neurons reliably respond to stimulus trains, without facilitation or depression. In contrast, when tectothalamic neurons fire at high frequency, SP is released in addition to glutamate, which amplifies the subsequent postsynaptic LPN neuronal responses to both tectal and cortical inputs. *In vivo* studies indicate that neurons in the superficial layers of the SC can fire at very high frequencies. In the anesthetized rat, firing rates of up to 120 Hz have been recorded in superficial layers of the SC (Prevost et al., 2007), and in the awake behaving monkey, firing rates of 250 Hz or more have been recorded in the superficial SC (Wurtz and Mohler, 1976). Thus, our stimulation parameters are well within the normal firing range of SC neurons.

### ***Functional implications***

A variety of studies have concluded that SP is released in response to stressful stimuli, and SP antagonists have been suggested to be an important therapeutic target for depression and/or anxiety (e.g. Ebner et al., 2009). We hypothesize that the release of SP from tectothalamic terminals may similarly function to increase reactions to threatening visual stimuli.

We recently studied the tectal projections to the dorsal (Pd) and central pulvinar nucleus (Pc) of the tree shrew (Chomsung et al., 2008). Luppino et al (1988) first described these projections as “diffuse” and “specific” respectively. By using a combination of anterograde and retrograde tracing techniques, as well as electron microscopy, we concluded that both the Pd and Pc receive topographic (specific) projections from the SC, and the Pd receives additional nontopographic (diffuse) projections, possibly arising from convergent axon collaterals. Because we also found

that the Pd (but not the Pc) projects to the amygdala, we suggested that the diffuse tectopulvinar projections are involved in coding the movement of large or threatening objects to initiate escape responses, while the specific tectopulvinar projections are involved in coding the precise location of small moving objects to initiate orienting or pursuit responses (Chomsung et al., 2008).

Whether a small portion of the rat LPN receives topographic connections from the SC (comparable to the tree shrew Pc) remains an open question. This is difficult to test because the tectorecipient zone of the rat LPN is quite small when compared to the large tectorecipient zones of the tree shrew pulvinar nucleus. However, both anatomical and physiology studies indicate that the majority of the LPN is organized in a nontopographic manner, and that LPN neurons have very large receptive fields (Mooney et al., 1984).

Mooney et al (1984) suggested the LPN neurons respond to visual events, such as the appearance of novel objects, rather than the specific features of visual stimuli. In particular, the majority of LPN neurons that could be antidromically driven from the SC responded best to visual stimuli moving across their receptive fields, similar to the responses of SC-LPN neurons which have been classified as movement-sensitive wide field vertical cells (Mooney et al., 1988). Convergent input from multiple wide field vertical cells likely accounts for the LPN cells' sensitivity to movement across widespread regions of the visual field. This organization makes the LPN well suited to signal the appearance of potential danger.

There also appears to be good overlap between tecto-LPN projections, regions of the LPN that project to the amygdala (Doron and Ledoux, 1999, 2000), and regions innervated by terminals that contain SP. Similarly, the paralamina nuclei, which also

receive “integrator” inputs from the SC (Smith et al., 2007), project to the amygdala (Doron and Ledoux, 1999, 2000) and are innervated by SP fibers (unpublished data). Thus, the tectorecipient zone of the LPN may be part of a complex of nuclei that receive convergent tectal inputs and project to the amygdala. In this context, our results suggest that the SP-mediated potentiation of synaptic inputs may serve to amplify responses to threatening objects that move across large regions of the visual field.

**Figure 1.**

SP is presynaptic and NK1 is postsynaptic in the LPN. A) An antibody against SP stains terminal boutons in the LPN. B) An antibody against NK1 stains dendrites and occasional somata in the LPN. C) A 12  $\mu\text{m}$  thick confocal image of tissue from the caudal LPN stained with NK1 and SP antibodies. An NK1-stained neuron (purple) is surrounded by SP-stained terminals (green). There was no double-labeling of NK1 and SP, indicating that the NK1 receptors are not located on SP terminals. D-F) Electron micrographs of the LPN illustrate that SP is located in terminal boutons that synapse (white arrows) with dendrites (D,E) and NK1 receptors are present on postsynaptic dendrites (F). Scale bars = 10  $\mu\text{m}$  in A (applies to B), 10  $\mu\text{m}$  in C, and 0.5  $\mu\text{m}$  in D (applies to E and F).

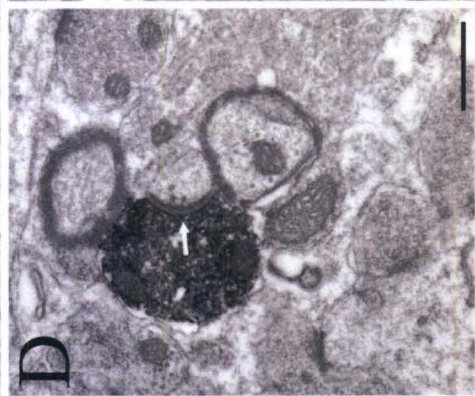
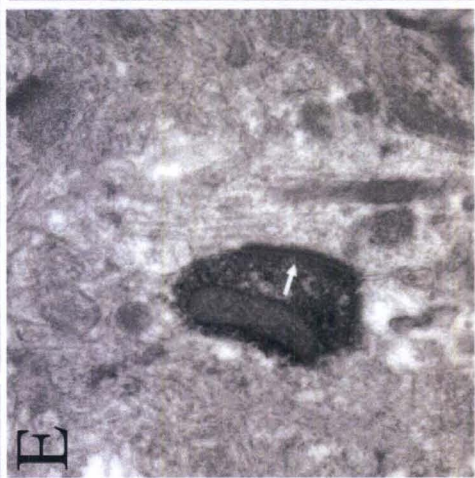
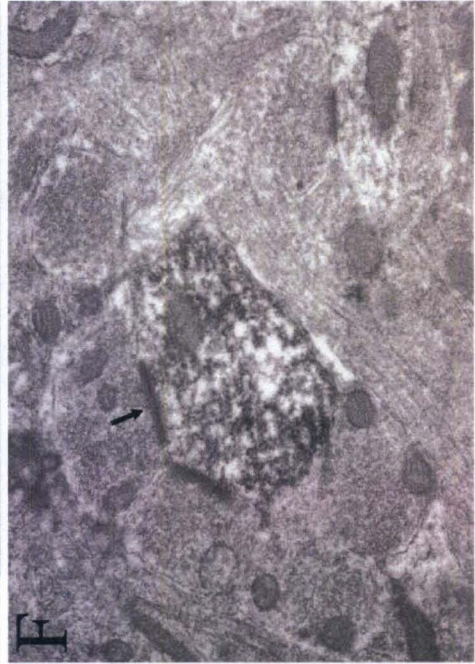
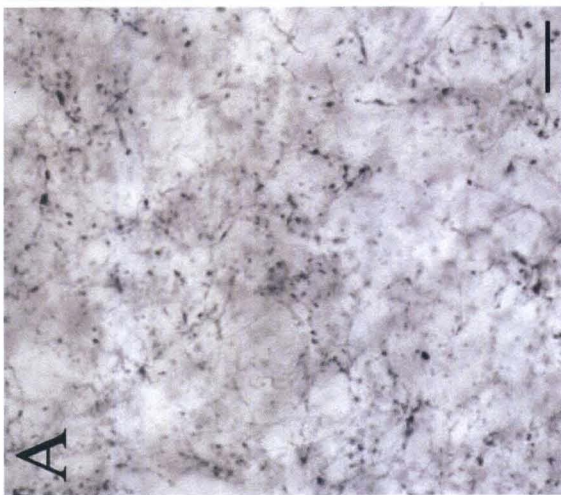
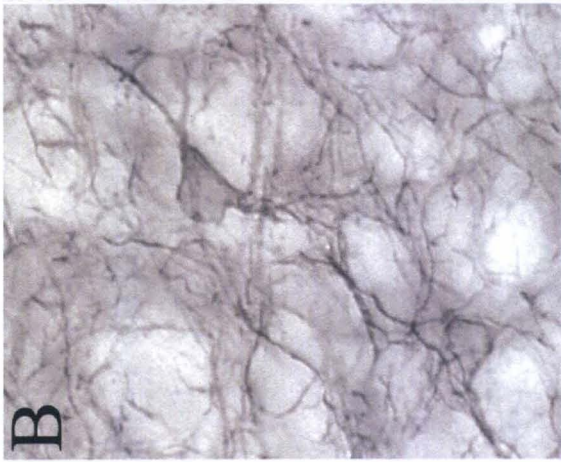
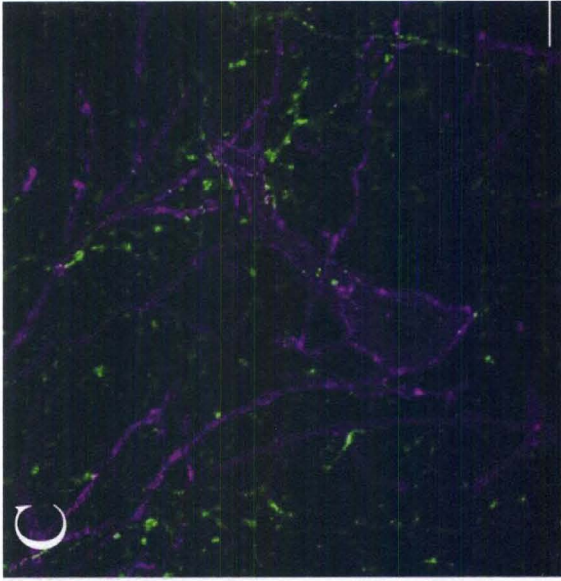




**Figure 2.**

Tecto-LPN terminals contain SP. A) A large injection of biotinylated dextran amine (BDA) was made in the superficial layers of the SC to label axons in the LPN by anterograde transport. LPN tissue was subsequently treated to reveal the tecto-LPN axons and SP. A 10  $\mu\text{m}$  thick confocal image of the caudal LPN illustrates the overlap of tecto-LPN axons (purple) and terminals that contain SP (green). The white areas of the image indicate tecto-LP terminals that contain SP. B-F) The excitatory neurotoxin ibotenic acid was injected unilaterally into the superior colliculus. SP staining in the LPN contralateral to the ibotenic acid injection was densely concentrated in the caudal portion of the nucleus, as in normal rats (B, boxed region shown at higher magnification in C). The inset shows neurons visualized with the NeuN antibody in the superior colliculus. SP staining was absent in the LPN ipsilateral to the ibotenic acid injection (D, boxed regions shown at higher magnification in E). The inset shows the lesion in the superior colliculus caused by the ibotenic acid injection in a section stained with NeuN. Scale bars = 5  $\mu\text{m}$  in A, 500  $\mu\text{m}$  in D (also applies to B), 1 mm in D inset (also applies to B inset) and 25  $\mu\text{m}$  in E (also applies to C).

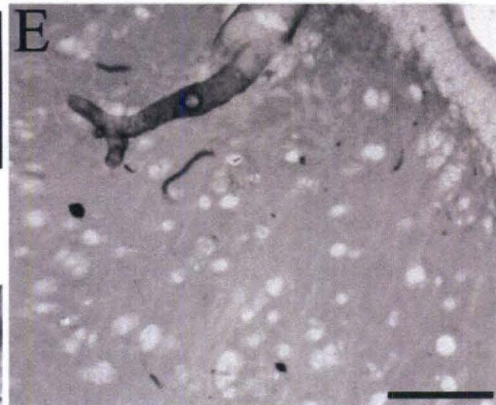
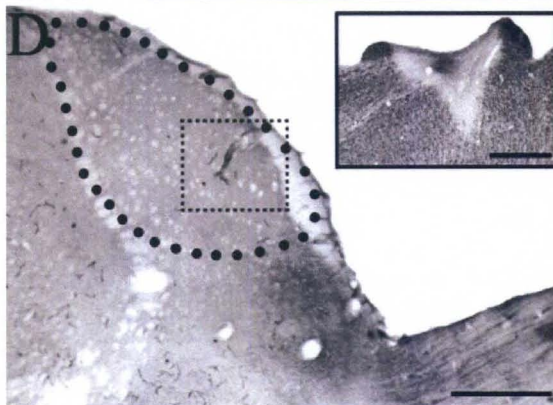
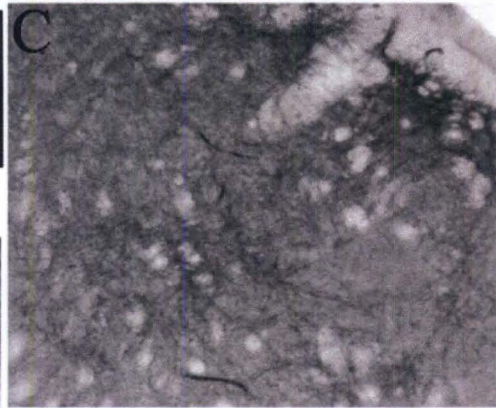
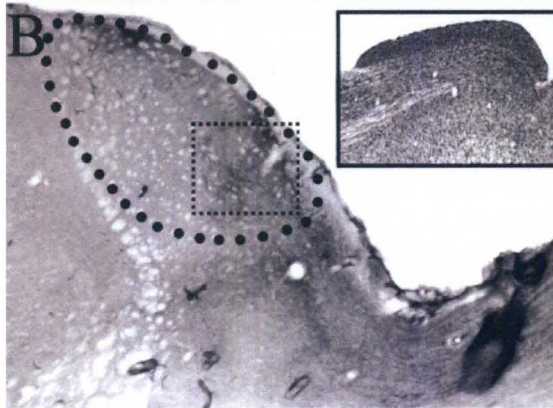
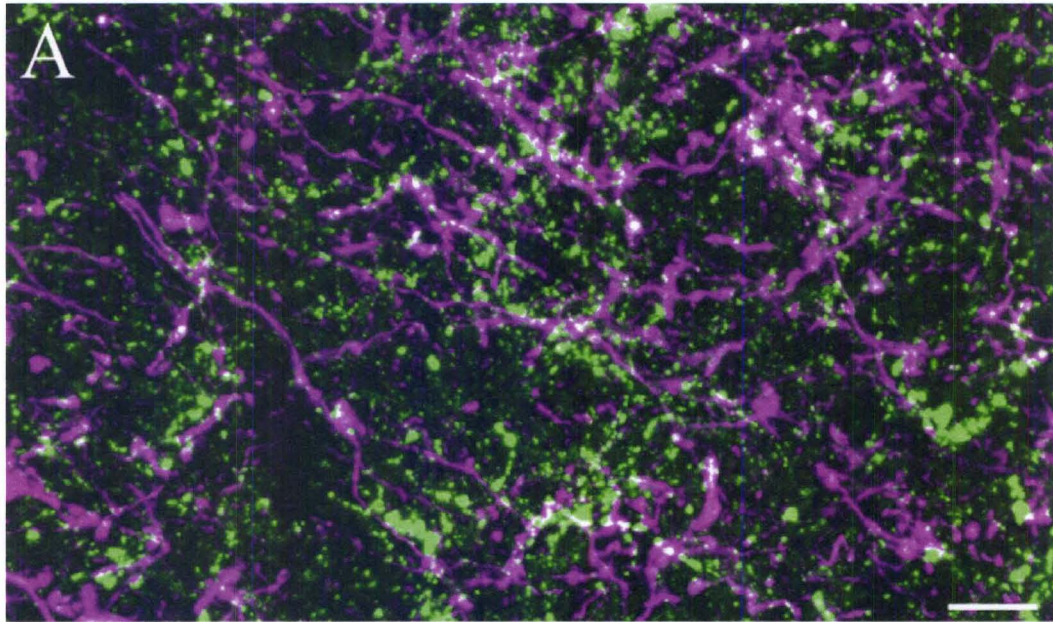


**Figure 3.**

Cortico-LPN and tecto-LPN inputs are glutamatergic and convergent. **A)** Schematic illustration of the recording and stimulation sites used to examine tectothalamic and corticothalamic EPSPs in the lateral posterior nucleus (LPN). Parasagittal slices that contained the most lateral regions of the superior colliculus (SC) were used. An array of 8 electrodes (black dots surrounded by white circles) was placed in the SC to activate the cut axons of tectothalamic cells located in more medial regions of the SC. A second array of 8 electrodes was placed just rostral to the LPN to activate the cut axons of corticothalamic cells (CTX). Our previous anatomical studies (Li et al., 2003; Masterson et al., 2009) revealed that only the rostral LPN is innervated by large corticothalamic terminals that originate from layer V cells. The caudal tectorecipient region of the LPN (light gray) is innervated only by small corticothalamic terminals that originate from layer VI. **B)** Tectothalamic EPSPs activate both NMDA and non-NMDA receptors. In the presence of the NMDA receptor antagonist APV, or the AMPA/kainate receptor antagonist CNQX, there was a decrease in EPSP amplitude and a shift in the latency of the peak amplitude. Tectothalamic EPSPs were abolished in the presence of both APV and CNQX. **C)** With increasing stimulation intensity, tectothalamic EPSPs show a graded increase in amplitude, and a small decrease in latency. **D)** Graph shows the average tecto-LPN EPSP amplitudes and latencies as a function of stimulation intensity for a sample of 7 cells.

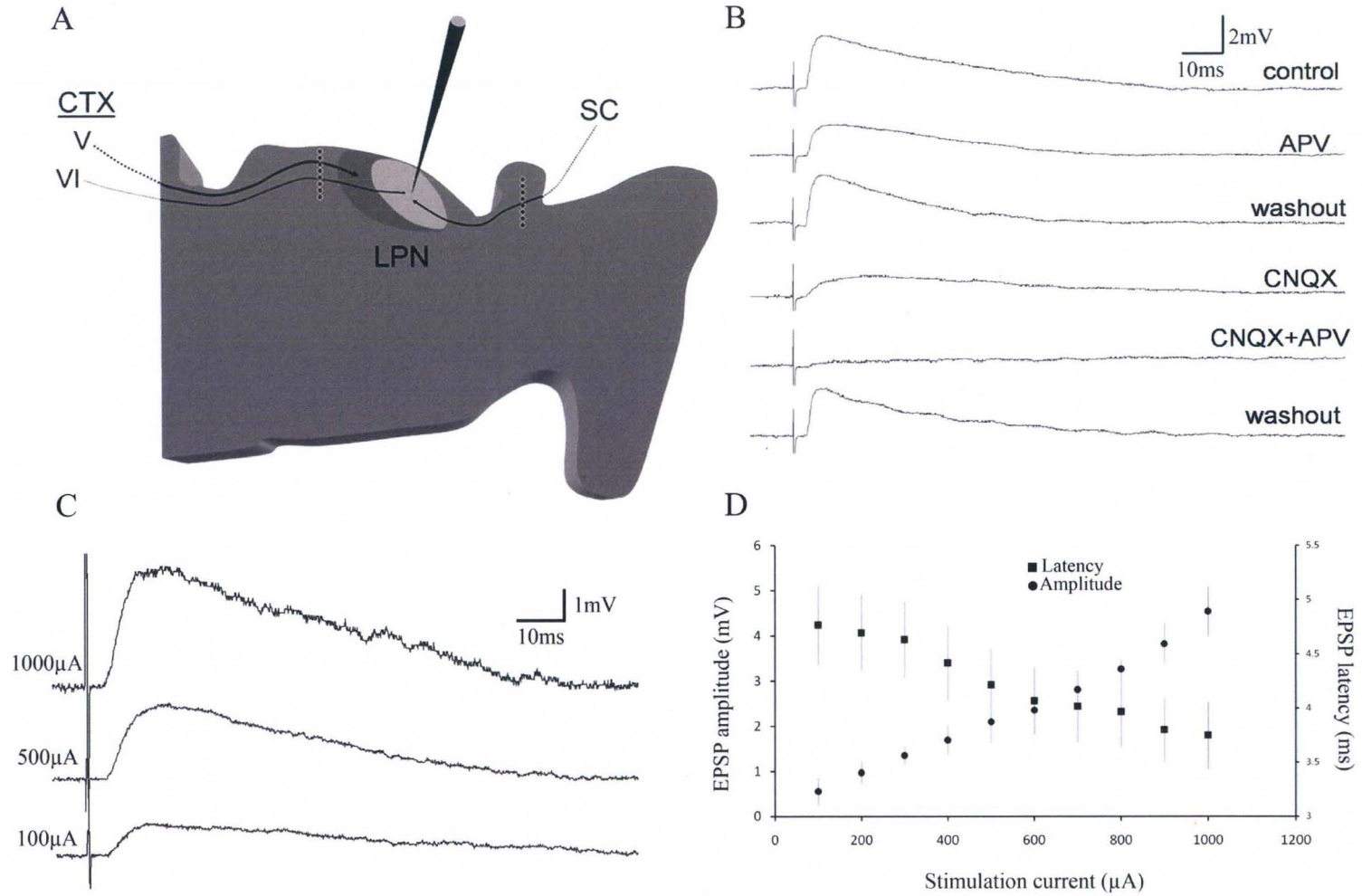


**Figure 4.**

Tecto-LPN and cortico-LPN EPSPs display distinct short term synaptic plasticity.

Stimulation experiments consisted of 20 pulses at 0.5, 1, 2, 5, and 10 Hz. **A)** EPSPs 1, 10

and 20 from a SC stimulation experiment. Stimulation of tectal fibers produced EPSPs

with stable amplitudes. **B)** EPSPs 1, 10, and 20 from a CTX stimulation experiment.

Stimulation of cortical fibers produced EPSPs that showed frequency-dependent

facilitation. **C and D)** Each point represents the normalized average of EPSPs evoked in

35 cells by 20 pulses at 0.5, 1, 2, 5 and 10Hz. The EPSP amplitudes were normalized by

dividing the EPSP amplitude evoked by each pulse in the train (EPSP<sub>n</sub>) by the EPSP

amplitude evoked by the first pulse of the train (EPSP<sub>1</sub>). **C)** Tectothalamic experiments.

**D)** Corticothalamic experiments.

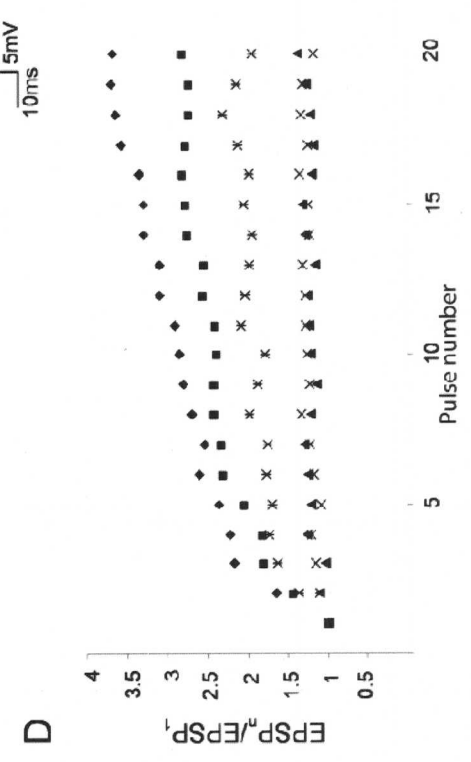
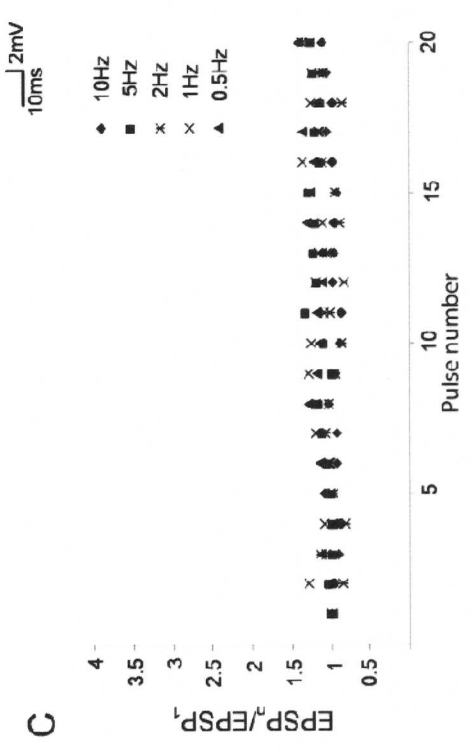
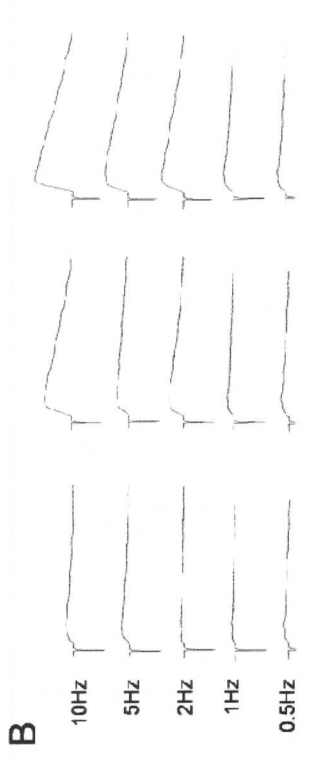
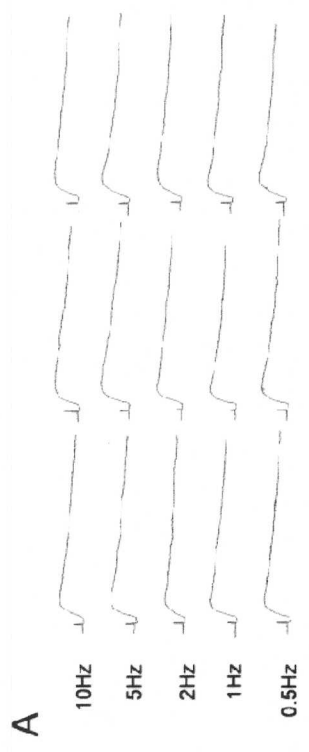


**Figure 5)**

Substance P increases the amplitude of cortico-LPN and tecto-LPN EPSPs. Substance P, or substance P and the NK1 antagonist L703,606, were bath applied during *in vitro* whole cell recordings and stimulation of tecto-LPN axons (SC) or cortico-LPN axons (CTX). In A-D the gray trace is the control EPSP (0 minutes) and the darker traces are EPSPs 10 and 20 minutes after application of substance P or substance P and L703,606. **A)** EPSPs generated by SC stimulation before and after substance P application. **B)** EPSPs generated by SC stimulation before and after substance P and L703,606 application. **C)** EPSPs generated by CTX stimulation before and after substance P application. **D)** EPSPs generated by CTX stimulation before and after in the substance P and L703,606. **E)** The histogram illustrates the potentiation of SC and CTX evoked EPSPs at 5, 10, 15 and 20 minutes after substance P application expressed as a percentage of control values (0 minutes).

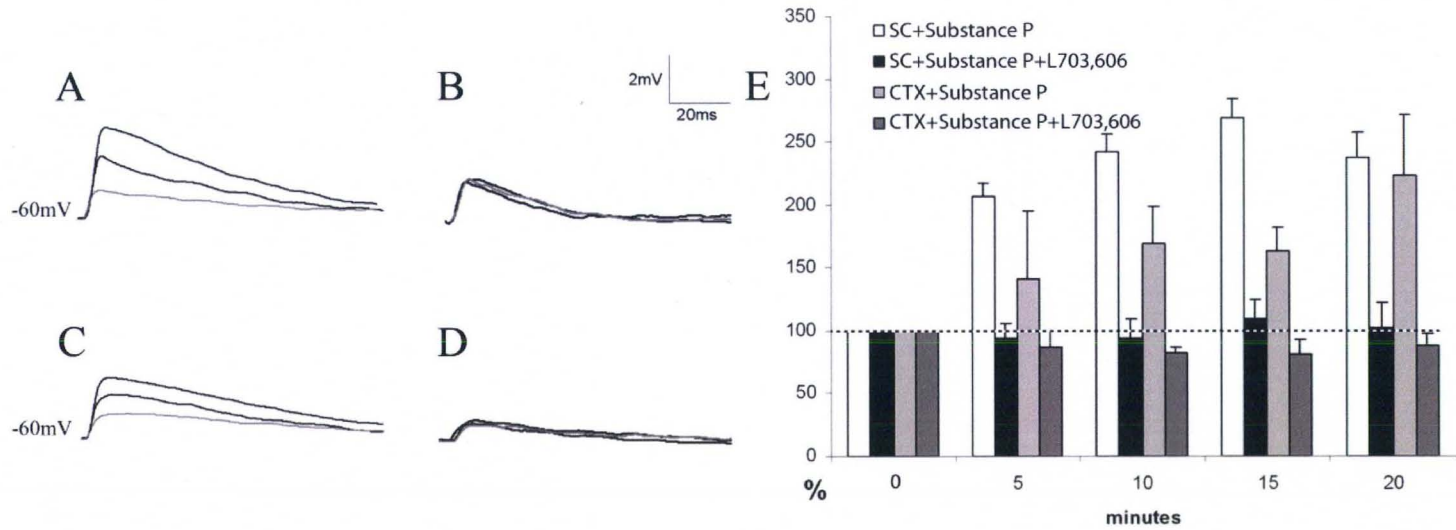




**Figure 6.**

SP effects are mediated by postsynaptic NK1 receptors. Voltage responses of LPN neurons (bottom traces) to 10 ms 50pA hyperpolarizing current pulses (top traces) (**A**) increase after 10 minutes of bath application of SP (**B**). **C**) The amplitudes of LPN neuron voltage responses to brief (20 ms) application of glutamate (lower trace) are increased following 10 minutes of bath application of SP (top trace indicated by arrow). The histogram illustrates the average increase in peak amplitude expressed as a percentage of control amplitudes ( $n = 16$ ). **D**) The increase in response to glutamate application is correlated with an increase in input resistance ( $r = 0.68$ ).

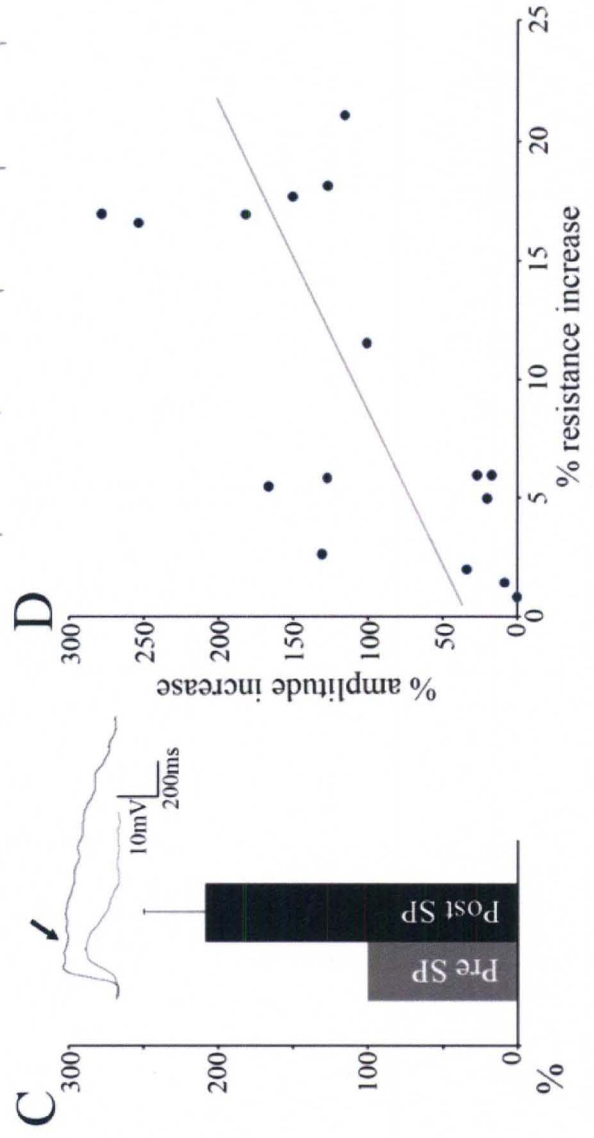
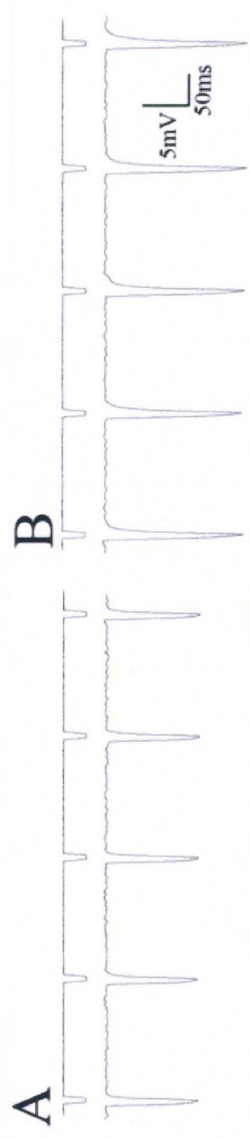


**Figure 7.**

High frequency stimulation of tecto-LPN axons increases the amplitude of subsequent tecto- and cortico-LPN EPSPs. In cells that responded to stimulation of both tecto-LPN (SC) and cortico-LPN (CTX) axons, tecto-LPN axons were stimulated at a frequency of 100 Hz for 0.5 seconds and the amplitudes of subsequent EPSPs evoked by single SC or CTX stimulus pulses were monitored. In A-D the gray trace is the control EPSP and the darker traces are EPSPs 10 and 20 minutes after 100 Hz SC stimulation. **A)** EPSPs generated by SC stimulation before and after 100 Hz SC stimulation. **B)** EPSPs generated by SC stimulation before and after 100 Hz SC stimulation in the presence of the NK1 antagonist L703,606. **C)** EPSPs generated by CTX stimulation before and after 100 Hz SC stimulation. **D)** EPSPs generated by CTX stimulation after 100 Hz SC stimulation in the presence of L703,606. **E)** The histogram illustrates the potentiation of SC and CTX evoked EPSPs at 5, 10, 15 and 20 minutes after 100 Hz SC stimulation expressed as a percentage of control values (0 minutes).

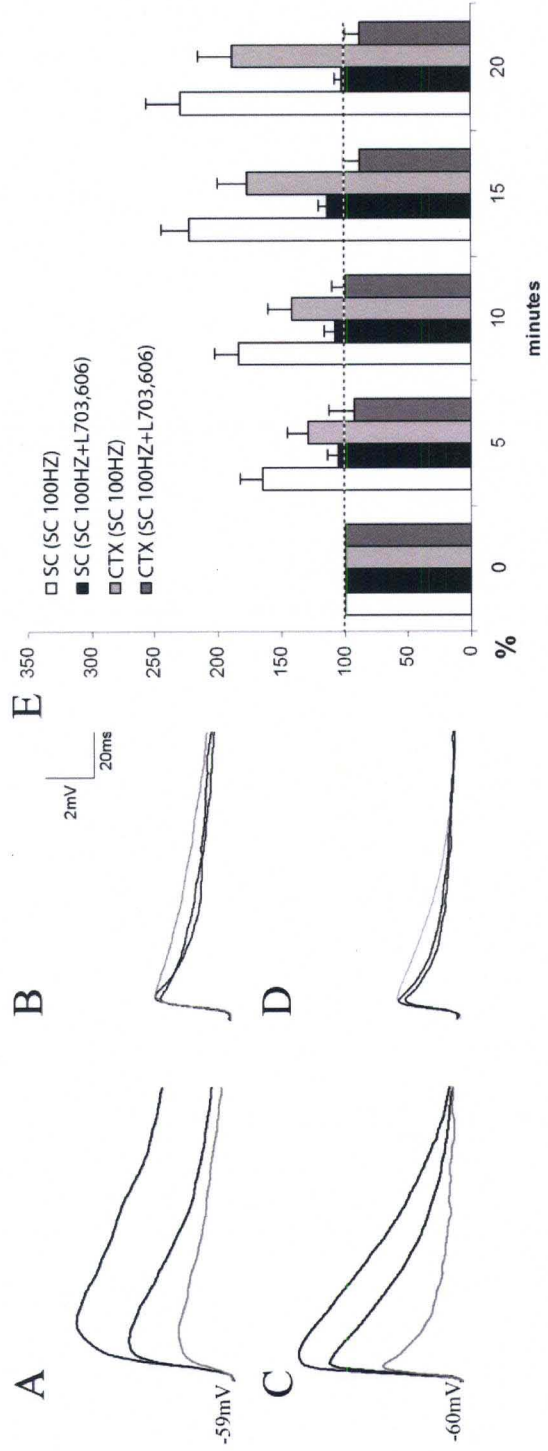


**Figure 8.**

High frequency stimulation of cortico-LPN input does not change the amplitude of subsequent tecto- or cortico-LPN EPSPs. In cells that responded to stimulation of both tecto-LPN (SC) and cortico-LPN (CTX) axons, cortico-LPN axons were stimulated at a frequency of 100 Hz for 0.5 seconds and the amplitudes of subsequent EPSPs evoked by single SC or CTX stimulus pulses were monitored. In A and B, the gray trace is the control EPSP and the darker traces are EPSPs 10 and 20 minutes after 100 Hz CTX stimulation. **A)** EPSPs generated by SC stimulation before and after 100 Hz CTX stimulation. **B)** EPSPs generated by CTX stimulation before and after 100 Hz CTX stimulation. At the completion of the experiment, the SC was then stimulated at 100 Hz for 0.5 seconds. The dotted trace (arrow) indicates the subsequent potentiation of the CTX EPSP. **C)** The histogram illustrates that there was no increase in the amplitudes of SC or CTX evoked EPSPs at 5, 10, 15 and 20 minutes after 100 Hz CTX stimulation. Amplitudes expressed as a percentage of control values (0 minutes).

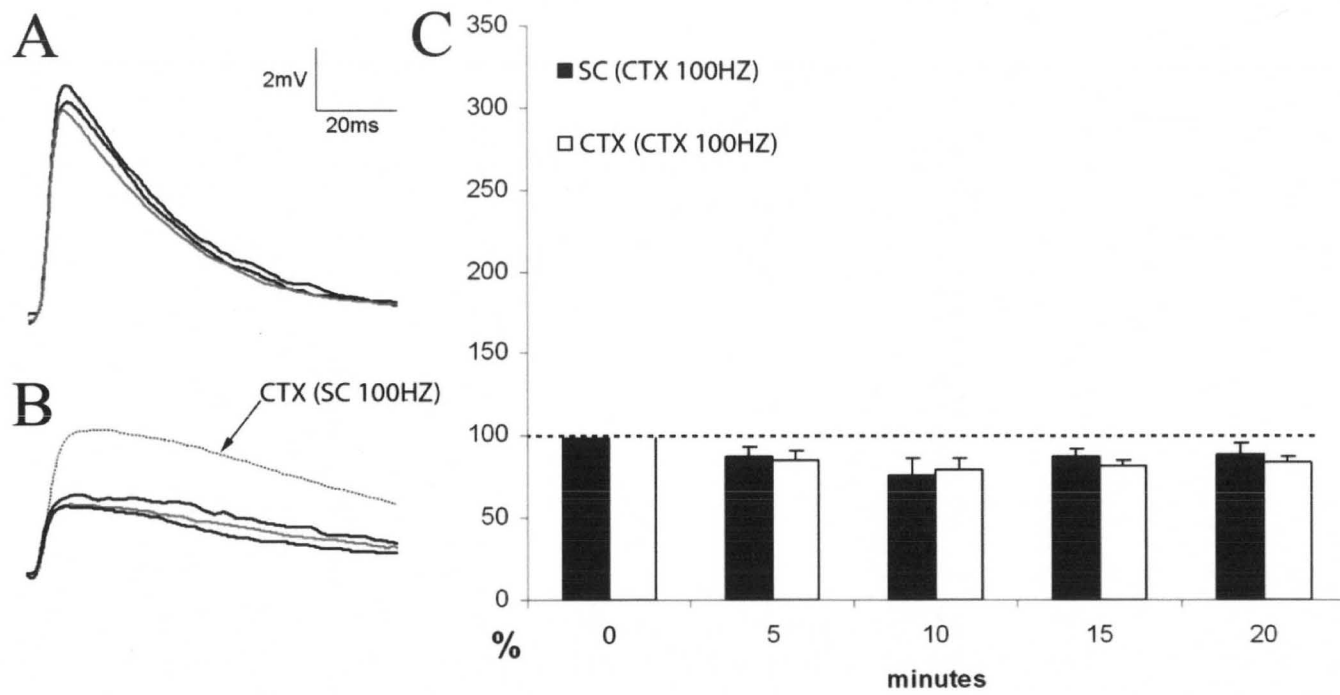
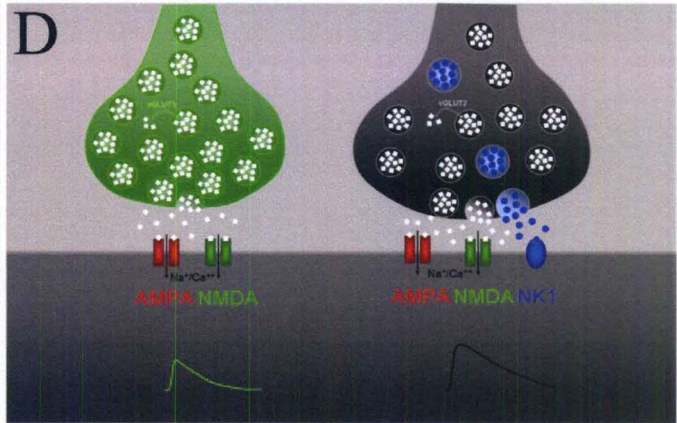
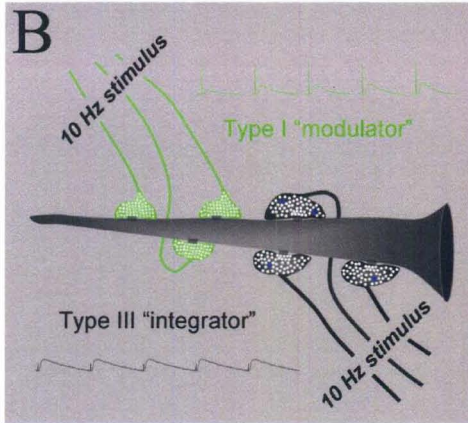
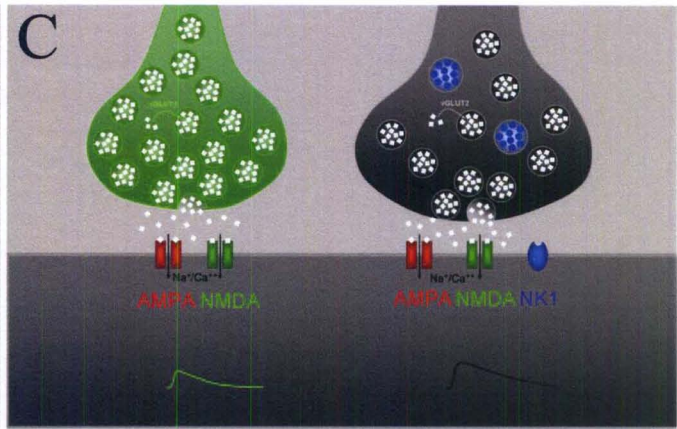
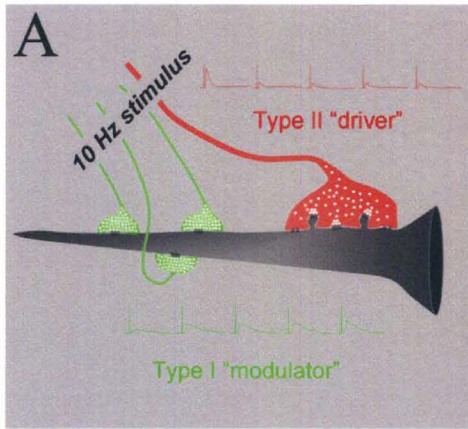


**Figure 9.**

Schematic summary of rat LPN glutamatergic synapses. **A)** In the rostral LPN, projection cells receive input to their proximal dendrites from a small number of large terminals with round vesicles (RL profiles, red) that originate from cortical layer V, and input to their distal dendrites from a large number of small terminals with round vesicles (RS profiles, green) that originate from cortical layer VI (Li et al., 2003c). Stimulation of RL profiles at 10 Hz produces EPSPs that depress (type II responses, red), characteristic of "driver" inputs (Sherman and Guillery, 1998; Li et al., 2003b), while stimulation of RS profiles at 10 Hz produces facilitating EPSPs (type I responses, green), characteristic of "modulator" inputs (Sherman and Guillery, 1998; Li et al., 2003b). **B)** In the caudal LPN, projection cells receive input to their proximal dendrites from a large number of medium sized terminals with round vesicles (RM profiles, black) that originate from the SC, and input to their distal dendrites from a large number of small terminals with round vesicles (RS profiles, green) that originate from cortical layer VI (Masterson et al., 2009). Stimulation of RM profiles at 10 Hz produces EPSPs that do not depress or facilitate (type III responses, black), characteristic of "integrator" inputs (Smith et al., 2007), while stimulation of RS profiles at 10 Hz produces facilitating EPSPs (type I responses, green), characteristic of "modulator" inputs. **C)** Glutamate (white squares) is transported into vesicles within RS (green) and RM (black) profiles by the type I (vGLUT1) and type II (vGLUT2) vesicular glutamate transporters respectively (Masterson et al., 2009). When stimulated at frequencies up to 10Hz, glutamate release activates postsynaptic AMPA and NMDA receptors. **D)** When stimulated at high frequency (100Hz), RM profiles additionally release SP (blue circles) which activates postsynaptic NK1 receptors and

increases the amplitudes of subsequent glutamatergic postsynaptic responses (represented by the green and black traces).





## **CHAPTER IV**

### **SUMMARY AND FUTURE DIRECTIONS**

#### **Summary**

The previous chapters have detailed the synaptic organization and electrophysiological properties of the tectothalamic pathway, a pathway centered in the caudal LPN. The caudal LPN is a neural structure in which streams of information mingle and merge. The vGLUT1 and vGLUT2 markers were particularly useful in teasing apart these visual streams. Although vGLUT1 has been shown to be a marker of corticothalamic terminals, the source of the subcortical vGLUT2 within the caudal LPN was unknown. We used a combination of lesion and tracer experiments to find that the origin of the vGLUT2 was within the superficial layers of the SC. Using these markers and various tracers, we were then able to determine the flow of information through the caudal LPN. Information from layer VI of the visual cortex is passed through small terminals onto distal dendrites of projection neurons. These same projection neurons receive visual information from the superficial layers of the SC through clusters of terminals on their proximal dendrites. This clustering of terminals most likely represents convergent input from multiple tectal axons.

Like the corticothalamic terminals, the tectothalamic terminals are glutamatergic and the EPSPs elicited by these synapses are mediated by postsynaptic NMDA and AMPA receptors. However, the tectothalamic synapses differ from the corticothalamic synapses in that the tectothalamic response to high frequency stimulation shows little frequency-dependent plasticity whereas the type I corticothalamic response shows a marked frequency-dependent facilitation. In addition, we found that the tectothalamic synapses contain the neuropeptide SP and EM analysis indicated that these SP-positive terminals synapse with dendrites that express the SP receptor NK1. Exogenous application of SP caused a depolarization of the cellular membrane, increased membrane resistance, and increased the EPSP amplitudes for both corticothalamic and tectothalamic responses. The application of SP also increased the cells response to puffs of glutamate. These effects were blocked by the co-application of the NK1 antagonist L703,606. These experiments suggest that the effects of SP are postsynaptic and are not limited to the activated postsynaptic site.

Many neuropeptides are only released from terminals in response to high frequency stimulation. The colocalization of SP and its receptor indicated a possible role for the high frequency stimulation of SC fibers in the tectothalamic pathway. To test this, we stimulated both the corticothalamic and tectothalamic fibers at 100Hz. High frequency stimulation of corticothalamic fibers had no effect on either corticothalamic or tectothalamic EPSP amplitudes. In contrast, high frequency stimulation of tectothalamic fibers caused a depolarization in cellular membrane, increased membrane resistance, and increased both corticothalamic and tectothalamic EPSP amplitudes. This implies that

tectothalamic fibers, firing at high frequency, release SP which acts postsynaptically through the NK1 receptor.

### **Future directions**

#### *Resolution of the anatomy within the tectothalamic circuit*

The anatomical experiments presented in the previous chapters provide strong evidence that the SP-positive terminals located in the caudal LPN originate from the superficial layers of the SC. However, attempts to double label the SP-positive neurons within the SC that project to the caudal LPN were unsuccessful. The inability to label SP-positive cells is likely due to the mechanisms of neuropeptide synthesis and transport. Although neuropeptides are initially synthesized in the cell soma, they often undergo modification while being transported down the axon. Therefore, the complete neuropeptide is specifically localized and concentrated in the axon terminal. Administration of colchicine, a toxin that inhibits microtubule formation, might cause a sufficient accumulation of SP in the soma to allow immunohistochemical detection (Larson, 1992)

Projection neurons in the caudal LPN receive convergent input from the visual cortex and the SC. We don't know exactly where this integrated information is sent. The projection neurons that were recorded from in these experiments have multiple potential targets: cortex, striatum, or amygdala. The *in vitro* preparation of the electrophysiological experiments was not conducive to the labeling and reconstruction of recorded cells. Anterograde labeling of cells during *in vivo* electrophysiological experiments would maintain the connectivity between projection cells in the caudal LPN and target structures. It has been reported that the projection from the SC to the LPN is

nontopographic (Mooney et al., 1984) but the experiments were indirect. A more direct measure of tecto-LPN projection patterns would be the complete reconstruction of axon arbors from single tecto-LPN cells. The absence or presence of topographic organization is important for interpreting the function of the tectothalamic pathway.

#### *Receptors and mechanisms of SP potentiation*

The electrophysiological experiments discussed in the previous chapters described the effects of SP in the caudal LPN but did not directly address the mechanisms underlying the potentiation. The effects of SP on membrane conductance in the LPN have been shown to be mediated by potassium channels, specifically potassium leak ( $K_{leak}$ ) channels (Paul and Cox, 2010). A decrease in the conductance of  $K_{leak}$  would increase membrane resistance and depolarize the cell. The potentiation of EPSPs characterized in chapter III could be attributed to an increase in membrane resistance, as this would decrease shunting and prevent the degradation of dendritic signals. Replication of the SP application experiments and the high frequency stimulation experiments in the presence of a potassium channel blocker, such as cesium, would determine the role of potassium channels in SP-induced potentiation of EPSPs in the caudal LPN.

The slow activation and long-lasting effects of SP imply G-protein coupling and an intracellular signal transduction pathway. The NK1 receptor is associated with excitatory activity in many areas of central nervous system (Go and Yaksh, 1987, Adelson et al., 2009, Paul and Cox, 2010) and has been shown to undergo endosomal internalization in the presence of SP (Mantyh et al., 1995). Many G protein-coupled receptors exhibit internalization as part of their signaling sequence. Preliminary

experiments were performed in which the NK1 receptor was visualized at 0, 5, 10, and 15 minutes post-SP application. Although the results were intriguing, issues of standardization and quantification of the confocal data were never satisfactorily solved. It would be interesting to know if receptor internalization occurs in response to either SP application or high frequency stimulation.

The superficial layers of the SC are themselves innervated by layer V neurons of the visual cortex. The arrangement of neural circuitry, wherein the caudal LPN receives both direct (layer VI input) and indirect (layer V input via the SC) visual information raises interesting questions as to the function of this nucleus. These attributes might allow the LPN to integrate visual information and to synchronize cortical regions, processes that would be critical for the orchestration of attention. The pulvinar, the primate equivalent of the rodent LPN, has been considered an important structure for visual attention. The purpose of SP in this circuit is impossible to ascertain through purely *in vitro* experimentation and it will be necessary to expand the research into an *in vivo* model. The chemical conjugate substance P-saporin specifically destroys NK1 receptor expressing cells. An *in vivo* experiment in which substance P-saporin were injected into the caudal LPN would eliminate the tectorecipient cells and potentially affect behavior. In the complex and constantly changing environment of the visual world, a neural circuit dedicated to the identification and evaluation of novel stimuli seems a necessity.

## REFERENCES

- Abramson BP, Chalupa LM (1998) Multiple pathways from the superior colliculus to the extrageniculate visual thalamus of the cat. *J Comp Neurol* 271:397-418.
- Adelson D, Lao L, Zhang G, Kim W, Marvizon JC (2009) Substance P release and neurokinin 1 receptor activation in the rat spinal cord increase with the firing frequency of C-fibers. *Neuroscience* 161:538-553.
- Afrah AW, Fiska A, Gjerstad J, Gustaffson H, Tjolsen A, Olgart L, Stiller C, Hole K, and Brodin E (2002) Spinal substance p release in vivo during the induction of long-term potentiation in dorsal horn neurons. *Pain* 96:49-55.
- Alvarado JC, Stanford TR, Vaughan JW, Stein BE (2007) Cortex mediates multisensory but not unisensory integration in superior colliculus. *J Neurosci* 27:12775-12786.
- Arsenault D, Zhang ZW (2006) Developmental remodelling of the lemniscal synapse in the ventral basal thalamus of the mouse. *J Physiol* 573:121-132.
- Baldauf ZB, Chomsung RD, Carden WB, May PJ, Bickford ME (2005) Ultrastructural analysis of projections to the pulvinar nucleus of the cat. I: Middle suprasylvian gyrus (areas 5 and 7). *J Comp Neurol* 485:87-107.
- Baron SA, Jaffe BM, Gintzler AR (1983) Release of substance P from the enteric nervous system: direct quantitation and characterization. *J Pharmacol Exp Ther* 227:365-368.
- Bartlett EL, Stark JM, Guillery RW, Smith PH (2000) Comparison of the fine structure of cortical and collicular terminals in the rat medial geniculate body. *Neuroscience* 100:811-828.

- Battaglia G, Spreafico R, and Rustioni A (1992) Substance P innervation of the rat and cat thalamus. I. Distribution and relation to ascending spinal pathways. *J Comp Neuro* 315:457-472.
- Bender D (1983) Visual activation of neurons in the primate pulvinar depends on the cortex but not on the colliculus. *Brain Res* 279(1-2):158-161.
- Bender D, and Butter C (1987) Comparison of the effects of superior colliculus and pulvinar lesions on visual search and tachistoscopic pattern discrimination in monkeys. *Exp Brain Res* 69:140-154.
- Benedek G, Fischer-Szatmari L, Kovacs G, Perenyi J, Katoh YY (1996) Visual, somatosensory and auditory modality properties along the feline suprageniculate-anterior ectosylvian sulcus/insular pathway. *Prog Brain Res* 112:325-334.
- Bourassa J, Deschenes M (1995) Corticothalamic projections from the primary visual cortex in rats: a single fiber study using biocytin as an anterograde tracer. *Neuroscience* 66:253-263.
- Brill J, Kwakye G, Huguenard JR NPY (2007) Signaling through Y1 receptors modulates thalamic oscillations. *Peptides* 28:250-256.
- Buchel C, Josephs O, Rees G, Turner R, Frith C, and Friston K (1998) The functional anatomy of attention to visual motion. *Brain* 121:1281-1294.
- Bundesen C, Larsen A, Kyllingsbaek S, Paulson OB, Law I. *Exp Brain Res*. 2002 Dec;147(3):394-406. Epub 2002 Oct 12.
- Burnett LR, Stein BE, Chapomis D, and Wallace MT (2004) Superior colliculus lesions preferentially disrupt multisensory orientation. *Neuroscience* 124(3):535-547.
- Casanova C, Molotchnikoff S (1990) Influence of the superior colliculus on visual responses of cells in the rabbit's lateral posterior nucleus. *Exp Brain Res* 80:387-396.
- Castro-Alamancos MA, Calcagnotto ME (1999) Presynaptic long-term potentiation in corticothalamic synapses. *J Neurosci* 19:9090-9097.



- Chalupa LM, Williams RW, Hughes MJ (1983) Visual response properties in the tectorecipient zone of the cat's lateral posterior-pulvinar complex: a comparison with the superior colliculus. *J Neurosci* 3:2587-2596.
- Chen C, Blitz DM, Regehr WG (2002) Contributions of receptor desensitization and saturation to plasticity at the retinogeniculate synapse. *Neuron* 33:779-788.
- Chen C, Regehr WG (2000) Developmental remodeling of the retinogeniculate synapse. *Neuron* 28:955-966.
- Chen C, Regehr WG (2003) Presynaptic modulation of the retinogeniculate synapse. *J Neurosci* 23:3130-3135.
- Chomsung RD, Petry HM, Bickford ME (2007) Synaptic organization of the projection from the temporal cortex to the tree shrew pulvinar nucleus Society for Neuroscience Abstracts 33:392.10
- Chomsung RD, Petry HM, Bickford ME (2008) Ultrastructural examination of diffuse and specific tectopulvinar projections in the tree shrew. *J Comp Neurol* 510:24-46.
- Cleland BG, Dubin MW, Levick WR (1971) Simultaneous recording of input and output of lateral geniculate neurones. *Nat New Biol* 231:191-192.
- Cox CL, Huguenard JR, Prince DA (1997) Peptidergic modulation of intrathalamic circuit activity in vitro: actions of cholecystokinin. *J Neurosci* 17:70-82.
- Crain BJ, Hall WC (1980) The organization of the lateral posterior nucleus of the golden hamster after neonatal superior colliculus lesions. *J Comp Neurol* 193:383-401.
- de Biasi S, Frassoni C, Spreafico R (1986) GABA immunoreactivity in the thalamic reticular nucleus of the rat. A light and electron microscopical study. *Brain Res* 399:143-147.
- Diez-Guerra FJ, Sirinathsingji DJ, Emson PC (1988) In vitro and in vivo release of neurokinin A-like immunoreactivity from rat substantia nigra. *Neuroscience* 27:527-536.
- Doron NN, Ledoux JE (1999) Organization of projections to the lateral amygdala from auditory and visual areas of the thalamus in the rat. *J Comp Neurol* 412:383-409.

- Doron NN, Ledoux JE (2000) Cells in the posterior thalamus project to both amygdala and temporal cortex: a quantitative retrograde double-labeling study in the rat. *J Comp Neurol* 425:257-274.
- Ebner K, Sartori SB, Singewald N (2009) Tachykinin receptors as therapeutic targets in stress-related disorders. *Curr Pharm Des* 15:1647-1674.
- Erisir A, Van Horn SC, Sherman SM (1997) Relative numbers of cortical and brainstem inputs to the lateral geniculate nucleus. *Proc Natl Acad Sci U S A* 94:1517-1520.
- Fabre-Thorpe M, Vievard A, and Buser P (1986) Role of the extrageniculate pathway in visual guidance. II. Effects of lesioning the pulvinar-lateral posterior thalamic complex in the cat. *Exp Brain Res* 62(3):596-606.
- Feig S, Harting JK (1998) Corticocortical communication via the thalamus: ultrastructural studies of corticothalamic projections from area 17 to the lateral posterior nucleus of the cat and inferior pulvinar nucleus of the owl monkey. *J Comp Neurol* 395:281-295.
- Fitzpatrick D, Penny GR, Schmechel DE (1984) Glutamic acid decarboxylase-immunoreactive neurons and terminals in the lateral geniculate nucleus of the cat. *J Neurosci* 4:1809-1829.
- Fremeau RT, Jr., Troyer MD, Pahner I, Nygaard GO, Tran CH, Reimer RJ, Bellocchio EE, Fortin D, Storm-Mathisen J, Edwards RH (2001) The expression of vesicular glutamate transporters defines two classes of excitatory synapse. *Neuron* 31:247-260.
- Go VL, Yaksh TL (1987) Release of substance P from the cat spinal cord. *J Physiol* 391:141-167.
- Govindaiah G, Cox CL (2006) Modulation of thalamic neuron excitability by orexins. *Neuropharmacology* 51:414-425.
- Granseth B, Ahlstrand E, Lindstrom S (2002) Paired pulse facilitation of corticogeniculate EPSCs in the dorsal lateral geniculate nucleus of the rat investigated in vitro. *J Physiol* 544:477-486.

- Guillery RW (1969) The organization of synaptic interconnections in the laminae of the dorsal lateral geniculate nucleus of the cat. *Z Zellforsch Mikrosk Anat* 96:1-38.
- Guillery RW (1995) Anatomical evidence concerning the role of the thalamus in corticocortical communication: a brief review. *J Anat* 187 ( Pt 3):583-592.
- Harting JK, Updyke BV, Van Lieshout DP (1992) Corticotectal projections in the cat: anterograde transport studies of twenty-five cortical areas. *J Comp Neurol* 324: 379-414.
- Herzog E, Bellenchi GC, Gras C, Bernard V, Ravassard P, Bedet C, Gasnier B, Giros B, El Mestikawy S (2001) The existence of a second vesicular glutamate transporter specifies subpopulations of glutamatergic neurons. *J Neurosci* 21:RC181.
- Hilbig H, Bidmon HJ, Ettrich P, Muller A (2000) Projection neurons in the superficial layers of the superior colliculus in the rat: a topographic and quantitative morphometric analysis. *Neuroscience* 96:109-119.
- Hirsch JA (2003) Synaptic physiology and receptive field structure in the early visual pathway of the cat. *Cereb Cortex* 13:63-69.
- Houser CR, Vaughn JE, Barber RP, Roberts E (1980) GABA neurons are the major cell type of the nucleus reticularis thalami. *Brain Res* 200:341-354.
- Hubener M, and Bolz J (1988) Morphology of identified projection neurons in layer 5 of the rat visual cortex. *Neuroscience letters* 94:76-81.
- Hutsler JJ, Chalupa LM (1991) Substance P immunoreactivity identifies a projection from the cat's superior colliculus to the principal tectorecipient zone of the lateral posterior nucleus. *J Comp Neurol* 312:379-390.
- Kaneko T, Fujiyama F (2002) Complementary distribution of vesicular glutamate transporters in the central nervous system. *Neurosci Res* 42:243-250.
- Kato N, and Yoshimura H (1993) Facilitatory effects of substance P on the susceptibility to long-term potentiation in the visual cortex of adult rats. *Brain Research* 617:353-356.

- Kelly LR, Li J, Carden WB, Bickford ME (2003) Ultrastructure and synaptic targets of tectothalamic terminals in the cat lateral posterior nucleus. *J Comp Neurol* 464:472-486.
- Krout KE, Loewy AD, Westby GW, Redgrave P (2001) Superior colliculus projections to midline and intralaminar thalamic nuclei of the rat. *J Comp Neurol* 431:198-216.
- Laberge D, and Buchsbaum M (1990) Positron emission topographic measurements of pulvinar activity during an attention task. *J Neurosci* 10:613-619.
- Larson PJ (1992) Distribution of substance P-immunoreactive elements in the preoptic area and the hypothalamus of the rat. *J Comp-Neurol* 316(3):287-313
- Lee SH, Cox CL (2006) Excitatory actions of vasoactive intestinal peptide on mouse thalamocortical neurons are mediated by VPAC2 receptors. *J Neurophysiol* 96:858-871.
- Lee SH, Cox CL (2008) Excitatory actions of peptide histidine isoleucine on thalamic relay neurons. *Neuropharmacology* 55:1329-1339.
- Li, J., Kelly, L. R., Carden, W. B., and Bickford, M. E. (2000) Synaptic organization of the cat medial LP nucleus: comparison of tectothalamic and corticothalamic terminals. *Society for Neuroscience Abstracts* 26:1469
- Li J, Bickford ME, Guido W (2003a) Distinct firing properties of higher order thalamic relay neurons. *J Neurophysiol* 90:291-299.
- Li J, Guido W, Bickford ME (2003b) Two distinct types of corticothalamic EPSPs and their contribution to short-term synaptic plasticity. *J Neurophysiol* 90:3429-3440.
- Li J, Wang S, Bickford ME (2003c) Comparison of the ultrastructure of cortical and retinal terminals in the rat dorsal lateral geniculate and lateral posterior nuclei. *J Comp Neurol* 460:394-409.
- Lindstrom S, Wrobel A (1990) Frequency dependent corticofugal excitation of principal cells in the cat's dorsal lateral geniculate nucleus. *Exp Brain Res* 79:313-318.

- Ling C, Schneider GE, Northmore D, Jhaveri S (1997) Afferents from the colliculus, cortex, and retina have distinct terminal morphologies in the lateral posterior thalamic nucleus. *J Comp Neurol* 388:467-483.
- Luppino G, Matelli M, Carey RG, Fitzpatrick D, Diamond IT (1988) New view of the organization of the pulvinar nucleus in Tupaia as revealed by tectopulvinar and pulvinar-cortical projections. *J Comp Neurol* 273:67-86.
- Lyon DC, Jain N, Kaas JH (2003) The visual pulvinar in tree shrews I. Multiple subdivisions revealed through acetylcholinesterase and Cat-301 chemoarchitecture. *J Comp Neurol* 467:593-606.
- Major DE, Luksch H, Karten HJ (2000) Bottlebrush dendritic endings and large dendritic fields: motion-detecting neurons in the mammalian tectum. *J Comp Neurol* 423:243-260.
- Mantyh P, Allen C, Ghilardi J, Rogers D (1995) Rapid endocytosis of a G protein-coupled receptor: Substance P evoked internalization of its receptor in the rat striatum *in vivo*. *Pharmacology* 92:2622-2626
- Mason R, Groos GA (1981) Cortico-recipient and tecto-recipient visual zones in the rat's lateral posterior (pulvinar) nucleus: an anatomical study. *Neurosci Lett* 25:107-112.
- Masterson SP, Li J, Bickford ME (2009) Synaptic organization of the tectorecipient zone of the rat lateral posterior nucleus. *J Comp Neurol* 515:647-663.
- Mathers LH (1971) Tectal projection to the posterior thalamus of the squirrel monkey. *Brain Res* 35:295-298.
- Mathers LH (1972) The synaptic organization of the cortical projection to the pulvinar of the squirrel monkey. *J Comp Neurol* 146:43-60.
- McCormick DA, von Krosigk M (1992) Corticothalamic activation modulates thalamic firing through glutamate "metabotropic" receptors. *Proc Natl Acad Sci U S A* 89:2774-2778.
- McHaffie JG, Kruger L, Clemo HR, Stein BE (1988) Corticothalamic and corticotectal somatosensory projections from the anterior ectosylvian sulcus (SIV cortex) in neonatal

- cats: an anatomical demonstration with HRP and 3H-leucine. *J Comp Neurol* 274:115-126.
- Melone M, Burette A, Weinberg RJ (2005) Light microscopic identification and immunocytochemical characterization of glutamatergic synapses in brain sections. *J Comp Neurol* 492:495-509.
- Miguel-Hidalgo JJ, Senba E, Takatsuji K, and Tohyama M (1991) Effects of eye enucleation on substance P-immunoreactive fibers of some retinorecipient nuclei of the rat in relation to their origin from the superior colliculus. *Neuroscience* 44:235-243.
- Montana V, Ni Y, Sunjara V, Hua X, Parpura V (2004) Vesicular glutamate transporter-dependent glutamate release from astrocytes. *J Neurosci* 24:2633-2642.
- Montero VM, Singer W (1984) Ultrastructure and synaptic relations of neural elements containing glutamic acid decarboxylase (GAD) in the perigeniculate nucleus of the cat. A light and electron microscopic immunocytochemical study. *Exp Brain Res* 56:115-125.
- Montero VM, Singer W (1985) Ultrastructural identification of somata and neural processes immunoreactive to antibodies against glutamic acid decarboxylase (GAD) in the dorsal lateral geniculate nucleus of the cat. *Exp Brain Res* 59:151-165.
- Mooney RD, Fish SE, Rhoades RW (1984) Anatomical and functional organization of pathway from superior colliculus to lateral posterior nucleus in hamster. *J Neurophysiol* 51:407-431.
- Mooney RD, Nikolettseas MM, Ruiz SA, Rhoades RW (1988) Receptive-field properties and morphological characteristics of the superior collicular neurons that project to the lateral posterior and dorsal lateral geniculate nuclei in the hamster. *J Neurophysiol* 59:1333-1351.1988.
- Norita M, Katoh Y (1986) Cortical and tectal afferent terminals in the suprageniculate nucleus of the cat. *Neurosci Lett.* 65(1):104-8.

- Oertel WH, Riethmuller G, Mugnaini E, Schmechel DE, Weindl A, Gramsch C, Herz A (1983) Opioid peptide-like immunoreactivity localized in GABAergic neurons of rat neostriatum and central amygdaloid nucleus. *Life Sci* 33 Suppl 1:73-76.
- Ogawa-Meguro R, Shigemoto R, Itoh K, and Mizuno N (1994) Immunohistochemical localization of substance P receptor in the superior colliculus. A light and electron microscope study in the rat. *Neuroscience Letters* (1994) 166:135-138.
- Ogier R, and Raggenbass M (2003) Action of tachykinins in the rat hippocampus: modulation of inhibitory synaptic transmission. *Euro J of Neuro* 17:2639-2647.
- Ogren MP, Hendrickson AE (1979) The morphology and distribution of striate cortex terminals in the inferior and lateral subdivisions of the Macaca monkey pulvinar. *J Comp Neurol* 188:179-199.
- Partlow GD, Colonnier M, Szabo J (1977) Thalamic projections of the superior colliculus in the rhesus monkey, *Macaca mulatta*. A light and electron microscopic study. *J Comp Neurol* 72:285-318.
- Paul K, Cox CL (2010) Excitatory actions of substance P in the rat lateral posterior nucleus. *Eur. J Neurosci* 31(1):1-13.
- Paxinos G, Watson C (2007) *The rat brain in stereotaxic coordinates*.
- Prevost F, Lepore F, Guillemot JP (2007) Spatio-temporal receptive field properties of cells in the rat superior colliculus. *Brain Res* 1142:80-91.
- Reichova I, Sherman SM (2004) Somatosensory corticothalamic projections: distinguishing drivers from modulators. *J Neurophysiol.* Oct;92(4):2185-97.
- Rinvik E, Ottersen OP, Storm-Mathisen J (1987) Gamma-aminobutyrate-like immunoreactivity in the thalamus of the cat. *Neuroscience* 21:781-805.
- Robson JA, Hall WC (1977) The organization of the pulvinar in the grey squirrel (*Sciurus carolinensis*). I. Cytoarchitecture and connections. *J Comp Neurol* 173:355-388.

- Rowland BA, Quessy S, Stanford TR, Stein BE (2007) Multisensory integration shortens physiological response latencies. *J Neurosci* 27:5879-5884.
- Saffroy M, Torrens Y, Glowinski J, and Beaujouan J (2003) Autoradiographic distribution of tachykinin NK<sub>2</sub> binding sites in the rat brain: comparison with NK<sub>1</sub> and NK<sub>3</sub> binding sites. *Neuroscience* 116:761-773.
- Sherman SM, Guillery RW (1998) On the actions that one nerve cell can have on another: distinguishing "drivers" from "modulators". *Proc Natl Acad Sci U S A* 95:7121-7126.
- Sherman SM, Thalamic (2001) relay functions. *Prog Brain Res.* 134:51-69.
- Sherman SM, Guillery RW (2002) The role of the thalamus in the flow of information to the cortex. *Philos Trans R Soc Lond B Biol Sci* 357:1695-1708.
- Smith PH, Bartlett EL, Kowalkowski A (2007) Cortical and collicular inputs to cells in the rat paralamina thalamic nuclei adjacent to the medial geniculate body. *J Neurophysiol* 98:681-695.
- Sun QQ, Baraban SC, Prince DA, Huguenard JR (2003) Target-specific neuropeptide Y-ergic synaptic inhibition and its network consequences within the mammalian thalamus. *J Neurosci* 23:9639-9649.
- Sun QQ, Huguenard JR, Prince DA (2002) Somatostatin inhibits thalamic network oscillations in vitro: actions on the GABAergic neurons of the reticular nucleus. *J Neurosci* 22:5374-5386.
- Takahashi T (1985) The organization of the lateral thalamus of the hooded rat. *J Comp Neurol* 231:281-309.
- Turner JP, Salt TE (1998) Characterization of sensory and corticothalamic excitatory inputs to rat thalamocortical neurones in vitro. *J Physiol* 510 ( Pt 3):829-843.
- Vidnyanszky Z, Borostyankoi Z, Gorcs TJ, Hamori J (1996) Light and electron microscopic analysis of synaptic input from cortical area 17 to the lateral posterior nucleus in cats. *Exp Brain Res* 109:63-70.



- von Krosigk M, Monckton JE, Reiner PB, McCormick DA (1999) Dynamic properties of corticothalamic excitatory postsynaptic potentials and thalamic reticular inhibitory postsynaptic potentials in thalamocortical neurons of the guinea-pig dorsal lateral geniculate nucleus. *Neuroscience* 91:7-20.
- Wassle H, and Illing RB (1980) The retinal projection to the superior colliculus in the cat: a quantitative study with HRP. *J Comp Neurol* 190:333-356.
- Wu Z, Guan B, Li Z, Yang Q, Liu C, and Chen J (2004) Sustained potentiation by substance p of NMDA-activated current in rat primary sensory neurons. *Brain Research* 1010:117-126.
- Wurtz RH, Mohler CW (1976) Organization of monkey superior colliculus: enhanced visual response of superficial layer cells. *J Neurophysiol* 39:745-765.
- Wurtz RH, Sommer MA (2004) Identifying corollary discharges for movement in the primate brain. *Prog Brain Res* 144:47-60.

## LIST OF ABBREVIATIONS

ABC	avidin-biotin-peroxidase complex
ACSF	Artificial cerebrospinal fluid
AMPA	$\alpha$ -amino-3-hydroxy-5-methyl-4-isoxazolepropionic acid
APV	2-amino-5-phosphonovaleric acid
BDA	biotinylated dextran amine
CNQX	6-cyano-7-nitroquinoxaline-2,3-dione
CS	clustered spiking
CTX	optic radiations (input from cortex)
DAB	3-3' diaminobenzidine
dLGN	dorsal lateral geniculate nucleus
DNQX	6,7-dinitro-2,3-quinoxalinedione
EPSP	excitatory postsynaptic potential
EM	electron microscope
FG	fluorogold
GABA	$\gamma$ -amino butyric acid
HRP	horseradish peroxidase
IC	inferior colliculus

IPSP	inhibitory postsynaptic potential
LDN	lateral dorsal nucleus
LGN	lateral geniculate nucleus
LPN	lateral posterior nucleus
LTP	long-term potentiation
NGS	normal goat serum
NK1	neurokinin receptor 1
NMDA	N-methyl-D-aspartate
NOT	nucleus of optic tract
OT	optic tract
Pc	central subdivision of pulvinar
Pd	dorsal subdivision of pulvinar
PB	phosphate buffer
PBS	phosphate buffered saline
PHAL	phaseolus vulgaris leucoagglutinin
PT	pretectum
RL	large terminals with round vesicles
RM	medium terminals with round vesicles
RS	regular spiking
SC	superior colliculus
SGI	stratum griseum intermediale
SGS	stratum griseum superficiale

SO	stratum opticum
SP	substance P
STR	superior thalamic radiation
SZ	stratum zonale
TRN	thalamic reticular nucleus
V1	primary visual cortex
vGLUT1	vesicular glutamate transporter 1
vGLUT2	vesicular glutamate transporter 2
vLGN	ventral lateral geniculate nucleus
VPL	ventroposterior lateral nucleus

## **CURRICULUM VITAE**

**NAME:** Sean Phillip Masterson

**DATE OF BIRTH:** August 19, 1974

**EDUCATION:**

B.A., Psychology

Indiana University Southeast, New Albany, Indiana

1996-2001

M.S., Anatomical Sciences and Neurobiology

University of Louisville, Louisville, Kentucky

2003-2005

Ph.D., Anatomical Sciences and Neurobiology

University of Louisville, Louisville, Kentucky

2003-2005

**AWARDS:**

Society for Neuroscience Graduate Student Travel Award

2006

Ruth L. Kirschstein National Research Service Award

2006

Predocutorial Training Grant, SUNY Stony Brook

2003

National Science Foundation Fellowship, Columbia University

2000

**PUBLICATIONS:**

Masterson SP, Li J, Bickford ME (2009) Synaptic organization of the tectorecipient zone of the rat lateral posterior nucleus. *J. Comparative Neurology* 515:647-663.

Masterson SP, Miller T, Nassim B (2003) Conversion of Cholic acid to methyl 3-alpha-carbethoxy-12-alpha-acetoxy-6-oxo-5-beta 7-en-24oate. *Steroids* 68(3):253-256.

Masterson SP, Li J, Bickford ME. Frequency-dependent release of substance P mediates heterosynaptic potentiation of glutamatergic synaptic responses in the rat visual thalamus. *J. Neurophysiology* (in press).

**ABSTRACTS:**

Masterson SP, Li J, Bickford ME (2009) Substance-P mediated long term potentiation in the visual thalamus. *Society for Neuroscience Abstracts*

Masterson SP, Li J, Bickford ME (2006) Synaptic integration of corticothalamic and tectothalamic inputs in the lateral posterior nucleus of the rat. *Society for Neuroscience Abstracts* 32: 241.4

Chomsung R, Masterson SP, Wei H, Bickford ME (2005) Tectal terminals contact neurons in the lateral posterior nucleus that project to the visual cortex. *Society for Neuroscience Abstracts* 31: 853.5

Masterson, SP, Chomsung R, Bickford ME (2005) Substance P potentiates tectal inputs to the lateral posterior nucleus in the rat. Society for Neuroscience

Abstracts 31: 853.6

Masterson S, Li J, Bickford ME (2004) Responses of regular spiking cells of the rat lateral posterior nucleus to tectal and cortical inputs. Society for Neuroscience

Abstracts 30:983.10